4-22-2015

Development of Point-of-Care Testing Sensors for Biomarker Detection

Xuena Zhu
Florida International University, xzhu006@fiu.edu

DOI: 10.25148/etd.FIDC000063

FLORIDA INTERNATIONAL UNIVERSITY

Miami, Florida

DEVELOPMENT OF POINT-OF-CARE TESTING SENSORS FOR BIOMARKER DETECTION

A dissertation submitted in partial fulfillment of

the requirements for the degree of

DOCTOR OF PHILOSOPHY

in

BIOMEDICAL ENGINEERING

by

Xuena Zhu

2015

To: Dean Amir Mirmiran
College of Engineering and Computing

This dissertation, written by Xuena Zhu, and entitled Development of Point-of-Care Testing Sensors for Biomarker Detection, having been approved in respect to style and intellectual content, is referred to you for judgment.

We have read this dissertation and recommend that it be approved.

_____
Anthony J. McGoron

_____
Helen Tempest

_____
Nikolaos Tsoukias

_____
Shuliang Jiao

_____
Chenzhong Li, Major Professor

Date of Defense: April 22, 2015

The dissertation of Xuena Zhu is approved.

_____
Dean Amir Mirmiran
College of Engineering and Computing

_____
Dean Lakshmi N. Reddi
University Graduate School

Florida International University, 2015

DEDICATION

I would like to dedicate this dissertation to my family whose love and support are the driving force of my life.

ACKNOWLEDGMENTS

This dissertation has been made possible by the collective support of my family, friends and mentors. I would like to thank my husband, my parents and my sister who are my greatest support system in life. Their unconditional love and support have kept me going through the hard times. My mentor Dr. Chenzhong Li has taught me a great deal and will be a father-figure for life. He has always had my best interest at heart and has provided me with every opportunity to grow. I am grateful for all the kindness and patience that he has shown me over the years. I would also like to thank my dissertation committee members Dr. Anthony Mcgoron, Dr. Helen Tempest, Dr. Nikolaos Tsoukias and Dr. Shuliang Jiao for their invaluable advice in steering me towards the right direction. My lab members Dr. Chang Liu, Dr. Evangelia Hondroulis, Dr. Rakesh Guduru, Pratikkumar Shah and Dali Sun have been great friends as well as colleagues and have helped me not just with academics but to grow as a person.

The friends I made in Miami have been my surrogate family and have helped me on every step of the way. They have come and gone but each one of them has touched my life in a special way and taught me to live life to the fullest. Their support and good wishes have been the driving force in helping me successfully finish my dissertation.

I would also like to acknowledge FIU Graduate School Presidential Fellowship and Dissertation Year Fellowship for financial supports through my doctoral study. I also thank AMERI (Advanced Material Engineering Research Institute, FIU) for technical support. This work has also been partially supported by grant NIH R15 ES021079-01 and W81XWH-10-1-0732 by U.S. Army Medical Research & Materiel Command (USAMRMC) and the Telemedicine & Advanced Technology Research Center (TATRC) to Professor Chenzhong

Li, Florida Department of Health James and Esther King Team Science Award (CJR), Florida State Bankhead Coley Technology Transfer Commercialization Partnership (CJR).

I truly thank all of you from the bottom of my heart.

ABSTRACT OF THE DISSERTATION

DEVELOPMENT OF POINT-OF-CARE TESTING SENSORS FOR BIOMARKER DETECTION

by

Xuena Zhu

Florida International University, 2015

Miami, Florida

Professor Chenzhong Li, Major Professor

Point-of-care testing (POCT) is defined as medical testing at or near the site of patient care and has become a critical component of the diagnostic industry. POCT has many advantages over tests in centralized laboratories including small reagent volumes, small size, rapid turnaround time, cost-effectiveness, low power consumption and functional integration of multiple devices. Paper-based POCT sensors are a new alternative technology for fabricating simple, low-cost, portable and disposable analytical devices for clinical diagnosis.

The focus of this dissertation was to develop simple, rapid and low cost paper-based POCT sensors with high sensitivity and portability for disease biomarker detection. Lateral flow strips (LFS) were used as the basic platform as it provides several key advantages such as simplicity, fast response time, on site and cost-effectiveness, and it can be used to detect specific substances including small molecules, large proteins and even whole pathogens, in a sample by immunological reactions. Earlier designs of paper strips lacked the quantitative information of the analyte concentration and could only provide single analyte detection at a time. In this study, a series of modifications were made to upgrade the platform to compensate for these limitations.

First, we developed a gold nanoparticle based LFS for qualitative colorimetrical detection of bladder cancer related biomarkers in standard solutions and in urine samples. Second, by incorporating an image processing program “ImageJ”, a semi-quantitative LFS platform was established. The capability of the strip was evaluated by testing a small DNA oxidative damage biomarker in urine and cell culture models. Third, we combined the electrochemical method and colorimetrical method for quantitative biomarker detection. Finally, we integrated a commercialized blood glucose meter to quantitatively detection of two non-glucose biomarkers by converting their signals to that of glucose. The upgraded sensor could provide a noninvasive, rapid, visual, quantitative and convenient detection platform for various disease biomarkers. In addition, this platform does not require expensive equipments or trained personnel, deeming it suitable for use as a simple, economical and portable field kit for on-site biomarker monitoring in a variety of clinical settings.

TABLE OF CONTENTS

CHAPTER PAGE

LIST OF TABLES

TABLE PAGE

LIST OF FIGURES

FIGURE PAGE

ABBREVIATIONS AND ACRONYMS

8-OHdG	8-hydroxy-2-deoxyguanosine
Ab	Antibody
AFM	Atomic force microscope
AuNPs	Gold nanoparticles
AuNPs-Ab	Gold nanoparticles labeled antibody
BCa	Bladder cancer
BSA	Bovine serum albumin
CdO	Cadmium oxide
CNTs	Carbon nanotubes
CuO	Copper oxide
DMEM	Dulbecco's Modified Eagle's Medium
DNA	Deoxyribonucleic acid
ECIS	Electrochemical immunosensor
ELISA	Enzyme-linked Immunosorbent Assay
EIS	Electrical impedance sensing
GFP	Green fluorescent protein
$HAuCl_4$	Hydrogen tetrachloroaurate solution
HCG	Human chorionic gonadotropin
HIS	Hospital Information System
IgG	Immunoglobulin G
K_2CO_3	Potassium carbonate
LFS	Lateral flow strip
LFIA	Lateral flow immunochromatographic assay

LFT	Lateral flow tests
MMP-9	Matrix metallopeptidase 9
$NaBH_4$	Sodium borohydride
NaCl	Sodium chloride
NIH	National institutes of health
NPs	Nanoparticles
PBS	Phosphate buffered saline
PCa	Prostate cancer
PGM	Personal glucose meter
PI	Isoelectric point
POCT	Point-of-care testing
PSA	Prostate-specific antigen
ROS	Reactive oxygen species
SEM	Scanning electron microscopy
STV-AuNPs	Streptavidin Coated Gold Nanoparticles
TiO_2	Titanium dioxide
µPADs	Microfluidic Paper-Based Analytical Devices
VEGF	Vascular endothelial growth factor
VLIS	Virtual Laboratory Information System
VUC	Voided urinary cytology

Chapter 1. Introduction

1.1. Motivation

The motivation of this dissertation was to develop paper-based point-of-care testing (POCT) sensors with high sensitivity, specificity, speed of performance and the advantages of simplicity for disease biomarker detection. POCT is defined as medical testing at or near the site of patient care. The driving notion behind POCT is to bring the test conveniently and immediately to the patient. This fundamental research could potentially benefit early disease diagnosis, which allows for immediate clinical management decisions to be made. Lateral flow immunochromatographic assay (LFIA) or simply lateral flow strip (LFS) were used as the basic platform as it provides advantages such as simple, rapid and low cost, and it can be used to detect various substances in a sample by using an immunological reaction. However, earlier designs of paper strips lacked the quantitative information of the analyte concentration and could only provide single analyte detection at a single time. To overcome these limitations, we applied the software "ImageJ" to semi-quantify the tests, integrated a paper electrode to carry out quantitative electrochemical measurements, and finally upgraded the platform to make it suitable to be combined with the commercialized blood glucose meter for universal biomolecule detection. The goal of this dissertation was to develop a noninvasive, rapid and quantitative detection method for disease biomarkers. In addition, the developed POCT sensor does not require expensive equipment or trained personnel, deeming it suitable for use as a simple, economical, portable field kit for on-site biomarker monitoring in a variety of clinical settings.

1.2. Specific aims

Specific Aim 1: To develop gold nanoparticles (AuNPs) based LFS and evaluate its ability to detect three bladder cancer (BCa) related biomarkers and an oxidative DNA damage biomarker.

LFS is the simplest and earliest design of paper-based POCT platform, and it has been widely used as in-field and POCT diagnostic tools for monitoring biological molecules and chemical contaminants. LFS were used as the basic platform throughout the entire dissertation study, thus, the first aim of the dissertation research was to fabricate a AuNPs based LFS. The reliability of the strip was first evaluated by three BCa related biomarkers (Creatinine, Matrix metallopeptidase 9 (MMP-9) and vascular endothelial growth factor (VEGF)) for their qualitative colorimetrical analysis. Then, by incorporating an image processing program "ImageJ", the strip was upgraded for semi-quantitative detection of a small DNA oxidative damage biomarker (8-hydroxy-2'-deoxy-guanosine, 8-OHdG). To the best of our knowledge, this is the first LFS-based sensing platform with the capability of 8-OHdG detection. This sensing platform could also help study nanomaterials induced toxicity within cells.

We expected to rapidly detect three BCa related biomarkers as well as 8-OHdG with high sensitivity by our developed LFS platform. The toxicity of three metallic nanoparticles in vitro was also investigated and estimated by measuring the concentrations of 8-OHdG after particles exposure, whose feasibility was validated by the comparison with two other established methods, Alamar Blue assay and Electrical impedance sensing (EIS) system.

Specific Aim 2: To integrate an electrochemical sensing component to the LFS platform to develop a device which combining the electrochemical and colorimetrical sensing methodologies for biomarker detection

A colorimetrical assay can only provide a qualitative or semi-quantitative analysis of the analytes, which is not a specific enough result in many cases. Electrochemical detection is an attractive method due to its capability of quantitative analysis, easy miniaturization to provide a portable formation, and less incident background. Many studies have focused on applying electrochemical detection to the traditional paper-based POCT analytical devices in order to compensate for the limitations of colorimetric detection. The major concern with the measurement of 8-OHdG by the electrochemical method is the potential interference of 8-OHdG containing short nucleotides. As the products of 8-OHdG repairing, both the 8-OHdG molecule and 8-OHdG containing short nucleotides are present in biological urine samples, with 8-OHdG forming the major component usually. Existence of 8-OHdG containing short nucleotides will significantly quench the signaling in electrochemical assay set up with parameters for the 8-OHdG molecule. The occurrence and proportion of 8-OHdG containing short nucleotides are relatively similar in normal biological samples, but might vary appreciably across normal person and patients. To overcome the drawbacks of the immunostrip assay and electrochemical method for 8-OHdG detection, the second aim deals with the development of an novel electrochemical immunosensor (ECIS) which integrates carbon nanotubes (CNTs) paper electrodes with a immunochromatographic strip for quantitative analysis of 8-OHdG in both PBS buffer and urine samples.

We expected that the new sensing device could combine the competitive AuNPs based lateral flow immunoassay with miniaturized paper electrodes for both colorimetrical and electrochemical detection. This novel platform could provide a fast diagnostic tool for quantitative DNA oxidative stress assessment with high sensitivity and specificity. Furthermore, the integrated platform can be further upgraded and optimized into a wireless-enabled biosensing system in future for telemedicine applications.

Specific Aim 3: To integrate personal glucose meters with the traditional lateral flow immunostrip for portable and quantitative detection of biomarkers

We successfully coupled the electrochemical sensing platform to the LFS in the previous specific aim. An important superiority of the coupled platform is that it can be potentially connected to a portable electronic device for quantitative and instant measurements, which is a key perspective for the future POCT development. At the same time, electrochemical detection usually based on a fact that the analyte itself should be electrochemically detectable. Therefore, in the specific aim 3, we tried to test an electrochemical integrated LFS platform by directly connecting to a portable device, which can detect any analytes with or without electrochemical properties by electrochemical method. The personal glucose meter (PGM) is one of the most successfully commercialized diagnostic devices on the market and it has been widely used by millions of diabetic patients to monitor their blood glucose levels every day because of its low cost, compact size, simple operation and reliable quantitative results. In order to take advantages of this well established technique, a novel design that combines the traditional LFS with a commercial PGM was developed for quantitative

detection of non-glucose targets. A small molecule, 8-OHdG, as well as a large protein, prostate specific antigen (PSA), were used as model analytes for concept demonstration.

We expected that the new device could quantitatively detect non-glucose targets by using a PGM. The results obtained from PGM-based method were compared with those from commercialized ELISA kits, demonstrating the feasibility of the new platform. Considering the inherent advantages of the PGM, the demonstration of this device therefore should provide new opportunities for the monitoring of a wide range of biomarkers as well as various target analytes in connection to different molecular recognition events.

1.3. Point of care testing

1.3.1. Definition and significance of POCT

POCT, also known as near patient or bedside testing, is any analytical test performed outside the laboratory, normally at or near the site of patient care.[1] Many of the early "diagnostic tests" were first done at the bedside—for example, urine testing. Over the past few years, however, analytical systems have been developed that enable a wide range of tests to be done quickly and simply without the need for sophisticated laboratory equipment.[2]

The driving notion behind POCT is to bring the test conveniently to the patient and to obtain immediate results of the testing so that appropriate treatment can be implemented, leading to an improved clinical or economic outcome. The use of POCT has been around for over 50 years, however there has be a recent increased use in the hospital and community settings due to rapid advances in genomics, transcriptomics, and proteomics which has accelerated the unraveling of disease pathogenesis, the discovery of disease biomarkers, and the

identification of pathogens. In addition, the emerging fields of nanotechnology and microfluidics have improved assay designs and performance, thereby bringing accurate and sensitive diagnostic tests to POCT.[3]

The main advantage of POCT is a rapid turnaround time, generating results sooner and therefore allowing for more immediate patient triage and effective treatment or discharge. This can lead to improved patient care, earlier discharge from the hospital, reduced medical costs and contribute towards reducing government waiting time targets. In addition to saving time, some POCT tests have been modified to simplify the test procedure, reduce the chance of operator error, and directly use a body fluid sample without pretreatment.[3] Successful design will eliminate the need for prior knowledge in sample analysis and can be performed by an outpatient or by any ward personnel.

1.3.2. Biosensors in POCT

POCT devices often employ biosensors (Figure. 1.1). A biosensor is commonly defined as an analytical device that combines a biological component with a physicochemical-detector component for the detection of analytes. This generally occurs through the use of miniaturized analysis systems, where biological components are immobilized on a solid-state surface, which, in turn, interacts with the analyte.[4] These interactions may be detected by using either electrochemical or optical methods.

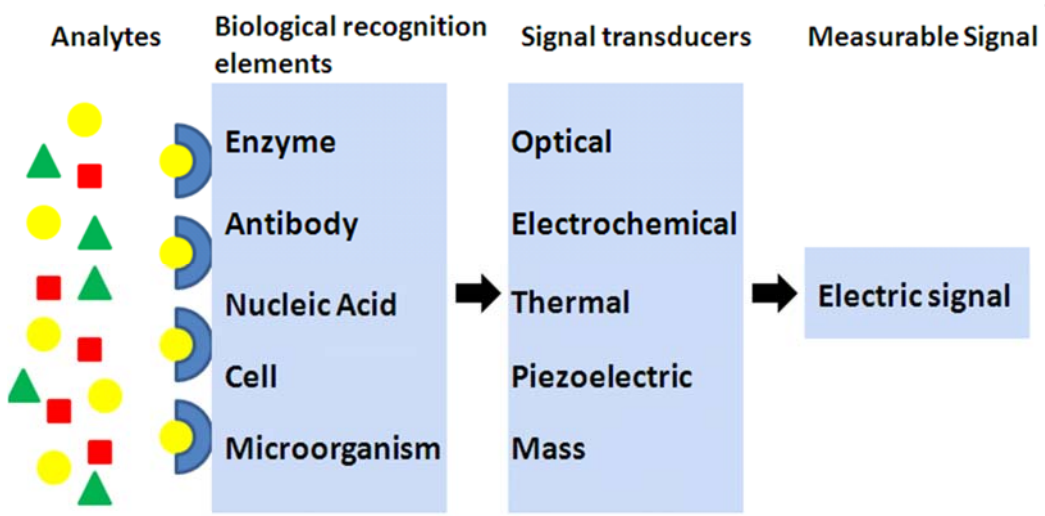

Figure 1.1. Schematic of biosensor

POCT analyzers currently available can be separated into various groups. Type 1: Qualitative strip-based POCT methods. Type 2: Unit-use analyzers, the simplest form of quantitative POCT device. For these two types of devices, most of the analysis takes place on the test strips and the reader is used only to read the results from the strips where the reaction has already taken place. Examples of type 2 include glucometers for home and the hospital POCT stations and the i-STAT Abbott (Abbott Park, IL, USA), a multi-parameter unit-use POCT instrument.[5] Type 3: Bench-top POCT analyzers, are generally more complex than unit-use machines and use different analytical principles, such as spectrophotometric substrate and enzyme-activity measurement; hematological particle counting; immunoassay; and, sensor-based blood-gas analysis.[6] Type 4: Hemostaseological coagulation analyzers, these POCT compatible machines show a high degree of complexity; although they are valid for use in POCT, only qualified personnel should operate them. Type 5: Continuous measurement with POCT systems, the most common example being continuous glucose monitoring,[7] and these systems are already available commercially. Type 6: Molecular

biology-based POCT devices used to detect infectious agents. The currently available novel POCT systems are in part forerunners of a new generation of laboratory systems which will dominate the market in 10–20 years' time (fourth-generation laboratory systems). These methods are characterized through miniaturization, parallel analyses and networking via information technology (IT).[6]

1.3.3. Telemedicine developed with POCT

Emerging Internet technologies are used to create and manage a Virtual Laboratory Information System (VLIS), integrated into a distributed healthcare environment. The main objective of the system is to organize the transference of clinical testing from the traditional large central laboratories to a cooperative scheme of several manageable POCTs.[8] Emerging information technologies allow these POCTs to be essentially connected within Hospital Information System (HIS) distributed environments, sharing on-line healthcare data among the different actors involved in patient treatment, which is also referred as telemedicine.

The fundamental parts of the telemedicine system are: the measuring devices (e.g., sensors), a device (e.g., mobile phone, IPAD) to format the readings for a communications link, a clinic server to which the data is transmitted, a database for storing the data, and a display of the data obtained from the server. Mobile devices are one of the most common methods employed and have been widely used for data collection and processing. The trend of using mobile and wireless communication for bio-sensing applications is becoming more and more apparent. For data collection, nano-structured materials will be used to build fully-integrated, non-invasive and bio-inspired wireless/mobile sensor for health monitoring including heart rate, blood glucose concentration, as well as different bimolecular levels. After data

collection, wireless/mobile devices will be continuingly used for the transmission of medical information to the hospital or health centre. For the patient, there is no longer the need to make an appointment with the doctor or to spend time and cost traveling only to receive a benign result. The systems can also be used to monitor the health condition of patients and to aid them in making a clinical decision as early as possible, an advantage for both disease control and therapy. From a clinical standpoint remote monitoring allows patients to record their readings in a more relaxed home environment, rather than to undergo the stress of travelling for a personal consultation.

1.4. Paper-based sensors

1.4.1 Unique properties of paper as a platform for disposable diagnostic devices

Paper is a well-known material for writing, printing, drawing and packaging. The potential utility of paper beyond these simple and traditional means stems from its unique properties, which include the following: it is available and manufactured in every part of the world very cheaply; it is biodegradable as well as biocompatible; it is flexible, easily coated and imprinted; it is made of a porous cellulose structure, so it wicks fluids and eliminates the requirement of an active pumping mechanism; its porous structure also serves as a filter for many analytical applications; and it is usually white and serves the best platform for colorimetric and fluorescent detection.[9]

1.4.2. Significance and development of paper-based sensors

Paper has been used in analytical laboratories since the early 20th century with a significant revolution when Martin and Synge were awarded the Nobel Prize for the invention of paper chromatography in 1952.[10] Over the years, with the development of novel nanomaterials and

nanofabrication technologies, many interesting and innovative concepts and prototypes for paper-based bioanalytical devices have been reported.

In 1956, the first paper device for the semi-quantitative detection of glucose in urine was demonstrated,[11] that further developed into immunochromatographic paper test strips (also known as lateral flow or dipstick tests), with the pregnancy test kit being a well-known example.[12] Although reliable, these simple and low cost devices are generally limited in providing a qualitative "yes/no" type of detection. The last few years has seen a shift in focus from basic design concepts to more advanced fabrication and patterning techniques in order to obtain more accurate and quantitative results. Whitesides and co-workers[13, 14] introduced the idea of fabricating microfluidic channels on paper for multiplex analyte detection. Since then, many new areas of fabrication and exploration have opened up, such as in paper-cut microfluidic devices[15-18] and microfluidic separation devices.[19-21] These new research avenues have resulted in sensors that can be analyzed by techniques other than colorimetry,[13, 14, 22-25] such as by electrochemical,[26-28] chemiluminescence[29] and electrochemiluminescence[30] methods.

Due to their enormous advantages, paper-based analytical devices can play vital roles in improving diagnostics and treatment of various diseases in resource-limited areas of the world, which are financially incapable of having advanced technologies.[13] A low-cost paper-based analytical device can fulfill the need of people in developing and poor regions of the world, which lack the facility of proper infrastructure and trained healthcare professionals at the site of patients.[13]

1.5. Lateral flow immunochromatographic assay (LFIA) or LFS

LFIA, also called lateral flow tests or simply strip tests, is the simplest and earliest design used for an analytical device platform. This technology offers additional advantages when compared to the conventional detection methods given that it is rapid, simple and cost-effective in comparison. The first application of strip assay was the pregnancy test with the detection of human chorionic gonadotropin (HCG) in the early 1980s.[31] The speed of the results observed directly by the naked-eye and the utilization of a membrane strip as the immunosorbent material provided an analytical platform that permits a one-step, rapid and low-cost analysis. To date, this technology has reached many fields of research such as pathogens and infectious diagnostic, food and environment monitoring. Figure 1.2 shows the typical design of LFS, having four major components: sample pad, conjugation pad, reaction membrane and absorbent pad. Typically, when a sample is applied, the antigen will bind to an antibody on the conjugation pad (conjugation antibodies are conjugated to signal molecules such as latex beads, colloid gold, etc.). The complex formed due to the antigen/conjugate antibody interaction then travels along the paper membrane through capillary action and is subsequently captured by antibodies available on the reaction zone of the paper strip.[10] A color change can be visualized with the naked eye within a few minutes, which indicates of the presence of the target analyte in the sample. However, earlier designs of paper strips were criticized for only providing a qualitative, 'yes/no' signal and lacked the quantitative information of the analyte concentration.[32] Moreover, such designs can only provide single analyte detection at a single time and they are difficult to integrate with multiple analyte detection.[32]

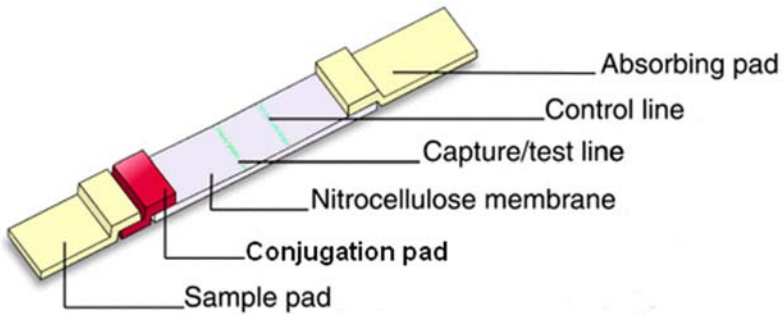

Figure 1.2. Lateral flow strip

To overcome the limitations of earlier LFS designs, such as single analyte detection, lack of quantitative information and lack of control over sample flow, many novel manufacturing techniques have been developed. In this dissertation study, we chose to use LFS as the basic platform as it provides several key advantages such as simplicity, fast response time, on site and cost-effectiveness, and it can be used to detect various substances in a sample by using an immunological reaction. Nevertheless, we reduced the disadvantage by integrating several novel techniques to the original platform. First, we applied a image processing program-ImageJ to the original colorimetrical measurements to semi-quantify the results. Second, we combined the traditional platform with a flexible paper electrode, which could perform a quantitative electrochemical detection beside the colorimetrical result. Third, to enlarge the application scope of test strip, we integrated the commercialized blood glucose meter with an upgraded platform, which can provide new opportunities for the monitoring of a wide range of biomarkers as well as various target analytes in connection to different molecular recognition events. Based on these improvements, the new strips can provide a noninvasive, rapid, visual and quantitative detection method for disease biomarkers. In addition, this method does not require expensive equipment or trained personnel, deeming it

suitable for use as a simple, economical, portable field kit for on-site biomarker monitoring in a variety of applications.

1.5. Biomarker detection

1.5.1 Biomarkers

A biomarker generally refers to a characteristic that is objectively measured and evaluated as an indicator of normal biological processes, pathogenic processes, or pharmacologic responses to a therapeutic intervention. Detection of biomolecules has been of significant interest in areas such as genomics, proteomics, medical diagnostics and environmental monitoring.

Lateral flow strips have been widely used to semi-quantitatively or quantitatively measure the concentration of common analytes, that is, glucose, HCG and BSA in a variety of body fluids (i.e. urine, blood, sweat, etc.) for a long period of time. Nowadays, by incorporating the new techniques, the paper-based devices can be further applied to many other biomarkers.

Cancer becomes one of the leading causes of death with more and more people being diagnosed with cancer every year. Currently, treatment efficiency of late stage cancer is poor. However, cancer at early stage is generally treatable, and the early detection of cancer is in urgent need. Cancer diagnosis is very important and becoming a practical way to improve the cure rate. Cancer biomarkers exist in body fluids or tumor tissues and encompass a wide range of molecules, including transcription factors, cell surface receptors and secreted proteins. It can be used for detection and can also help doctors to make decisions on patients as early as possible about the possible response to a given drug and what the most effective

dose might be providing valuable prognostic information. Traditional diagnostic techniques are usually costly, time-consuming, require specialized laboratory-based equipment, dedicated sample preparation processes and professional operators. Paper-based devices simplify the system. Wang *et al.* combined microfluidic paper-based analytical devices (μPADs) with the CL-ELISA for the simultaneous determination of α-fetoprotein, CA125 and carcinoembryonic antigen in human serum samples.[33] Liu *et al.* developed a disposable electrochemical immunosensor diagnosis device that integrates the immunochromatographic strip technique with an electrochemical immunoassay, and the device has been successfully applied for the detection of PSA in human serum samples.[34]

Along with cancer diagnosis, paper-based devices can also be used for the detection of other diseases. Many studies on diabetes developed methods to quantified glucose, lactate or cholesterol in human serum and urine samples by incorporating the electrochemical detection with paper-based microfluidic devices.[26, 35] In-field and point-of-care diagnosis of genetic diseases by DNA–DNA hybrids and dual labels were also developed with one example being an ultrasensitive nucleic acid biosensor based on horseradish peroxidase-gold nanoparticles dual labels and LFS biosensor.[36] A nanoparticle-based electrochemical immunosensor has been reported for the detection of phosphorylated acetylcholinesterase, which is a potential exposure biomarker for organophosphate pesticides and chemical warfare nerve agent exposures.[37] Heart-type fatty acid-binding protein is an early cardiac marker of acute myocardial infarction, which is the predominant cause of mortality and disability in most developed countries[38] and requires a rapid assay system. Renneberg's

group developed a quantitative lateral-flow assay for rapid detection of fatty acid-binding protein.[30]

Furthermore, paper-based devices have been widely used in environmental and food safety monitoring. Determination of metal ions in waste solutions is important in public health and environmental monitoring, for example, measurement of Au(III), Fe(III), Pb(II) and Zn(II) in industrial waste solutions by incorporating electrochemical method and microfluidic platform.[28, 39] Detecting and quantifying mycotoxins is essential for food safety monitoring. One group has developed a semi-quantitative detection of Ochratoxin A, a type of mycotoxin, by an aptamer-based chromatographic strip assay.[40]

1.5.2. Detection mechanism by LFS

The two predominant approaches to the LFS are the non-competitive (or sandwich) and competitive (or competitive inhibition) reaction schemes. These can best be explained graphically, as shown in Figures 1.3.a and 1.3.b. The double antibody sandwich format is used when testing for large analytes with multiple antigenic sites, such as LH, hCG, and HIV. In this case, less than an excess of sample analyte is desired so that some of the microspheres will not be captured at the capture line, and will continue to flow toward the second line of immobilized antibodies, the control line. This control line uses species-specific anti-immunoglobulin antibodies, specific for the conjugate antibodies on the microspheres. The competitive reaction scheme is used most often when testing for small molecules with single antigenic determinants, which cannot bind to two antibodies simultaneously. If this format is chosen, it is important to pay close attention to the amount of antibody bound to the

microspheres in relation to the amount of free antigen. Some of the microspheres will bind at the capture line giving a weak signal and making the test result ambiguous.

Three BCa related biomarkers (Creatinine, Matrix metallopeptidase 9 (MMP-9) and vascular endothelial growth factor (VEGF)), a DNA oxidative damage biomarker (8-hydroxy-2-deoxyguanosine (8-OHdG) and a PCa related biomarker (prostate-specific antigen (PSA)) were used in this dissertation study as representatives for demonstrating the feasibility and applicability of developed platforms (both sandwich and competitive formats of detection).

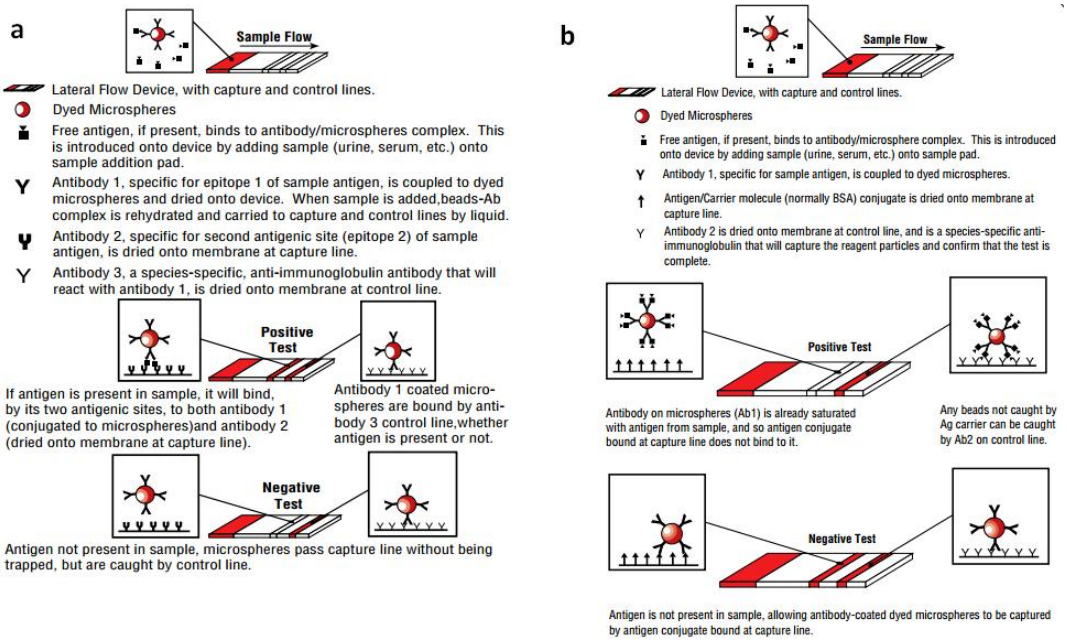

Figure 1.3. (a) Direct (double antibody sandwich) reaction scheme; (b) Competitive reaction scheme. Image taken from the website of Bangs Laboratories, inc..

Chapter 2. General experimental methods

2.1. Introduction

In this dissertation study, LFS were used as the basic platform and upgraded further with other elements to improve the design and enlarge the application of the strip. Some common experimental procedures present in each chapter will be summarized here.

2.2. Fabrication of AuNPs based LFS

2.2.1. Preparation of AuNPs

A well-established citrate reduction method[41] was employed to generate AuNPs of various diameters. Different sizes of AuNPs produce different reflected color. Preliminary data shows that AuNPs with a diameter of ~20 nm intrinsically gives a better visibility on paper based strip when accumulated on test line, and many studies[42-44] also used this size for similar applications, therefore we used AuNPs with average size around 20 nm as the labels.

Briefly, hydrogen tetrachloroaurate solution ($HAuCl_4$) (50 mL, 0.01%) was added to a Erlenmeyer flask (250 mL), stirred and brought to the boil on a hotplate. Trisodium citrate solution (1 mL, 1%) was added rapidly to the boiling solution under constant stirring. Gradually, the color changed from pale yellow to wine red (Figure 2.1). After the color change ceased, the solution was boiled for another 10 min and stirred without heating for another 10 min to complete the reduction of the gold chloride. The size of the particles were characterized by the Zetasizer after the solution reached room temperature.

The wine red colored solution contains AuNPs with a size of approximately 20 nm (Zetasizer, Figure. 2.2a) and its corresponding maximum absorbance is exhibited at 520 nm as shown in Figure. 2.2b (UV-VIS spectrophotometer). It is well known that the strong

absorbance at 520 nm is attributed to the surface plasmon resonance of AuNPs and the maximum absorption peak will be shifted or disappeared if the nanoparticles aggregate together.[45, 46]

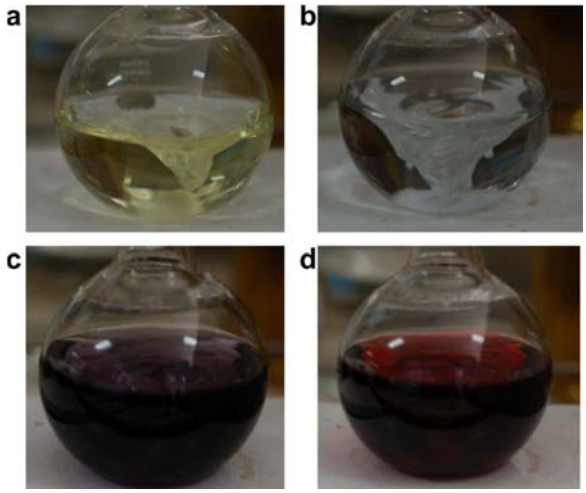

Figure 2.1. Color changes during the preparation of colloidal AuNPs: (a) 0 min, (b) 5 min, (c) 10 min and (d) 20 min (with an average size ~20 nm).

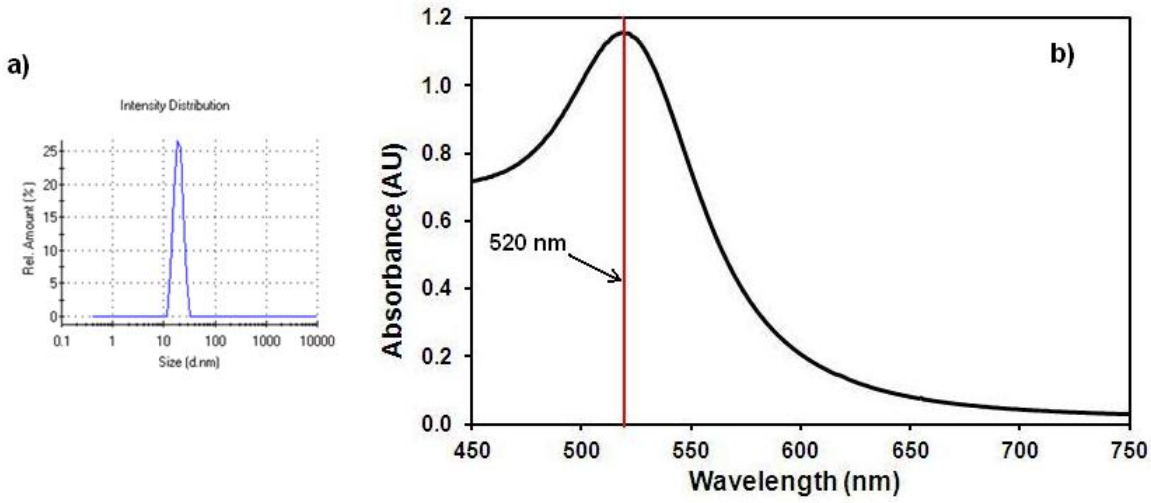

Figure 2.2. (a) Intensity distribution vs. size of AuNPs solution (average size ~20 nm) measure by Zetasizer; (b) UV-Vis spectrum of ~20 nm AuNPs

2.2.2. Synthesis of antibody conjugated AuNPs

For antibody labeling, the AuNPs solutions was concentrated 5-fold (5X) in advance and the pH was adjusted to 8.0~8.5 with 0.1 M Potassium carbonate (K_2CO_3). Before conjugation, the optimal concentration of the antibody was determinated by following the protocol from Y Zhao. et al..[47] Simply, antibody solutions with different concentrations were mixed with gold solution (5X, pH 8.0~8.5) and incubated for 15 min at room temperature, and then 10% Sodium chloride (NaCl) solution was added. The color of samples changes from brilliant red to blue as the concentration of antibody decreases (Figure 2.3). The optimum concentration for labeling was the lowest concentration of antibody that did not change color. For example, five folds (5X) concentrated AuNPs with an optimal concentration 0.5 mg mL^{-1} of anti-8-OHdG antibody was used for the DNA oxidative damage study.

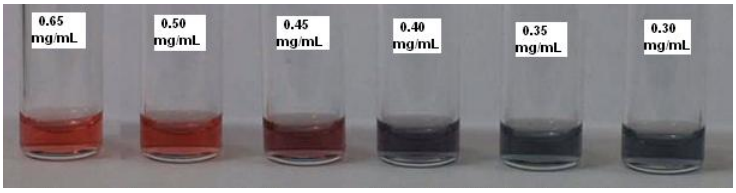

Figure 2.3. Determination of the optimal mAb concentration for conjugation

Purified antibody (60 µL) with optimal concentration (for bladder cancer biomarkers detection: anti-Creatinine pAb, 20 µg mL^{-1}; anti-MMP-9 mAb, 180 µg mL^{-1}; and anti-VEGF mAb, 180 µg mL^{-1}. For DNA oxidative damage biomarker detection: mouse anti-8-OHdG monoclonal antibody, 0.54 mg mL^{-1}) was added to a tube, which containing 750 µL pre-concentrated (5X) AuNPs solutions. The mixture was stirred gently at room temperature for 1 h first, and then stabilized by adding 10% BSA (90 µL) in sodium borate (20 mM) for a final concentration of 1% and incubated for another 20 min. After the tube was centrifuged for 15

min at 7,000 rcf, two phases were obtained: a clear to pink supernatant of unbound antibodies and a dark red, loosely packed sediment of the AuNPs-Abs conjugates. The supernatant was discarded and the pellet was resuspended in BSA/PBS (900 µL, 1%). Following the same centrifugation step, the supernatant was removed again and the soft sediment of conjugates was resuspended in 900 µL buffer 1, which contained sodium phosphate (20 m_M), Tween 20 (0.25%), sucrose (10%), and BSA (5%). Tween 20 provides buffer control and also has a slight surfactant quality that aids in resolubilization of the particles. BSA can provide a blocking function which can prevent non-specific binding. The sucrose serves as a preservative and a resolubilization agent. The final conjugate solution was stored at 4 °C until use.

Initially, we used a green fluorescent protein (GFP) labeled antibody as a model to demonstrate the feasibility of this conjugation protocol. As illustrated in Figure 2.4a, the fluorescence image demonstrated the efficiency of conjugation. Figure 2.4b showed that the corresponding maximum absorbance of AuNPs was shifted from 520 nm to 530 nm after antibody conjugation.

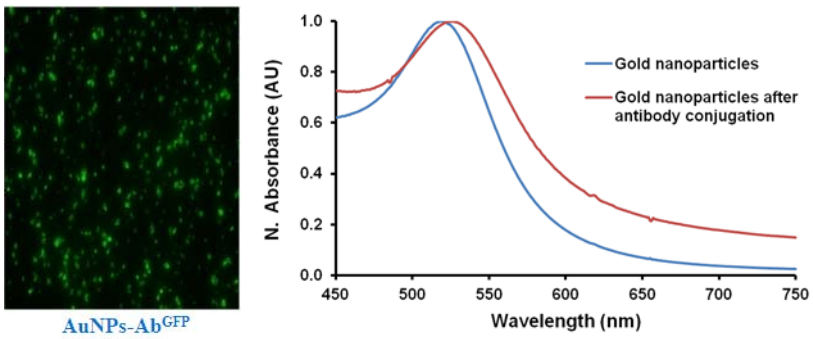

Figure 2.4. (a) Fluorescence images of the antibody conjugated AuNPs; (b) UV-Vis spectrum of ~20 nm AuNPs before and after antibody conjugation

2.2.3. Preparation of conjugation pad

30 μL AuNPs-Ab conjugates solution prepared as outlined in section 2.2.2 was dispensed by pipette onto a glass fiber pad (conjugate pad) (5 mm × 9 mm). Following which, all pads were dried at room temperature and stored in desiccators at 4 °C before use.

2.2.4. Preparation of reagents preloaded on the nitrocellulose membrane

2.2.4.1. Preparation of BSA-8 hydroxyguanosine conjugates

8-hydroxyguanosine (5 mg) was dissolved in $NaIO_4$ (1mL, 50 mM) and the mixture was incubated for 1 h in the dark. The reaction was stopped by adding Ethylene glycol (2.5 μL) for 5 min. The mixture was then mixed with BSA (2 mL, 25 g L^{-1}, pH=9.5, adjusted by K_2CO_3 (50 g L^{-1})) under constant stirring dropwise and incubated for another 1 h. After that, Sodium borohydride ($NaBH_4$, 2 mL, 24 g L^{-1}) was added and the mixture was incubated in the dark at 4 °C overnight (12-16 h). Finally, the conjugates were dialyzed against 1X PBS and stored at -20 °C.

2.2.4.2. Preparation of other antibodies

Creatinine pAb (20 μg mL^{-1}), anti-MMP-9 pAb (36 μg mL^{-1}), anti-VEGF pAb (18 μg mL^{-1}), Rabbit anti-Mouse IgG (1 mg mL^{-1}), Rabiit anti-Sheep IgG (1 mg mL^{-1}) and Goat anti-mouse IgG (1 mg mL^{-1}) were diluted from the original concentrations which directly obtained from manufacture.

2.2.4.3. Buffer used for capture reagent preparation

Nitrocellulose membranes can bind proteins electrostatically independent of pH, but pH can affect the immobilization efficiency of a particular protein by altering its properties in

solution. The tendency of the antibody to partition onto the membrane increases as the solubility of the capture reagent which is influenced by pH is reduced. Solubility is minimal when the protein has no net charge, for example, at the isoelectric point, pI. Thus, to minimize protein solubility and maintain a stable solution, the pH was adjusted to the pI of the capture reagent. Most antibodies have isoelectric points between pH 6.5 and 9.0. Using a buffer at pH 7.0 - 7.5 was commonly recommended by many studies and manufacture. In this study, 1X PBS (pH 7.4) was used for capture reagent preparation.

2.2.5. Assembly of the LFS

A typical test strip consists of four components: sample loading pad, conjugation pad, nitrocellulose membrane, and absorption pad, all of which were affixed onto a plastic backing plate (Figure 2.5).

The sample pad (5 mm by 19 mm) made of glass fiber was treated with buffer 2 (pH 8.0) which contains 0.15 mM NaCl, 0.05 M Tris-HCl and 0.25% Triton X-100 in advance. Use of an appropriate buffer minimizes the non-specific adsorption, increases the sensitivity and reproducibility of the biosensor. Based on many studies,[42-44] we compared the performances of different running buffers, and established that buffer 2 yielded the best results. Sample pads were then dried at room temperature and stored in desiccators at 4 °C before use.

For BCa related biomarkers detection: Anti-Creatinine pAb (20 μg mL^{-1}), anti-MMP-9 pAb (36 μg mL^{-1}) and anti-VEGF pAb (18 μg mL^{-1}) were used as the test line (T) capture reagents, while Rabbit anti-Mouse IgG and Rabiit anti-Sheep IgG (1 mg mL^{-1}) were used as the control line (C) capture reagent, respectively.

For DNA oxidative damage biomarker detection: BSA-8 hydroxyguanosine conjugates were used as the test line capture reagent, while goat anti-mouse IgG (1 mg mL^{-1}) was used as the control line capture reagent.

For PSA detection: Anti-PSA mAb were used as the test line capture reagent, while goat anti-mouse IgG (1 mg mL^{-1}) was used as the control line capture reagent.

These capture reagents were dispensed by the Linomat 5 dispenser onto a nitrocellulose membrane as test and control lines. Finally, all of components including sample pad, conjugate pad, nitrocellulose membrane and absorbent pad were assembled on a plastic adhesive backing layer. Each part overlapped 2 mm to ensure the solution migration through the strip during the assay (Figure 2.5).

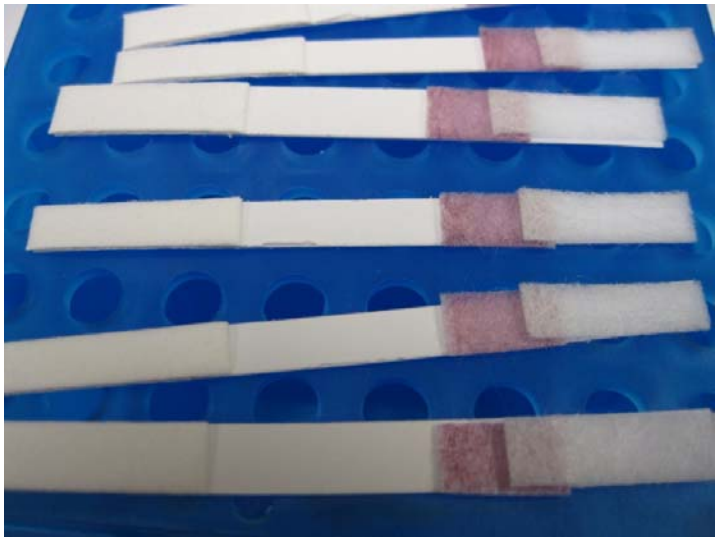

Figure 2.5. Typical AuNPs based LFS.

2.3. Preparation of standard solutions and samples

2.3.1. For BCa related biomarkers detection

Standard solution of Creatinine (Sigma-Aldrich), MMP-9 and VEGF (R&D systems, Inc,) (0.03 mg mL^{-1}, 50 ng mL^{-1} and 120 ng mL^{-1}, respectively) were commercially obtained without further processing, and kept at 4 °C before use. After institutional review board (IRB) approval, urine samples from 10 potential BCa patients were collected by Dr. Rosser's Translational Research Laboratory (MD Anderson Cancer Center Orlando) and shipped to us following the standard procedures. Urine samples were stored at -20 °C after received. Before use, urine samples were thawed to room temperature, and then centrifuged at 7,000 rcf for 10 min. Following which, supernatants were collected, filtered through a Whatman no. 1 filter paper and stored in a tube.

2.3.2. For DNA oxidative damage biomarker detection and nanotoxicity assessments

Stock solutions of 8-OHdG (500 μg mL^{-1}) were prepared before use by dissolving the 8-OHdG powder in purified PBS (1X) solution, DMEM and cell lysis buffer respectively. Working standards ((0.1–100000) ng mL^{-1}, (1–80) ng mL^{-1} and (1–80) ng mL^{-1}) were prepared further in the corresponding media.

2.3.3. For 8-OHdG detection by electrochemical method

8-OHdG standard solutions ((1-1000) ng mL^{-1}) were prepared as outlined in section 2.3.2. Urine samples were obtained from drug free, non-smoker, healthy volunteers within the department following the protocol approved by both Florida International University (FIU) and the Telemedicine and Advanced Technology Research Center [TATRC] IRB. Samples were stored frozen (-20℃) in aliquots of 4 mL until analyzed. Before use, urine samples were

thawed to room temperature and then centrifuged at 7,000 rcf for 10 min to remove any precipitate. Following which, the supernatants were collected and diluted 10-fold with PBS (1X) to minimized the interference induced by variation of urine components and further used as control. The diluted urine samples were serially spiked with 8-OHdG to make solutions of 0, 1, 10, 20, 50, 80, 100, 150, 200 and 1000 ng mL^{-1} concentration levels prior to the test.

2.3.4. For biomarker detection by PGM

8-OHdG standard solutions ((0.1-200) ng mL^{-1}) were prepared as outlined in section 2.3.2. PSA solution were directly obtained from manufacture (Sigma-Aldrich), working standards ((1-200) ng mL^{-1}) were prepared with 1X PBS before use. Urine samples were prepared as outlined in section 2.3.3 without dilution.

2.4. Paper strip assay and colorimetrical analysis

Standard solution or sample (100 μL) was added onto the sample pad, and the solution migrated toward the absorbent pad. Photographs were taken by a digital camera or scanner after 10 min for further colorimetrical analysis.

2.5. Detection mechanism for LFS

There are various possible formats of LFS depending on the type of target analyte.[48] The two kinds of format frequently used are sandwich assay and competitive assay.

2.5.1. Sandwich assay

Sandwich assay format (Fig. 2.6A) was employed to test analytes presenting several epitopes such as cancer protein biomarkers (i.e. MMP-9, VEGF and PSA). The sandwich assay can employ two different antibodies (polyclonal and monoclonal) that bind distinct epitopes of the analyte: a labeled monoclonal or polyclonal antibody is placed in a dehydrated state onto a glass-fiber membrane (conjugate pad) to serve as detector reagent and a polyclonal or monoclonal antibody specific to the analyte is sprayed at the test line of the nitrocellulose membrane to serve as the capture reagent. An additional antibody specific to the detection antibody could be used to produce a control signal. When a sample extract is applied to sample pad, the liquid migrates up by capillary force and the detector reagent is then released. Some of the analyte binds to the detection antibody and some will remain free in the solution. Subsequently, the mixture passes through the capture zone and both unbound analytes and bound analytes bind to the capture antibody. The response in the capture zone (test line) is directly proportional to the amount of analyte in the sample.[49]

2.5.2. Competitive assay

The competitive format is employed most often when testing analytes with low molecular weight or presenting a single antigenic determinant.[50] In a competitive format (Fig. 2.6B), an analyte-protein conjugate (e.g. 8-OHdG-BSA) coated on the test zone of a nitrocellulose membrane captures a labeled anti-analyte monoclonal antibody complex, allowing color particle (e.g. colloidal gold) to concentrate and form a visible line on the test zone. Another specific antibody coated on the control line allows the capture of the excess antibody complex. One band of color will therefore be visible in the control zone regardless of the presence of target analytes or not, confirming correct test development. Conversely to

sandwich, a negative sample will result to the formation of two band colors visible (test line and control line),[51] and the intensity of the test line is inversely proportional to the amount of analyte in the sample.

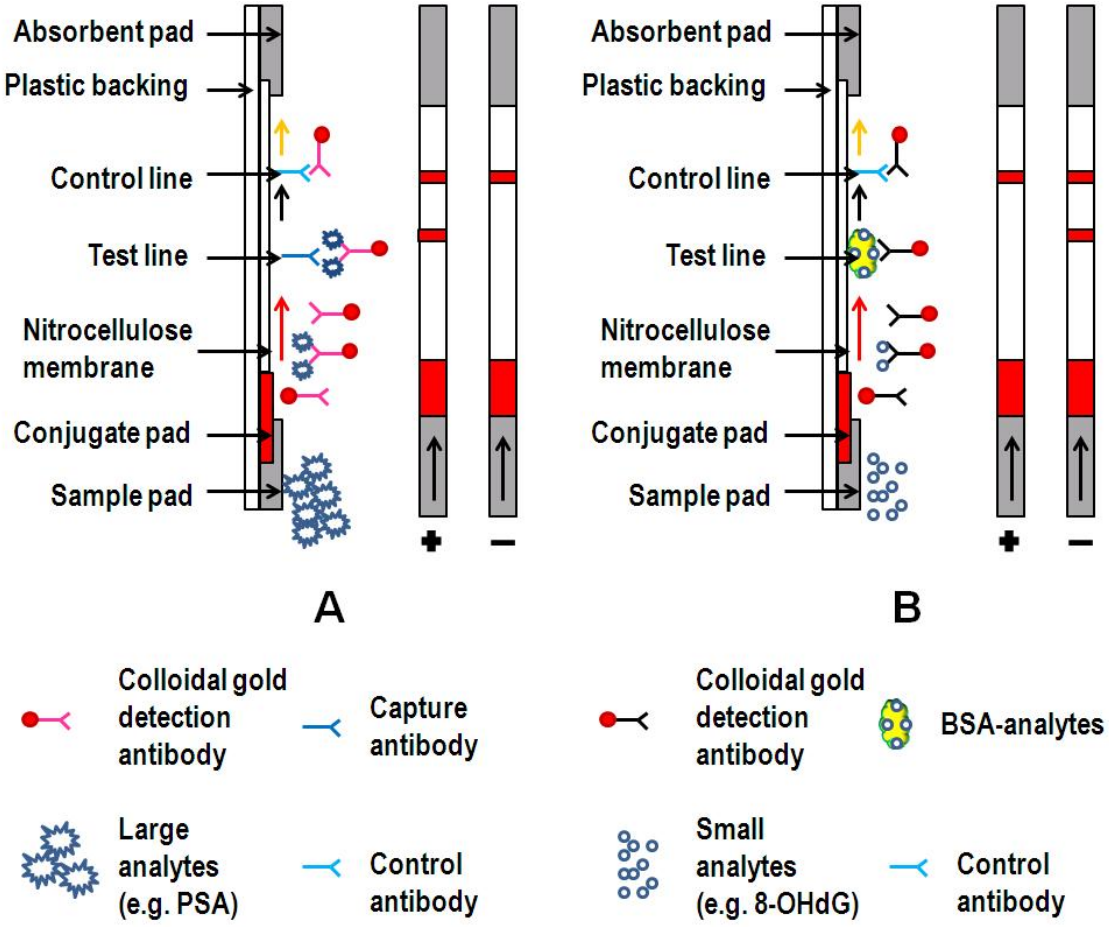

Figure 2.6 Schematic representation of lateral flow tests with sandwich format (A) and competitive format (B). In sandwich format the response on the test line is proportional to the analyte concentration. In contrast, with competitive format the signal response on the test line is inversely proportional to the analyte concentration. (+) = positive; (–) = negative. The lower line is the test line and the upper line is the control line.

Chapter 3. Development of gold nanoparticles based LFS and its applications on the detection of bladder cancer related biomarkers and an oxidative DNA damage biomarker

3.1. Development of LFS for bladder cancer related biomarker detection

3.1.1. Introduction

In the last decade, progresses in technologies have driven a new era in the analysis of both biological agents and chemical contaminants. These analytical techniques have been described and reviewed extensively in the literature.[52-55] Most of them are sensitive and specific, but suffer from being time consuming, laborious and multi-complex. In addition, these technologies are unaffordable to the farmers and some laboratories in the developing countries. Therefore, there is an emergent need to develop highly accurate, rapid and cheap analytical tools. To achieve this goal, many attempts have been focused on the development of rapid POCT such as LFS. LFS is a well-established diagnostic tool in laboratory and has been continually developed in the last three decades. It has been widely used as in-field and POCT diagnostic tools for monitoring biological warfare agents, infectious diseases and cancer.[35, 37, 40, 42-44, 56-63]

Cancer of the urinary bladder is a common malignancy worldwide.[64, 65] Bladder cancer (BCa) can be classified into two groups based on histopathology and clinical behavior: non-muscle invasive papillary tumors (Ta or T1) (80%) and muscle invasion tumors (20%). Nevertheless, more than 70% of patients with Ta/T1 lesions confined to the mucosa will have recurrence during the first two years. If left untreated these initially non-invasive lesions can progress to being muscle invasive.[66, 67] The recurrence phenomenon of non-invasive bladder tumors makes BCa one of prevalent cancers world-wide and is therefore a great burden to healthcare systems.[68] Gold standard for initial clinical diagnosis and staging of BCa involves cystoscopic examination of the bladder together with cytologic examination for malignant cells in the urine. Cystoscopy is an unpleasant invasive procedure and has certain side effects.

Voided urinary cytology (VUC) remains the method of choice for the non-invasive detection of BCa, but it is complex and lacks of sensitivity and accuracy.

While a number of biomarkers identified for BCa diagnosis may have utility in solid tissue or patients' serum, urine-based assays have obvious advantages for the detection of urological cancers, specifically BCa. Most importantly, urine is available for collection non-invasively. In addition, the ease of the collection of urine ensures patient compliance and allows for copious sample collection and repeat sampling. Based on the previous studies by Dr. Rosser and his colleagues,[67, 69-78] a 14-protein multiplex diagnostic signature has been revealed. 10 of the 14 proteins associated with the diagnostic signature have been validated by ELISA. Thus the development of a non-invasive high-throughput urine-based assay using reliable diagnostic markers would be of tremendous benefit to both patients and the healthcare system.

Dr. Rosser's group has rich experience on validation urine-based bladder cancer biomarkers. By cooperating with Dr. Rosser's group, 3 of 10 well-validated BCa related biomarkers were chosen as representatives for testing the feasibility of our strips in this section. Here we designed and developed a LFS of sandwich format for qualitative analysis of three BCa related biomarkers (Creatinine, Matrix metallopeptidase 9 (MMP-9) and vascular endothelial growth factor (VEGF)) in standard solutions as well as in urine samples from ten patients who potential with bladder cancer. The reliability of the sensor was further investigated by comparing the results to those of commercially available ELISA kits did by Dr. Rosser's group. The strips could provide a potential approach for simple and fast qualitative detection of these three biomarkers in urine samples.

3.1.2. Experimental

3.1.2.1. Materials and Apparatus

Sheep polyclonal to Creatinine antibody (US Biological (Salem, MA)). Rabbit polyclonal secondary antibody to Mouse IgG and Rabbit polyclonal secondary antibody to Sheep IgG (Abcam (Cambridge, MA)). Human Total MMP-9 DuoSet and Human VEGF DuoSet (R&D Systems, Inc. (Minneapolis, MN)). Glass fiber, nitrocellulose membrane, absorbent materials and polyester backing materials (Millipore (Billerica, MA)). Sucrose, Tween® 20 (polyoxyethylene-20-sorbitan monolaurate) and Tris.HCl (1 M) (Fisher Scientific (Fairlawn, NJ)). Creatinine standard solution, Bovine serum albumin (powder), Sodium chloride (NaCl), Sodium phosphate (Na_3PO_4), Gold chloride trihydrate ($HAuCl_4 .3H_2O$) and Potassium carbonate (K_2CO_3) (Sigma-Aldrich (St. Louis, MO)). Triton X-100, Tri-Sodium Citrate Dihydrate, Phosphate buffered saline (PBS, 1X, pH=7.4) and Drying Oven (VWR (West Chester, PA)). Dispenser Linomat 5 was from CAMAG (Wilmington, NC) and Zetasizer was from Malvern Instruments, Woodstock, GA. Canon T1i camara was bought from Canon, JP.

3.1.2.2. Fabrication of LFS

General procedures found in section 2.2.

3.1.2.3. Preparation of standard solution and urine samples

General procedures found in section 2.3.1.

3.1.2.4. Strip assay

General procedures found in section 2.4.

3.1.3. Results and discussion

3.1.3.1. Principle of the cancer biomarkers detection by LFS

The principle of the immuno strip is based on the specific immunoreactions occurring between the antibodies and cancer biomarkers and is illustrated in Figure 3.1. In this section, we choose the sandwich type design (Figure 3.1a) for all three biomarkers, given that the biomarkers described contain multiple antigenic binding sites (section 2.5.1)

As shown in Figure 3.1b, two clear lines on the membrane is a positive result (+). A single line in the control zone is a negative result (-). However, false positive and negative response will be given by the immunostrip in some conditions. For example, the pH of the gold nanoparticle solution and the concentration of the antibody are very important for efficient conjugation. Non-specific binding between the antibodies on the test line and the gold nanoparticles from conjugation pad due to inefficient conjugates will lead to false positive response. In addition, correct antibody pair is another important factor for accurate immunostrip response. After interacting with the antibody in the conjugation pad, the analyte still can be captured by the antibody on the test line through another antigenic site, avoiding the false negative responses. The conditions of the running buffer (i.e. salts, pH) which affect the binding efficiency between the antigen and antibody could also cause false negative response. So optimization of the fabrication condition is very crucial for the accurate immunostrip response.

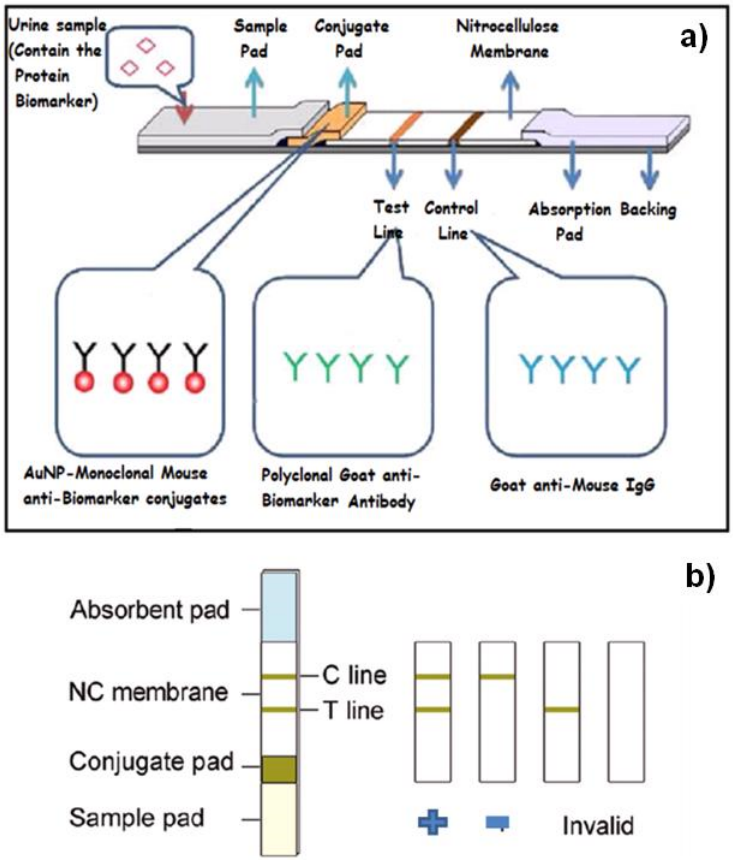

Figure 3.1. (a) Schematic Drawings for the principle of sandwich type lateral flow strips based on gold nanoparticles and (b) the structure of a strip together with the illustrations for testing results.

3.1.3.2. Individual biomarker detection by standard samples (Creatinine/MMP-9/VEGF)

In order to demonstrate the feasibility of the device, first, we used a standard solution of each individual biomarker with high concentration. 100 µL Standard sample with available concentration (Creatinine: 30 µg/mL; MMP-9: 50 ng/mL; VEGF: 120 ng/mL) were applied to the strips separately, and photographs were taken by digital camera after 10 min.

Figure 3.2 shows the typical responses of the strips to the three biomarkers with presented concentrations. As these are intended to be single-use strips, each sample was tested in

triplicate to ensure the repeatability and reliability of the results. From figure 3.2, we can see that there is only one red line (Control line) after applying the blank sample to the strip, containing no biomarker. While, apparently, there are two lines, both test and control lines, appeared by using standard solutions without exception. The results indicate that the device could be used as an analytical platform for individual biomarker detection.

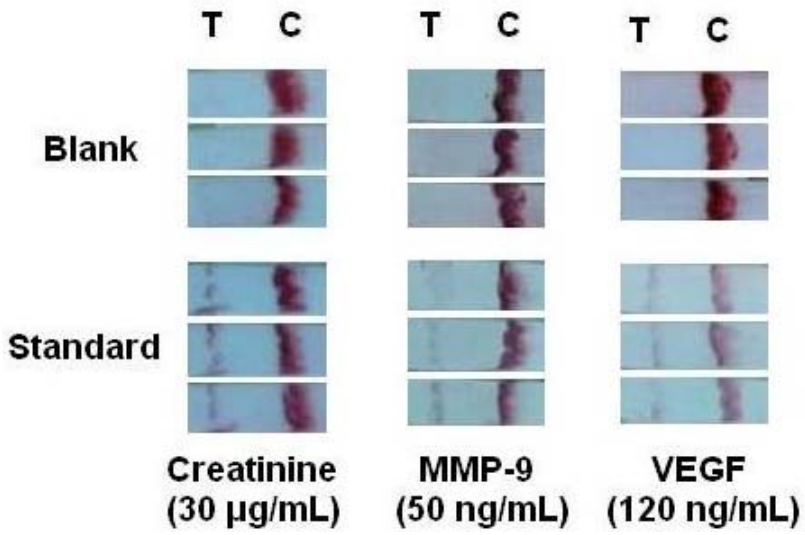

Figure 3.2. Typical responses of the strips to three biomarkers. Top: Blank samples without any biomarker; Below: Standard samples with individual biomarker (Creatinine: 30 µg/mL; MMP-9: 50 ng/mL; VEGF: 120 ng/mL).

3.1.3.3. Individual biomarker detection using urine samples

After confirming the feasibility of the strips for these biomarkers detection, it then can be used for the clinical urine sample testing. 10 urine samples potentially with bladder cancer (No. 0087, 0129, 1057, 1150, 0130, 0054, 0110, 0781-2, 0212, and 0403) obtained from Dr. Rosser's Translational Research Laboratory were applied to the strips following the same method for the standard solution. After 10 min, photographs were taken by using digital

camera. Figure 3.3 displays the representative responses of the strips (three types) to these urine samples. Each individual image was a representative image from the triplicate results.

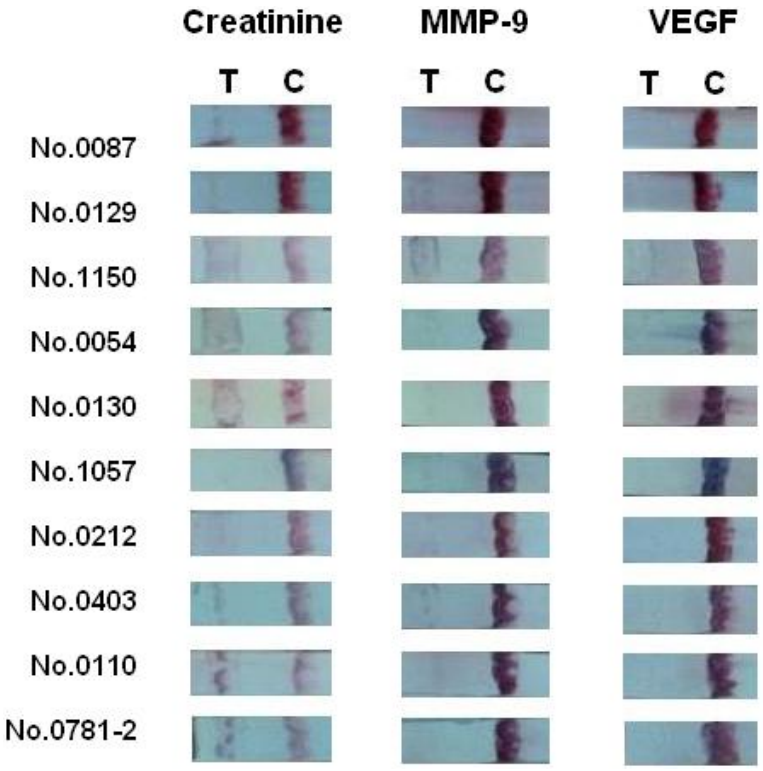

Figure 3.3. Representative results of strips (three types) to 10 clinical urine samples.

As shown in Figure 3.3, some of the strips present only one red line (control line), while, the rest give two lines (both test and control line) in the reaction window. Take No. 0087 as an example, there are two lines in Creatinine strips and one line in both MMP-9 and VEGF strips, indicating that No. 0087 only contains detectable amount of Creatinine. In the same way, we can conclude that No. 1150 contains detectable amounts of all three biomarkers according to our device. Further, follow the same analysis, we marked "+" as the sample contains certain biomarker, while "-" if it doesn't, which are summarized in Table 3.1. Table

3.1 gives a clearer and more straightforward idea of the situation of samples compared with the image.

Table 3.1. Summary of the results of the urine samples with +/-. Positive (+) represents that the sample contains certain biomarker, while negative (-) represents that the sample doesn't contain this biomarker.

Sample	Biomarkers		
	Creatinine	MMP-9	VEGF
Blank	–	–	–
Standard	+	+	+
No.87	+	–	–
No.129	+	+	–
No.1150	+	+	+
No.0054	+	–	–
No.0130	+	–	–
No.1057	–	+	–
No.0212	+	–	–
No.0403	+	+	–
No.0110	+	–	–
No.0781-2	+	–	–

Table 3.1 also gives combination result of the multiplex biomarkers to some extent. The level of only a single biomarker in any biological samples may not be able to provide a reliable

diagnostic conclusion. The ability to detect and quantify several biomarkers simultaneously in the same sample via a semi-robust multiplexed assay will reduce the assay costs and improve efficiency. A concept graph is illustrated in Figure 3.4. In addition to BCa diagnosis, comprehensive tests for the levels of multiplex biomarkers will also help us to better understand the underlying physiology of BCa and to monitor the BCa treatment progress.

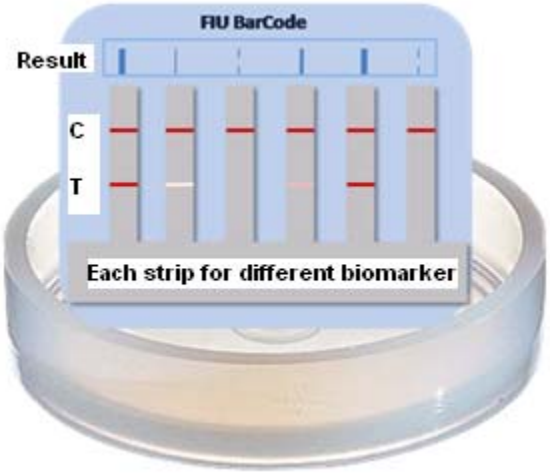

Figure 3.4. Illustration of a BarCode based multiplex detection devices.

In theory, multiple biomarkers could be tested simultaneously on a single test strip simply by pre-coating regions with multiple chemical and/or immunological reactants. However, practically, this approach is hampered by the increased likelihood of misinterpreting results when multiple lines are to be inspected. In addition, the difficulty of fabricating the test strips in which no two lines appreciably overlap will be another major practical concern. At this stage, we tested these biomarkers separately by using a single functional strip. However, we can perform a multiplex analysis by using a format as Table 3.1.

3.1.3.4. Comparison of the results of strips to those of the commercial ELISA kits

The efficacy of the novel strips to accurately detect BCa was further investigated by comparing the results to those obtained from commercial available ELISA kits. These ELISA assays are performed according to manufacturer recommendation. Briefly, standards or urine samples were added in triplicate to 96 well plates directed at a specific biomarker, followed by the addition of biotinylated antibody. The absorbance values were read on a microplate reader (Bio-tek, SynergyTM HT, VT) at a wavelength determined by the manufacturer. The above was repeated for each of the three biomarkers. For each biomarker, a standard curve was prepared using purified standards for each protein assessed. Signal intensities of each biomarker were converted to concentration values by reference to the standard curve.

Previous statistics (Median (min, max)/Mean +/- SD) from urine samples (127 subjects: 64 subjects with BCa and 63 subjects without a BCa) did by Dr. Rosser's group show: 0.9 (0, 1002)/46 +/- 141 ng mL^{-1} for cancer subjects and 0 (0, 14.25)/0.35 +/- 1.81 ng mL^{-1} for healthy subjects (MMP-9); 333 (0, 9814)/835 +/- 1725 pg mL^{-1} for cancer subjects and 0 (0, 904)/66 +/- 194 pg mL^{-1} for healthy subjects (VEGF), giving a general idea of the clinical range of these biomarkers in urine. Based on these statistic data, we defined a value over a certain threshold as positive (+), with which we can transfer the digital value obtained from the ELISA kit into positive (+)/negative (-) style which is similar to Table 1. At the end, we concluded a consistency testing form of the two methods (see Figure 3.5). From Figure 3.5, we can find that the consistency of the results is very high for all three biomarkers (Creatinine: 90%; MMP-9: 80%~100%; VEGF: 90%). The test strip provides a simple, low cost and portable platform for BCa related biomarker detection and could potentially be used as a screening tool for BCa through multiple diagnostic markers in future.

Sample	Biomarkers		
	Creatinine	MMP-9	VEGF
Blank	–	–	–
Standard	+	+	+
No.87	+	–	–
No.129	+	+	–
No.1150	+	+	+
No.0054	+	–	–
No.0130	+	–	–
No.1057	–	+	–
No.0212	+	–	–
No.0403	+	+	–
No.0110	+	–	–
No.0781-2	+	–	–
Consistency	90%	80%~100%	90%

Figure 3.5. Consistency of the results obtained from strips and ELISA. Red circle: data got from ELISA kits is in agreement with LFS (Table 3.1); Blue circle: inconclusive; None: the data obtained from ELISA kits is disagreement with that in Table 3.1.

3.1.4. Conclusions

We demonstrate here a novel POCT device in LFS format that provides a rapid qualitative measurement of three BCa-related biomarkers (Creatinine, MMP-9 and VEGF) in both standard solutions and clinical urine samples for the very first time. The diagnostic signature given by the strips can be further developed into a combination result in the near future. This kind of comprehensive test for the levels of multiplex biomarkers will help us to better understand the underlying physiology of BCa and to monitor the BCa treatment progress in addition to BCa diagnosis. In the end, by comparing the results obtained from the novel strips to those of the commercial ELISA kits, we can conclude that the strips can provide a useful tool for quick and non-invasive BCa diagnostic.

3.2. Development of LFS for an oxidative DNA damage biomarker detection

3.2.1. Introduction

In the previous section, we developed a LFS for colorimetrical detection of three BCa-related biomarkers. The qualitative assay is simple and fast, demonstrating that a feasible and reliable platform of LFS was established for our own applications. Nevertheless, in most cases, quantitative information is still necessary and important for analyzing the concentration of the target. In this section, an image processing program "ImageJ" was used for further quantitative analysis of the colorimetrical results of the LFS. A DNA oxidative damage biomarker, 8-OHdG was used as a model to demonstrate the concept, and the strip can also be used as a useful screening tool for nanotoxicity assessment.

In living cells endogenous reactive oxygen species (ROS) are produced as a result of various physiological processes, metabolic and other biochemical reactions. ROS, at low concentrations can serve as signaling molecules, necessary for the normal cellular activities. However, an increase in the level of ROS from exogenous sources such as ultraviolet or ionizing radiation, cigarette smoking, hazardous chemicals, etc.[79] can lead to an abnormal oxidant system called oxidative stress.[80] In the presence of oxidative stress, ROS generated in vivo can cause extensive oxidative damage to biomolecules. DNA is a particularly important target for oxidation, as damage may lead to heritable alternations. It is well known that the study of oxidative DNA damage is clinically important.[80] Numerous studies have shown that oxidative DNA damage links pathogenically to a variety of aging-associated degenerative diseases such as cancer, coronary heart disease and diabetes.[81]

Among the four constituent bases of DNA, guanine in particular is the most readily oxidized. Upon oxidation, a hydroxyl group is added to the C-8 position of deoxyguanosine in DNA,[82] resulting in the production of 8-hydroxy-2'-deoxyguanosine (8-OHdG), one of the predominant forms of free radical-induced lesions of DNA. 8-OHdG is probably the most studied oxidative DNA damage product due to its relative ease of measurement and pre-mutagenic potential.[83-86] Evidence shows that 8-OHdG can give rise to G-to-T transversion mutations in key genes known to be involved in the development of cancer,[87] so, elevated 8-OHdG levels have been noted in numerous tumors[84, 85] and thus is widely used as a biomarker for oxidative stress and carcinogenesis. [88-90] Urinary 8-OHdG, in particular, has been measured most frequently to indicate the extent of oxidative damage because it is noninvasive and technically less involved.

The traditional methods for 8-OHdG quantitative analysis are high-performance liquid chromatography (HPLC) with electrochemical detection (ECD),[91, 92] gas chromatography-mass spectrometry (GC-MS),[93] HPLC tandem mass spectrometry,[94, 95] and Enzyme-linked Immunosorbent Assay (ELISA).[96] These methods have been successfully used to analyze 8-OHdG in cell lysates, fluid samples and organs. However, these are lab based techniques requiring costly and cumbersome equipment and trained personal to perform the measurements. Thus, these techniques are of limited use in close proximity to patients. There is a great need for a portable POCT device for use by the mass public for easily available biological samples such as urine, saliva, blood, etc.[97] An ideal POCT device would serve the purpose of rapid and accurate detection of 8-OHdG with a user friendly operation eliminating the need for lab facilities and professionals.[98] This POCT device would provide results in

minutes rather than days or weeks and eliminate the concerns involved with the transport and storage of biological samples.

Significant progress in nanotechnology has had a measurable impact on industrial technology. However, the increased utilization of nanomaterials may negatively affect human health and the environment.[99-101] Oxidative stress is one of the most discussed mechanisms regarding the negative effects of nanomaterials on human health. Many studies[83, 84, 102-109] have shown that some metal oxide nanoparticles can cause ROS generation that leads to oxidative stress and DNA damage in the body. Therefore, characterization and reliable toxicity screening tools are required for new and existing nanomaterials, ensuring their compatibility for medical applications and for the safety of the environment. There are a number of different approaches that can be taken to assess the toxic effects of NPs, which can be categorized into three classes based on their objects of measurement. 1. Cell proliferation/viability assay, which is also called cytotoxicity measurement in other publications, includes Trypan Blue assay,[102, 110-113] Alamar Blue assay,[102, 111, 114] Neutral Red assay,[115, 116] lactate dehydrogenase (LDH) assay,[102, 110, 111, 117-120] Formazan-based assays (MTT, MTS, WST),[102, 110, 111, 115-117, 119, 120] and clonogenic assay.[102, 110, 111] 2. Direct or indirect intracellular ROS measurement, such as lipid peroxidation measurement,[102, 110, 111, 114, 121] glutathione (GSH) assay,[102, 111, 114-116, 119, 122] Electroparamagnetic resonance (EPR) assay,[111, 112] and 2, 7-dichlorofluorescin (DCFH) assay[102, 111-116, 119, 122] 3. Assays on the genomic level, like Comet assay,[102, 110-113, 116, 118, 120, 123] and DNA damage biomarker assay.[110, 112, 124]

In this section, we designed and developed a novel LFS for quantitative 8-OHdG detection for the very first time. The feasibility of the strip was first evaluated by testing 8-OHdG in

standard solutions. Afterwards, the strip was used to measure 8-OHdG concentrations in cell model (rat epithelial cells (CCL-149)) to assess the nanotoxicity (in respect of oxidative stress) of three particles (CuO, TiO_2 and CdO) in vitro on the genomic level. One of the most apparent pathways for NPs caused sickness or organ dysfunction is through prolonged inhalation exposure. Lung function changes have been reported after prolonged inhalation exposure to multiple NPs. Because of this, lung epithelial cells are the most physiologically relevant in vitro model to study nanotoxicity. Rat epithelia cell line has been widely used as a model[110, 125-129] to study nanotoxicity or cellular oxidative stress, therefore, CCL-149 was used as the cell model in this study. At the end, we compared the results obtained from strips to those from Alamar Blue assay and Electrical impedance sensing (EIS) system to demonstrate the reliability of our strips for nanotoxocity assessment. In conclusion, the novel strip we developed can potentially provide a portable sensing system for rapid 8-OHdG measurement in readily available biosamples, which also can be further used as a screening tool for nanotoxicological investigations.

3.2.2. Experimental

3.2.2.1. Materials

PBS (1X, PH=7.4), Triton X-100 and Tri-Sodium Citrate Dihydrate (VWR (West Chester, PA)). Gold chloride trihydrate ($HAuCl_4 \cdot 3H_2O$), Bovine serum albumin (powder), Sodium borohydride ($NaBH_4$), Sodium periodate ($NaIO_4$), Ethylene Glycol, Potassium carbonate (K_2CO_3), Sodium phosphate (Na_3PO_4), Sodium chloride (NaCl), Copper oxide (CuO), Cadmium oxide (CdO) and Titanium dioxide (TiO_2) (Sigma-Aldrich (St. Louis, MO)). Tween® 20 (polyoxyethylene-20-sorbitan monolaurate), Sucrose and Tris–HCl (1 M) (Fisher Scientific (Fairlawn, NJ)). Plastic backing, Nitrocellulose membrane, Absorbing pad and

cellulose paper (Millipore (Billerica, MA)). 8-hydroxy-2-deoxy Guanosine and 8-hydroxy Guanosine (Cayman chemical (Ann Arbor, MI)). Mouse monoclonal antibodies to 8 hydroxyguanosine and polyclonal Goat anti Mouse IgG (Abcam (Cambridge, MA)). Alamar Blue, DMEM, fetal bovine serum, and penicillin–streptomycin (Invitrogen (Merelbeke, Belgium)). Rattus epithelial cells, CCL-149 was from ATCC (Manassas, VA).

3.2.2.2. Equipment

HP Scanjet G3110 Photo Scanner (Hewlett-Packard, Palo Alto, CA). Zetasizer (Malvern Instruments, Woodstock, GA). Drying Oven (VWR (West Chester, PA)). Dispenser Linomat 5 (CAMAG (Wilmington, NC)). ImageJ (http://imagej.nih.gov/ij/download.html) was downloaded from the internet.

3.2.2.3. Fabrication of AuNPs-based competitive LFS

General procedures found in section 2.2.

3.2.2.4. Preparation of standard solution and samples

General procedures found in section 2.3.2

3.2.2.5. Particle source and characterization

TiO_2-NPs (Ø < 25 nm) and CuO-NPs (Ø < 50 nm) were obtained in powder form from Sigma-Aldrich. The dry powder of NPs was suspended in deionized water (1 mg mL^{-1}) and cell culture medium (1 mg mL^{-1}) respectively, and then sonicated using a sonicator bath at room temperature for 20 min (120 V/50-60 HZ) to form a homogeneous suspension. For size measurement, sonicated NPs stock solutions (1 mg mL^{-1}) were then diluted to working

solutions (100 μg mL^{-1}). TEM was used to characterize the size and shape of the NPs. A drop of aqueous NPs suspension was placed onto a carbon-coated copper grid, air-dried and observed with TEM (2000FX, JEOL). DLS was used to determine the hydrodynamic size and zeta potential of the NPs suspension both in the DI water and culture medium.

3.2.2.6. Cell culture and NPs solution preparation

Rat epithelial cells (CCL-149) were obtained from ATCC and cultured in DMEM/F-12 medium supplemented with FBS (10%) and penicillin-streptomycin (5%) at 5% CO_2 and 37 °C. At confluence, cells were harvested using trypsin (0.25%) and sub-cultured into 12-well plates (10^6 cells per well), 24-well plates (5×10^4 cells per well) or EIS chips (6×10^4 cells per well) according to the selection of experiments. Cells were allowed to attach the surface for 24 h prior to NPs treatment, and cells not exposed to NPs served as controls in each experiment. CuO, CdO and TiO_2 NPs were suspended in cell culture medium and diluted to the same concentration (100 μg mL^{-1}). The appropriate dilutions of NPs were then sonicated using a sonicator bath at room temperature for 20 min (120 V/50-60 HZ) to avoid NPs agglomeration prior to administration to the cells.

3.2.2.7. Assays on nanoparticles-induced toxicity assessment in cells

3.2.2.7.1. Cellular oxidative stress assessment from 8-OHdG concentrations by strips

Cells were seeded in 12-well plates with 10^6 cells per well. After 24 h of cell attachment, prepared NPs solutions were added to the corresponding wells with a final concentration of 100 μg mL^{-1}. In order to investigate the overall oxidative stress induced by NPs in cells, concentrations of 8-OhdG both in the cell culture medium and within the cells after NPs exposure (12 h) were tested by the LFS. First, the cell culture medium of different

experimental groups were collected at the end of exposure time (12 h) by pipets and put in tubes. After centrifugation (2900 rpm or 1000 xg, 5 min), the supernants were collected and marked as “cell culture media sample” for following strip test. Second, the cells left in the wells and pellets in the tubes after previous centriguation were resuspended and lysed by cell lysis buffer containing Tris (20 mM, pH=8.0), NaCl (137 mM), Triton X-100 (1%), Glycerol (10%) and EDTA (5 mM). The cell lysates were obtained by collecting the supernant of the mixture after centrifugation (2900 rpm or 1000 xg, 5 min) and marked as “cell lysates sample” for following strip test. Strip test procedures performed as outlined in section 2.4.

3.2.2.7.2. Alamar Blue assay

Cells were seeded in 24-well plates with 5×10^4 cells per well. One day later (24 h) and at time point 0, medium or medium containing NPs (100 μg mL^{-1}, final) were added on top of cells. Since incubation of Alamar Blue takes 6 hours, the reagent of 10 % sample volume was added at time point -6, 0, and 6 hours. Thus measurement of net absorbance at 570 nm was carried at time point 0, 6, and 12 hours. All data points were subtracted by reference number which came from the reading of the mixture of medium and Alamar Blue only, and then normalized to the average of triplicates at time point 0.

3.2.2.7.3. Cytotoxicity assay by Electrical Impedance Sensing (EIS) System

Cell suspension (0.6 mL, 6×10^4 cells) was applied into each well in the EIS chip for the experiments. After 24 h of cell attachment, prepared NPs solutions (100 μL) were added to the corresponding wells with a final concentration of 100 μg mL^{-1}. The resistance changes produced by the attachment of cells to the electrodes were monitored over a 36 h time period (both before and after NPs addition). The EIS chip design was previously reported. [125] In

short, as cells are placed in each well of the chip, they settle down onto the electrode surface creating a barrier for the flowing current increasing the resistance measurements. Thus, it is possible to monitor the cell attachment and proliferation from the change in resistance measurements.

3.2.3. Results and discussion

3.2.3.1. Principle of 8-OHdG detection by LFS

The principle of the immuno strip based on the specific immunoreactions occurring between the antibodies and the DNA damage biomarker (8-OHdG) is illustrated in Figure 3.6. Competitive format was chosen in this section for 8-OHdG testing, as this small molecule contains a single antigenic binding site, which cannot bind to two antibodies simultaneously (2.5.2).

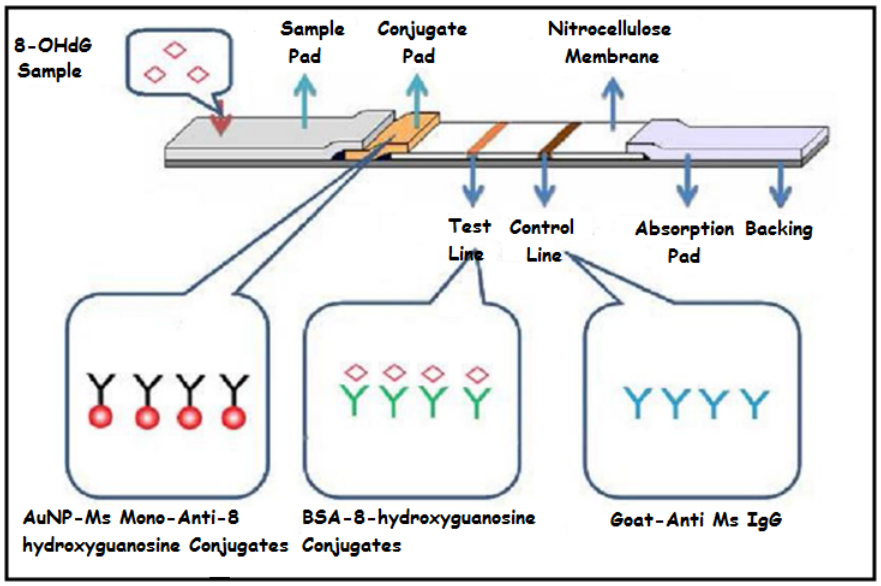

Figure 3.6 Mechanism of competitive LFS for 8-OHdG testing

3.2.3.2. Quantitative analysis by using Software ImageJ

A series of 8-OHdG standard solutions with concentrations of 0, 0.1, 1, 10, 50, 100, 500, 1000, 10,000 and 100,000 ng mL^{-1} in 1X PBS buffer were prepared and applied to the strips. After 10 min, photographs were taken by using a digital camera, then software ImageJ[130] was used for the quantitative analysis.

Figure 3.7 shows the typical responses of the test strip to 8-OHdG with increasing concentrations from 0 to 100,000 ng mL^{-1} dissolved in 1X PBS. The color intensity of the test line deceased when the sample concentration increased in general, which was consistent with the theory of detection of competitive format. The visual detection limit is defined herein as the minimum target analyte concentration required by the test line (T-line) for showing no obvious staining effect. Following this definition, the visual detection limit achieved by the standard sample is above 1000 ng mL^{-1}. The visual detection range is from 0 to 10,000 ng mL^{-1}.

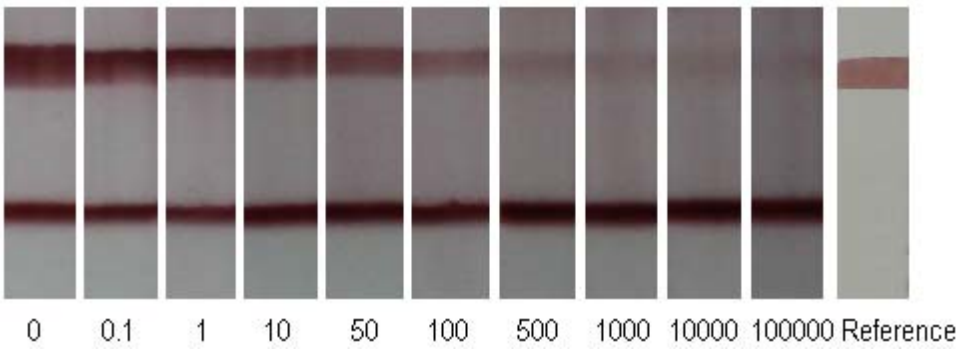

Figure 3.7. Typical responses of the competitive AuNPs based test strips to different concentrations of 8-OHdG; Top line: Test-line; Bottom line: Control-line. The concentration unit for those shown on the bottom is ng mL^{-1}.

In order to quantitatively extract the detection limit and detection range of this method, the test strips were further subjected to optical density analysis. The signals from both the T-line averaged from three parallel runs, and one from red color tape (reference) were digitized to optical density using software of ImageJ and expressed by the integral area of the cross-section of the T-line (areaT) and reference-line (areaR) within a fixed peak width. In order to eliminate the influence of artificial effects caused by camera (i.e. lighting, distance, etc.), a relative optical density (ROD) defined as areaT/areaR was used in the signal analysis. The optical density profiles of both the T-line and C-line recorded under different analyte concentrations are shown in Figure 3.8 with the optical densities of the T-line and C-line being normalized with respect to that of baseline. The optical intensity of the T-line quite obviously increased with the decrease of the analyte concentration. The discrimination of intensities is more intuitive compared to the photograph.

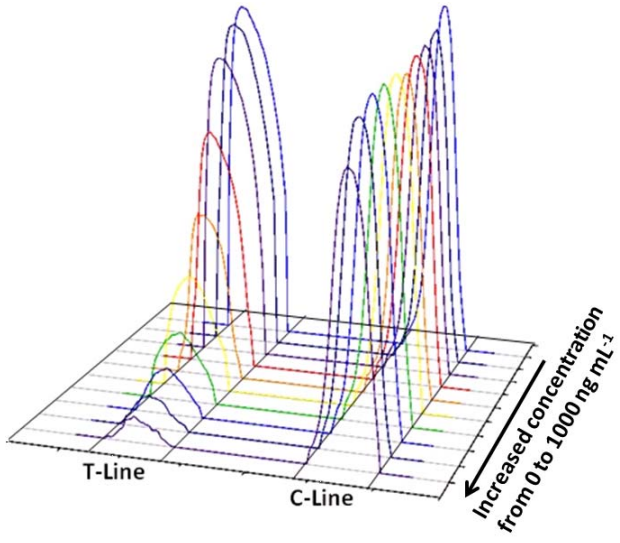

Figure 3.8. Optical density profiles of the T-line and C-line recorded by using software ImageJ and Sigmaplot after running a series of standard solutions with different 8-OHdG concentrations dissolved in 1X PBS.

After optical density analysis, we can get a representative calibration curve of 8-OHdG as shown in Figure 3.9. A normalized intensity (NI) defined as ROD/ABD (average blank density) of the T-line was used as the y-axis, concentration of 8-OHdG was used as the x-axis. As these are intended to be single-use strips, each data point represents the average response from three strips and the error bars represent the standard deviation. With the definition of the detection limit as the minimum concentration of analyte required for inducing a 10% NI decrease, it was determined as 0.9 ng mL^{-1} for standard sample.

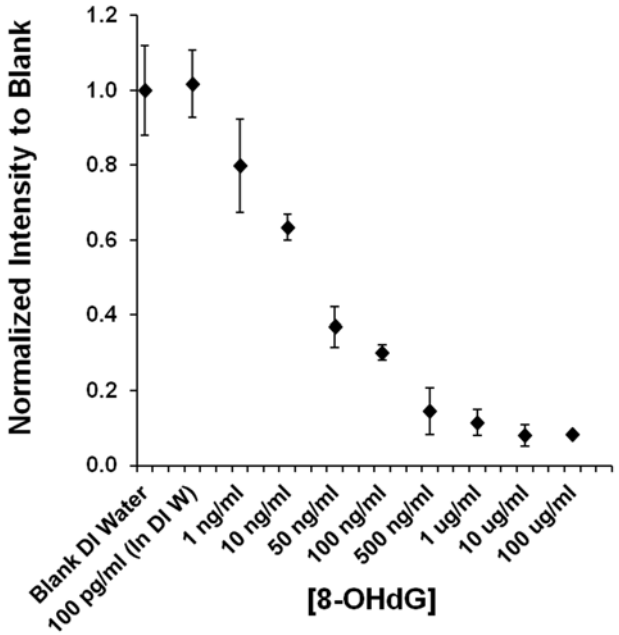

Figure 3.9 Dose-response curves for 8-OHdG based on optical density analysis using standard samples. Values are mean ± SD from three independent experiments.

3.2.3.3. Nanomaterials induce oxidative stress assessment in cells

3.2.3.3.1. Characterization of toxic NPs

The primary sizes of the NPs were determined using Transmission electron microscopy (TEM). As shown in Figure 3.10, the size of nano-TiO_2 was about 20 ± 5 nm (a). The nano-

CuO had the size of about 50 nm (b). The size was consistent with the data specified by the manufacturer.

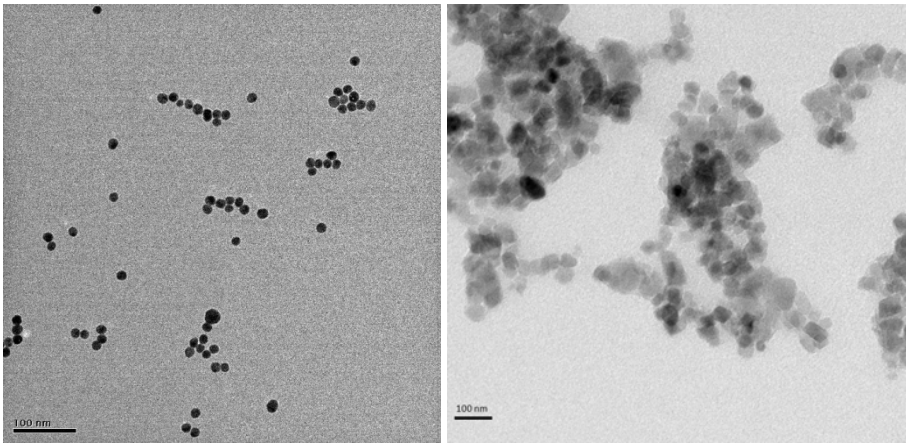

Figure 3.10 Size of NPs observed by TEM. (a) Left: the size of TiO_2-NPs was about 20 ± 5 nm and bar scale is 100 nm and (b) Right: the size of CuO-NPs was about 50 nm and bar scale is 100 nm.

Furthermore, dynamic light scattering (DLS) technique was used to characterize the behavior of the NPs, and the hydrodynamic sizes and surface charges were measured using a Zetasizer in a biological environment (i.e., DMEM cell culture medium). The NPs were suspended in deionized water or DMEM for analysis of their agglomerate sizes and zeta potential. Zeta potential measurements revealed that TiO_2-NP had the surface charge ranging from -10.5 ± 0.6 mV (n = 3) (in medium) to -15 ± 1.1 mV (n = 3) (in water), and the average particle hydrodynamic diameter ranged from 574 nm (PDI = 0.551) (in medium) to 1510 nm (PDI = 0.492) (in water). CuO-NPs demonstrated mean agglomerate sizes ranging from 338 (PDI = 0.346) (in medium) to 1350 nm (PDI = 0.312) (in water), and the surface charge ranged from -12.5 ± 0.5 mV (n = 3) (in medium) to -6 mV ± 0.2 (n = 3) (in water). These differences in zeta potential of TiO_2 and CuO-NPs can influence particle uptake as well as toxicological

parameters like ROS generation and genomic damage. Particle size observed by DLS did not coincide with the results obtained from the TEM. The larger size of the NPs in the hydrodynamic state compared to the size obtained by the TEM might be due to the tendency of the NPs to aggregate in aqueous state. This finding is supported by other investigators.[119, 131, 132]

The three metal oxides used in this study are relevant NPs types and are in widespread use in a number of consumer products. CuO NPs are utilized in various applications such as industrial catalysts, semiconductor devices, antimicrobial preparations, heat transfer fluids, and cosmetics.[114, 133-135] TiO_2 NPs have excellent optical performance and electrical properties and are produced for applications in paints and coatings and also in cosmetics as UV-absorbers. CdO can be used in batteries, electroplating baths, pigments, plastics, catalyst, ceramic glazes, synthetic products, and a variety of other materials.[136] Nevertheless, many studies[112-116, 119-121, 137] have demonstrated that these metal oxide NPs can induce cytotoxicity and DNA damage. Thus, they have been selected here as models for nanotoxicity assessment.

3.2.3.3.2. Effects of NPs on 8-OHdG level as a biomarker of oxidative stress in cells

A series of 8-OHdG solutions with concentrations of 0, 1, 10, 20, 40 and 80 ng mL^{-1}, both in cell lysis buffer and cell culture medium (DMEM), were prepared and applied to the strips. “Cell lysates sample” and “cell culture media sample” obtained in section 3.2.2.7.1 were also applied to the strips. After 10 min, photographs were taken by using a photo scanner **(**Figure 3.11), and then software ImageJ was used for the quantitative analysis. Figure 3.11 (a) and (c) show that the optical intensity decreased obviously when the concentration of 8-OHdG increased, both in the cell lysis buffer and in the cell culture medium, which is still consistent

with the mechanism of the competitive format and can be used as a calibration standard. Figure 3.11 (b) and (d) demonstrate the results by using different NPs, in which the color intensities of all the three experimental groups (NPs) are slightly lighter compared to the control indicating that these metallic NPs can lead to more 8-OHdG generation. Among the three experimental groups, CuO NPs seemed to cause most oxidative damage in cells with highest 8-OHdG generation in both the cell lysate and the cell culture medium.

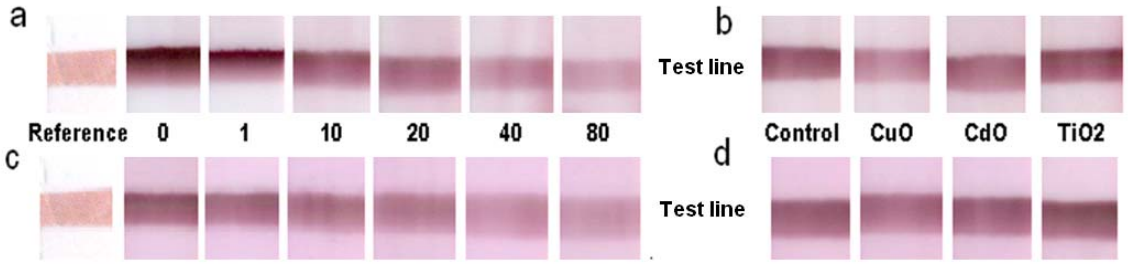

Figure 3.11 The photographs of test line based on 8-OHdG samples dissolved in cell lysis buffer (a) and cell culture medium (c); the photographs of test line based on cell lysate (b) and culture medium (d) after cells were treated with NPs solutions. The concentration unit for those shown in the middle is ng mL^{-1}.

Figure 3.12 illustrates the linear fitting curves for 8-OHdG both in the cell lysis buffer (a) and the cell culture media (b) with correlation coefficients of 0.957 and 0.9632, respectively. 8-OHdG concentrations in the three experimental groups can be estimated by these two curves (n = 6) presented in Figure 3.13. The CuO groups, both in the cell lysate (a) and the cell culture medium (b), have the highest 8-OHdG concentrations (23.24 ± 2.65 and 13.78 ± 1.04 ng mL^{-1}, respectively), followed by the CdO groups (12.35 ± 1.42 and 8.43 ± 0.68 ng mL^{-1}, respectively). While TiO_2 (1.76 ± 0.19 and 2.86 ± 0.14 ng mL^{-1}, respectively) shows no toxicity effect on oxidative stress in cells with similar 8-OHdG concentrations compared to the control (2.17 ± 0.15 and 2.56 ± 0.18 ng mL^{-1}, respectively).

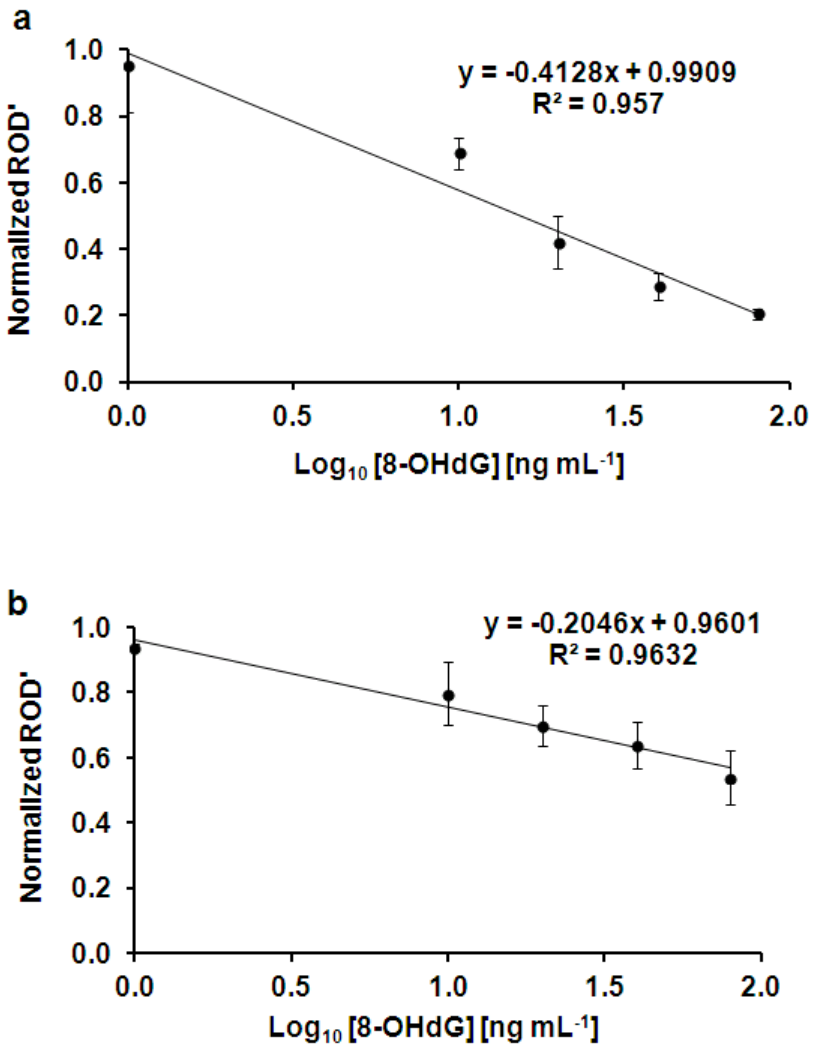

Figure 3.12 Calibration curves for 8-OHdG both in cell lysis buffer (a) and cell culture media (b). Values are mean ± SD from three independent experiments. ROD': ROD (relative optical density)/ ABD (average blank density)).

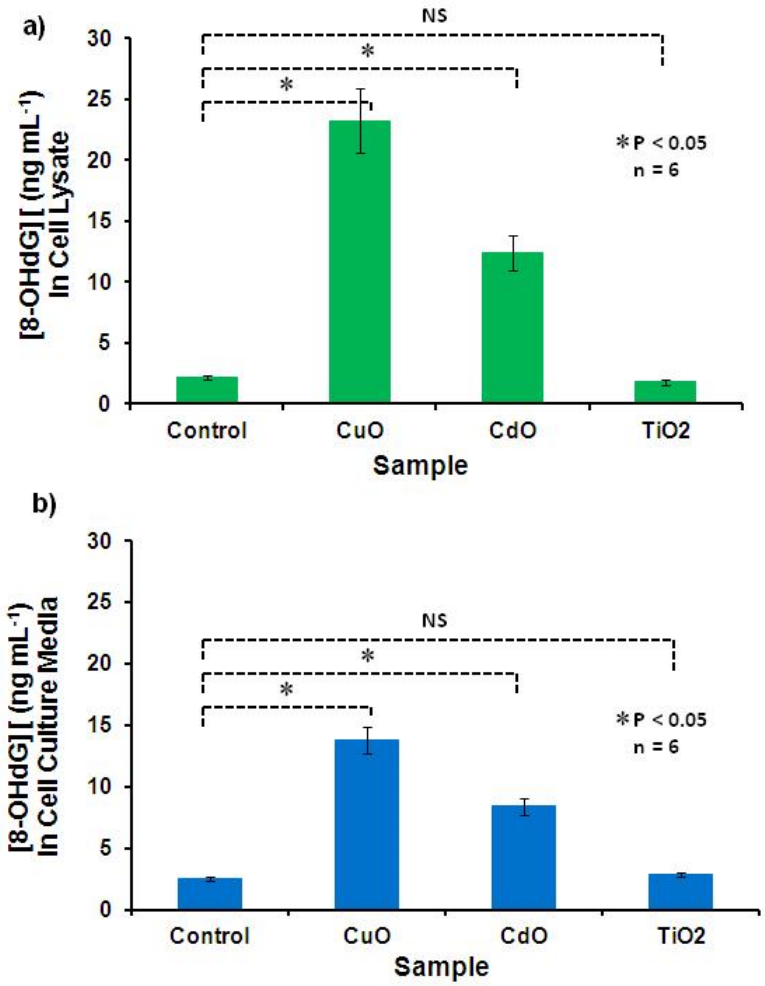

Figure 3.13 Estimated 8-OHdG concentrations in cell lysate (a) and in cell culture media (b) after cell were exposed to different NPs solutions.

3.2.3.3.3. Cytotoxicity study of NPs by Alamar Blue assay

Although nanotoxicity of these three particles choosen have been studied individually or in combination, we still need to characterize their toxic effects simultaneously in our rat epithelial cell model by a well established method, which can serve as the reference for our newly developed detection method. Thus, Alamar Blue assay in a time course manner was carried out with or without the presence of NPs (Figure 3.14) in this section to validate the results of strips obtained in the previous section . At time point 0 h while NPs were absent in

the medium during the Alamar Blue incubation phase, four groups exhibited nearly no difference in cell metabolic activity. At the range from 0 h to 12 h, control (no NPs) and TiO_2 showed normal cell growth and increased total metabolic activity, which was consistent with many other studies stating TiO_2 with a similar size had limited cytotoxicity. Nevertheless, the other NPs CuO and CdO prevented the normal cell growth. Even at the point 6 hours after adding NPs, the total metabolic activity falled by 40% around in both settings.

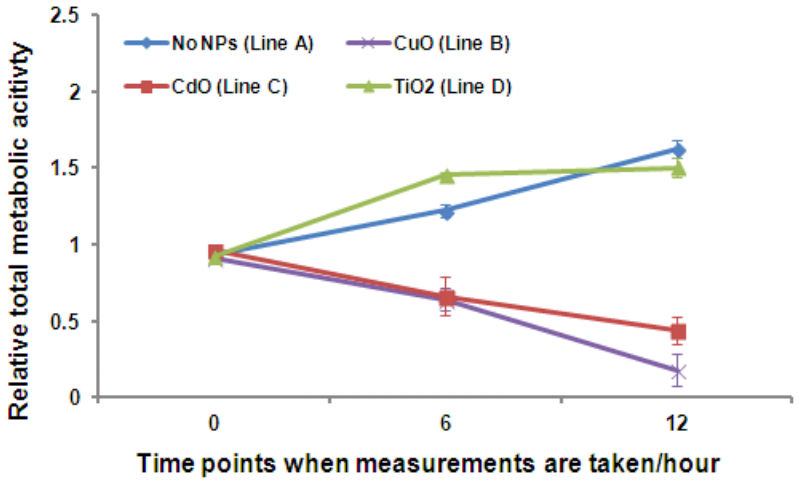

Figure 3.14 Alamar Blue assay for CuO, CdO and TiO_2 on CCL-149 (n = 6). Lines A represent the Cells only (cells with medium only). CuO (line B), CdO (line C) and TiO_2 (line D) are added at the initial time point.

3.2.3.3.4. Cytotoxicity study of NPs by Electrical Impedance Sensing (EIS) system

The whole cell based EIS system, previously published by our lab[125], was also applied to determine the cytotoxiciy of CuO, CdO, and TiO_2 NPs on rat epithelial cells (CCL-149). The EIS system measures the resistance produced by growing cell monolayers over electrodes and can detect changes in resistance that may occur with cell density changes in the cell layer after NPs exposure, and thus provides a kinetic monitor of cell viability. In this section, the

three NPs (CuO, CdO and TiO_2) (100 ug mL^{-1}) were added to the wells after 24 h of cell attachment, and the resistance changes produced by the attachment of cells to the electrodes were monitored over a 36 h time period. This setup would provide the kinetics of the interactions of the NPs with the cells.

Figure 3.15 illustrates the resistance readings for five different settings: Blank (medium only), CuO-24 hrs (CuO, 50 nm, 100 µg mL^{-1}, added after 24 hours of cell attachment), CdO-24 hrs (CdO, 100 µg mL^{-1}, added after 24 hours of cell attachment), TiO_2-24 hrs (TiO_2, 20±5 nm, 100 µg mL^{-1}, added after 24 hours of cell attachment) and a control of cells only (mouse epithelial cells, CCL-149). As shown in Figure 3.15, resistances in all five groups increased within the first 24 h with more and more cells attaching to the surface of electrodes before adding NPs. Nevertheless, upon inoculation of the NPs after 24 h, the trends became extremely different. Once the CuO was added to the cells (Line B), we observed a rapid decrease in the resistance values measured, eventually returning to readings similar to the blank (Line E), indicating cell detachment and the harsh cytotoxic effect of CuO towards the CCL-149, and being consistant with the results onbtained by our strips and Alamar Blue assay. The cytotoxic measurements of TiO_2 NPs towards the CCL-149 (Line D) showed slight difference in resistance values to those observed for the control (Line A). From this observation, it is evident that TiO_2 NPs (25 nm) have fewer cytotoxic effects on the cells compared to the CuO NPs (50 nm) with the same concentration (100 ug mL^{-1}) and similar size, which is also comparable with the results got from our strips and Alamar Blue assay. When cells were exposed to CdO, noticeable changes in resistance (Line C) were observed compared to the control (Line A), which is consistent with the fact that it is extremely toxic and affects the growth mechanism of the cells given by Alamar Blue assay. CdO was used

here as a negative control and employed to demonstrate the ability of the EIS system. Cadmium is a toxic material that has been shown to cause lysosomal damage and DNA breakage in mammalian cells and disrupt mitochondrial function and promote apoptosis.[137] However, the value decreased slowly compared to the CuO NPs (Line B), indicating a slower detachment rate of the cells. The observed phenomena may be attributed to the fact that the smaller NPs (CuO, 50 nm) can enter the cell and damage the cells more easily.

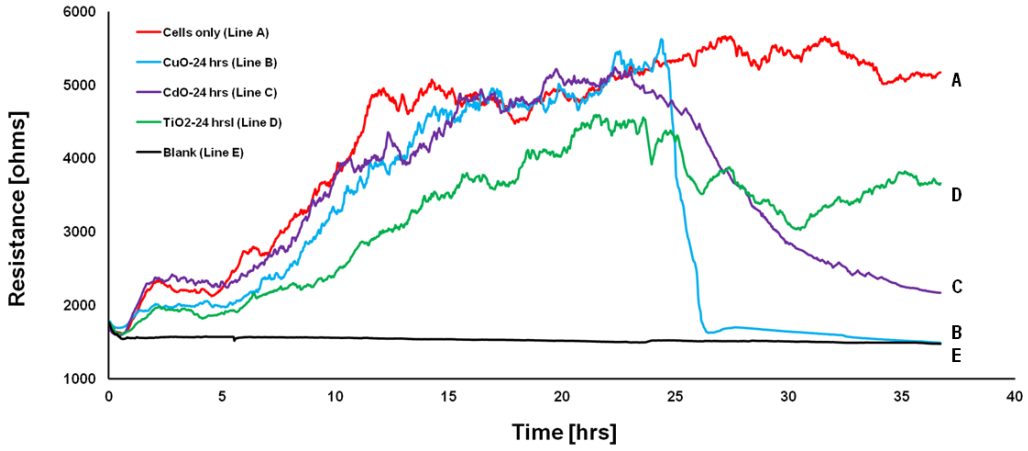

Figure 3.15 Resistance readings for CuO, CdO and TiO_2 on CCL-149. Lines A and E represent the Cells only (cells with medium only) and Blank (medium only) resistance readings. CuO (line B), CdO (line C) and TiO_2 (line D) are added after 24 hours of cell attachment.

Comparing the above sections, we notice that the high toxicity of CuO NPs leads to almost 100% cell detachment within 2 h after NPs addition (Figure 3.15, line B), which could be a response to the DNA damage (illustrated in Figure 3.13, CuO NPs induce the highest 8-OhdG generation in cell) as a way to prevent a mutagenic outcome. It is also possible that DNA damage to some extent is a consequence of cytotoxicity. However, from the present data, it is hard to clarify which process is the driving force. On the other hand, the TiO_2 NPs

cause cytotoxic effects (Figure 3.15, line D), however, without apparent increase in 8-OHdG levels, indicating different mechanisms underlying these effects.

The results show that there was a high variation among different NPs with similar size and concentration regarding their ability to cause cytotoxicity and DNA oxidative lesions. Results from Alamar Blue Assay and EIS system were generally consistent with those from our strips, indicating that the test strip can be served as a simple and low cost alternative method for oxidative stress assessment in cells.

3.2.4. Conclusions

In this work, we successfully designed and presented a novel LFS for an oxidative DNA damage biomarker (8-OHdG) detection. Besides an instant eye-based qualitative detection, a quantitative analysis was also obtained through an image processing program "ImageJ". The detection is quite quick (~10 minutes) and of high sensitivity (as low as 0.9 ng mL^{-1}, which is comparable to that of commercialized ELISA kit). By using the same strip, we further assessed the nanotoxicity of three metal oxides (CuO, TiO_2, CdO) NPs on rat epithelial cells (CCL-149) through measuring 8-OHdG concentrations produced in cells after NPs exposure. Feasibility of this method was validated by the comparison with two other established methods, Alamar Blue assay and EIS system on the level of cell proliferation/viability. In conclusion, the strip can provide a useful platform for quantitative or qualitative 8-OHdG measurement and a high throughput analysis capable in mass screening in nanotoxicological investigations.

Chapter 4. Integrate the electrochemical sensing platform to the LFS for biomarker detection

This chapter was submitted as follows (with slight modifications): X. Zhu, P. Shah, S. Stoff, H. Liu and C. Z. Li, "A paper electrode integrated lateral flow immunosensor for quantitative analysis of oxidative stress induced DNA damage", *Analyst*, 139 (11), 2850 - 2857, 2014.

4.1. Introduction

LFS can provide a low-cost, easy-to-use and portable platform and have been widely used in many areas.[35, 40, 42, 56, 62, 138] In LFS, the primary goal is to visualize colorimetrically the qualitative or semi-quantitative status of the analytes. Readout of the test results is performed optically, either by a machine such as a reflectometer or by the unaided human eye. In the previous chapter, we successfully designed and developed a LFS for semi-quantitative 8-OHdG detection in both standard solution and cell model with the help of an image processing program "ImageJ". However, LFS is known to be more prone to develop false positive (indicates that a person has a specific disease or condition when the person actually does not have it, which would increase the expense because of the reexamination) or false negative result (indicates a person does not have a disease or condition when the person actually does have it, which may miss the best treatment time) if applied to real samples, such as urine and blood, especially patient originated ones. The absorption of antibodies on the surface of AuNPs heavily relies on the hydrophobic and ionic interaction. A "bad" sample with either high ionic strength, high urea concentration or low pH[139] accelerates the dissociation of the antibody-AuNPs complex, leading to false results.

Electrochemical detection is an attractive method due to its capability of quantitative analysis, eases to be miniaturized to be portable, and produces less background. Therefore, in our specific aim 2, we tried to integrate an electrochemical sensing system to the LFS to develop a device which combining the electrochemical detection method with the previous colorimetrical detection method. Many studies have focused on applying electrochemical detection to the traditional POCT analytical devices in order to compensate for the limitations of colorimetric detection. Yang et al.[140] pioneered the use of paper based electrodes

fabricated by sputtering silver directly onto a paper substrate through the development of a disposable Clark-type oxygen sensor. Dungchai et al.[26] demonstrated a paper screen-printed electrode based device for electrochemically quantitative analysis of glucose, lactate and uric acid. Nie et al.[28] followed a similar approach using paper based electrodes to detect heavy metal ions and glucose. These results reveal that the combination of electrochemical detection on paper based devices is a promising route to generate robust and cost efficient quantitative analytical tools.

Most of these researches are based on a fact that the analyte itself can be electrochemically detectable. The DNA oxidative damage biomarker we used in the specific aim 1, 8-OHdG, has redox properties and can be detected by electrochemical method when it undergoing oxidation via a two-electron two-proton charge transfer reaction (Figure 4.1[141]), which has been well characterized for quantitative measurement.[142] Thus, we used 8-OHdG as a representative in this section to evaluate the new developed platform.

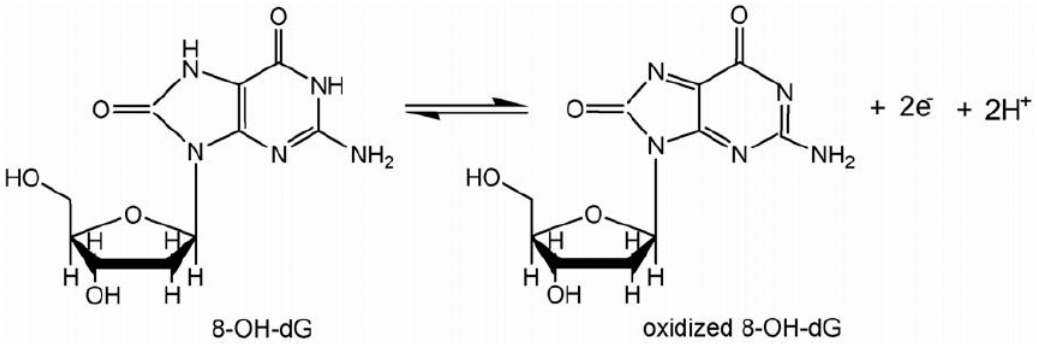

Figure 4.1. Schematic showing electroactive behavior of 8-OHdG.

8-OHdG displays a defined oxidation peak at a potential of 0.42 V (vs. Ag/AgCl reference electrode), which can be detected by Chronoamperometry technique. Chronoamperometry offers a better signal-to-noise ratio than other electrochemical techniques in this type of applications, and the use of a thin slab of fluids mechanically clamped to the electrodes is more resistant to vibration than analysis in a larger volume of solution.[143] The chronoamperometric measurement of current—reflecting charge transfer to/from the redox-active species as a function of time at constant applied voltages—begins with an initially large capacitive current. Upon the decay of the initial capacitive current within 1–2 s, Faradaic current (the current that is proportional to the concentration of the analyte) dominates. The current, i, decays as $t^{-1/2}$ as described by the Cottrell equation.[143] (eqn (1))

$$i = \frac{\mathrm{nFAD}^{1/2}\mathrm{C}}{\pi^{1/2}\mathrm{t}^{1/2}} \qquad (1)$$

where n is the number of electrons, t is the time, F is Faraday's constant, A is the area of the electrode, D is the diffusion coefficient of analytes, and C is the initial concentration of the reactants. The designed paper-based electrochemical device confines fluids in the paper channel, inhibits the convective movement of fluids, and thus facilitates the chronoamperometric measurements by minimizing the disturbances of the stationary boundary layer in the vicinity of electrodes due to vibration, thermal or density-based convection, and other disturbing sources.[28]

As we mentioned previously, 8-OHdG is one of the predominant forms of free radical-induced lesions of DNA. Because oxidative DNA lesions, i.e., oxidized nucleosides and bases, are reasonably water soluble and excreted into the urine without being further metabolized, urinary 8-OHdG is considered an important biomarker of generalized and

cellular oxidative stress.[144] In fact, urinary 8-OHdG levels have been most frequently measured to indicate the extent of oxidative damage, since it is a non-invasive and technically less involved procedure.[145] The major concern with the measurement of 8-OHdG by electrochemical method is the potential interference of 8-OHdG containing short nucleotides. As the products of 8-OHdG are repaired, both 8-OHdG molecule and 8-OHdG containing short nucleotides are present in biological urine samples[145], with 8-OHdG being the major form usually. Existence of 8-OHdG containing short nucleotides will significantly quench the signaling in electrochemical assay set up for 8-OHdG molecule. The occurrence and proportion of 8-OHdG containing short nucleotide is relatively similar in normal biological samples, but might vary appreciably across healthy individuals and patients.

To overcome the drawbacks of strip assay and electrochemical method for 8-OHdG detection, we designed and report here a novel sensing system by integrating carbon nanotubes (CNTs) paper electrodes and immunochromatographic strip (referred to as an electrochemical immunosensor, ECIS) for quantitative analysis of 8-OHdG in both standard solution and urine samples. The sensing device combined competitive AuNPs based immunoassay of lateral-flow format with miniaturized paper electrodes for both colorimetrical and electrochemical detection. On the one hand, electrochemistry does not rely on the conjugation of AuNPs and antibodies, and thus could functions normally when the colorimetric method gives false positive results due to dissociation of AuNPs from antibody. On the other hand, immunostrip assay is able to respond to both the 8-OHdG molecule and the 8-OHdG containing short nucleotides and thus functions normally for biological samples containing high 8-OHdG containing short nucleotides. The optimized system was capable of achieving a detection limit of 2.07 ng mL^{-1} for 8-OHdG while only requiring 10 min to

complete the assay, which is comparable with the commercialized ELISA kit (detection limit is around 0.5 ng mL^{-1}). The normal range of urinary 8-OHdG is given differently by using different methods (10-20 ng mL^{-1} by sophisticated methods (i.e. HPLC-ECD, GC-MS and CE-ECD)[146-149] and 20~60 ng mL^{-1} by ELISA method[81, 150-152]). Based on these data, we can conclude that this novel device can provide a simple and fast tool for quantitative assessment of DNA oxidative stress in urine samples. Furthermore, the integrated platform can be further upgraded and optimized into a wireless-enabled biosensing system in future.

4.2. Experimental

4.2.1. Materials and equipment

Nitrocellulose membrane, glass fibers, absorbent materials and polyester backing materials (Millipore (Billerica, MA)). Buckeye CNT paper (Buckeye Composites NanoTechLabs, Inc. (Kettering, OH)). Silver/Silver Chloride conductive ink (Conductive Compounds, Inc. (Hudson, NH)). Mouse monoclonal antibodies to 8-hydroxyguanosine and polyclonal Goat anti Mouse IgG (Abcam (Cambridge, MA)). 8-hydroxy Guanosine and 8-hydroxy-2-deoxy Guanosine (Cayman chemical (Ann Arbor, MI)). Gold chloride trihydrate ($HAuCl_4 \cdot 3H_2O$), Sodium periodate ($NaIO_4$), Sodium phosphate (Na_3PO_4), Sodium chloride (NaCl), Sodium borohydride ($NaBH_4$), Potassium carbonate (K_2CO_3), Ethylene Glycol and Bovine serum albumin (powder) (Sigma-Aldrich (St. Louis, MO)). Silver conductive adhesive paste, Tri-Sodium Citrate Dihydrate, Triton X-100 and Phosphate buffered saline (PBS, 1X, PH=7.4) (VWR (West Chester, PA)). Tris–HCl (1 M), Tween® 20 (polyoxyethylene-20-sorbitan monolaurate) and Sucrose (Fisher Scientific (Fairlawn, NJ)). Zetasizer was from Malvern Instruments, (Woodstock, GA). Laminator (Office Depot). HP Scanjet G3110 Photo Scanner (Hewlett-Packard (Palo Alto, CA)). Dispenser Linomat 5 (CAMAG (Wilmington, NC)).

Drying Oven (VWR (West Chester, PA)). Cyclic voltammetric (CV) and Chronoamperometric measurements were performed with an electrochemical analyzer CHI 660C (CH Instruments, Austin, TX).

4.2.2. Preparation of the immunochromatographic strip

The LFS specific for 8-OHdG detection were prepared following similar method outlined in section 2.2 with slight modification. The strip consists of four components: sample loading pad, conjugated pad, nitrocellulose membrane, and absorption pad, all of which were pasted onto a plastic backing plate. AuNPs with average diameter 20 nm were synthesized by citrate reduction method (section 2.2.1). Ab-AuNPs conjugates and BSA-8 hydroxyguanosine conjugates were prepared according to the reported protocol in section 2.2.2 and 2.2.4.1. A desired volume (25 μL) of Ab-AuNPs mixture was dispensed by pipette onto a glass fiber pad (6 mm × 5 mm), which was dried at room temperature and stored in desiccators at 4 °C before use. The sample loading pad (6 mm × 16 mm) was made from glass fiber and soaked with a buffer containing 0.15 mM NaCl, 0.05 M Tris-HCl and 0.25% Triton X-100. The pad was dried in an oven for 20 min at 50 °C and stored in desiccators at room temperature. BSA-8 hydroxyguanosine conjugates were used as the test line (T) capture reagent, while goat anti-mouse IgG (1 mg mL^{-1}) was used as the control line (C) capture reagent. These capture reagents were dispensed by the Linomat 5 dispenser at different locations on a nitrocellulose membrane (30mm × 10 cm) as the test and control lines (separation distance is 13 mm). The membrane was mounted onto the adhesive backing plate in advance. The prepared plate (with nitrocellulose membrane and absorption pad) was cut into 6 mm-wide strips using a strip cutter and stored at 4 °C until use. Finally, all of other parts were assembled on the

adhesive backing layer. Each part overlapped 2 mm to ensure solution migration through the strip during the assay.

4.2.3. Fabrication of CNTs conductive paper integrated immunostrip (ECIS)

The structure of ECIS (Figure 4.2a) is similar to that of the traditional LFS. Besides the four required components, two electrodes were integrated into the original strip to carry out the electrochemical detection function. Briefly, CNTs conductive paper (2 mm in width) bought from Buckeye Composites was used as the working electrode. The CNTs paper was placed on the control line with the sensing surface facing down, and its extension beyond the strip was laminated with a silver plated copper wire to be connected to an electrochemical analyzer. Ag/AgCl ink painted copper paper (4 mm in width) was placed at a 1 mm distance from the CNTs paper on the side farthest from the absorption pad to serve as the reference/counter electrode. Finally, the entire strip was laminated (Fig. 4.2b) in order to ensure complete contact between the sample, membrane and electrodes.

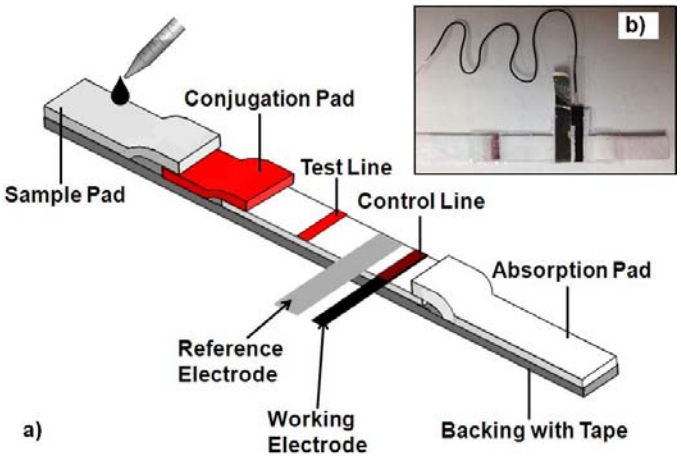

Figure 4.2 (a) A schematic for ECIS; (b) Photograph of a representative ECIS.

4.2.4. Preparation of standard and spiked urine samples

General procedures found in section 2.3.3.

4.2.5. Coupled chronoamperometric and colorimetric measurements of 8-OHdG

Chronoamperometric measurements were performed with an electrochemical analyzer CHI 660C or a portable electrochemical analyzer connected to a personal computer. A fully-integrated ECIS sensor was connected to the analyzer in advance and conductivity of the loop was examined. 100 μL of standard solution or of urine sample solution containing the desired concentration of 8-OHdG was applied to the sample application zone. After waiting for a specified time period (10 min), chronoamperimeric measurements (fixed potential: 0.42 V, sample duration: 20s) were performed by using the software. At the same time, a photograph of the strip was then taken using a digital scanner. The software ImageJ was used to quantify the intensity of test lines for colorimetric analysis.

4.2.6. Quantitative analysis

Current readout from chronoamperimeric measurements and color intensity from colorimetric tests are expressed as the mean ± SD of six experiments. The data were analyzed quantitatively either by using ImageJ and/or Excel software.

4.3. Results and discussion

4.3.1. Material selection for electrochemical sensing system-CNTs Paper

Suitable materials of electrode need to be selected for the electrochemical sensing system. We fabricated several screen-printed electrodes by using different electrode materials and different substrates, such as silver-based electrodes and gold thin-film electrodes. We also

tried various commercialized screen-printed electrodes which are constructed by more advanced nanomaterials including graphene electrodes, gold nanoparticle decorated electrodes and CNTs electrodes. These electrodes have their own advantages and disadvantages in terms of sensitivity, simplicity and cost-effectiveness. However, based on their performances on 8-OHdG detection and the design of the sensor, a flexible electrode which can be easily integrated into the strip and of high electrochemical activity is preferred. CNTs conductive paper, bought from NanoTechLabs, Inc., was finally selected as the electrochemical sensing component as it is flexible as well as has high electrochemical activity. Before using the CNTs conductive paper to create the test strip, we characterized the CNTs paper by using scanning electron microscope (SEM). The surface structure of CNTs conductive paper is shown in Figure 4.3. Instead of the sheet or net structure most often found in CNTs, the figure shows a forest structure which can provide a larger surface area and better sensitivity, both qualities which are suitable for our applications.

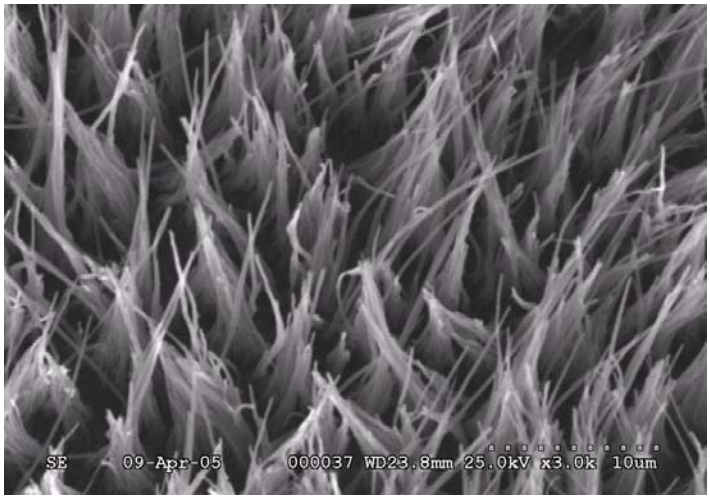

Figure 4.3 SEM characterization of CNTs paper

4.3.2. Principle of the ECIS for 8-OHdG detection

The method of the biosensor is based on two principles: the first principle is that of competitive-type immunoreactions in the LFS as demonstrated in the previous chapter; the second principle is the ability of 8-OHdG to be electrochemically detected when undergoing oxidation via a two-electron two-proton charge transfer reaction (Figure 4.1)

In a typical assay, a sample solution containing a desired concentration of 8-OHdG is applied to the sample application pad (Figure 4.4 (A)). The sample moves along the strip due to capillary force and rehydrates the AuNP-anti-8-OHdG in the conjugation pad. Then the immunoreactions between 8-OHdG and AuNP-anti-8-OHdG conjugates occur and the formed AuNP-anti-8-OHdG-8-OHdG complexes continue to migrate along the strip (Figure 4.4 (B)). When they reach the test zone, the unbound AuNP-anti-8-OHdG conjugates are captured by the BSA-8-hydroxyguanosine conjugates immobilized on the test zone via the same immunoreactions. The accumulation of AuNPs on the test zone induces a characteristic red band which is visible with the naked eye (Figure 4.4 (C)). This color change accomplishes the colorimetric detection of 8-OHdG in a sample and the color intensity is inversely proportional to the concentration. The capillary action causes the liquid sample to migrate further. Once the solution passes through the control zone, the AuNP-anti-8-OHdG Ab-8-OHdG complexes and excess AuNP-anti-8-OHdG conjugates are captured on the control zone by the pre-immobilized polyclonal Goat anti-Mouse IgG, thus forming a second red band showing that the biosensor is operating properly (Figure 4.4 (D)). Chronoamperometric measurement of the control line was performed (exactly 10 min after applying the sample) using electrochemical analyzer providing the data to produce the Current vs. Time curves (Figure 4.4 (E)). Qualitative analysis of the colorimetric test is

simply performed by observing the color change of the test zone, and quantitative analysis is realized by reading the optical intensities of the red bands with a scanner (just after the chronoamperometric measurement). The peak area (Figure 4.4 (F)) is proportional to the amount of the captured Au-NPs in the test zone, which is inversely proportional to the concentration of 8-OHdG in the sample solution.

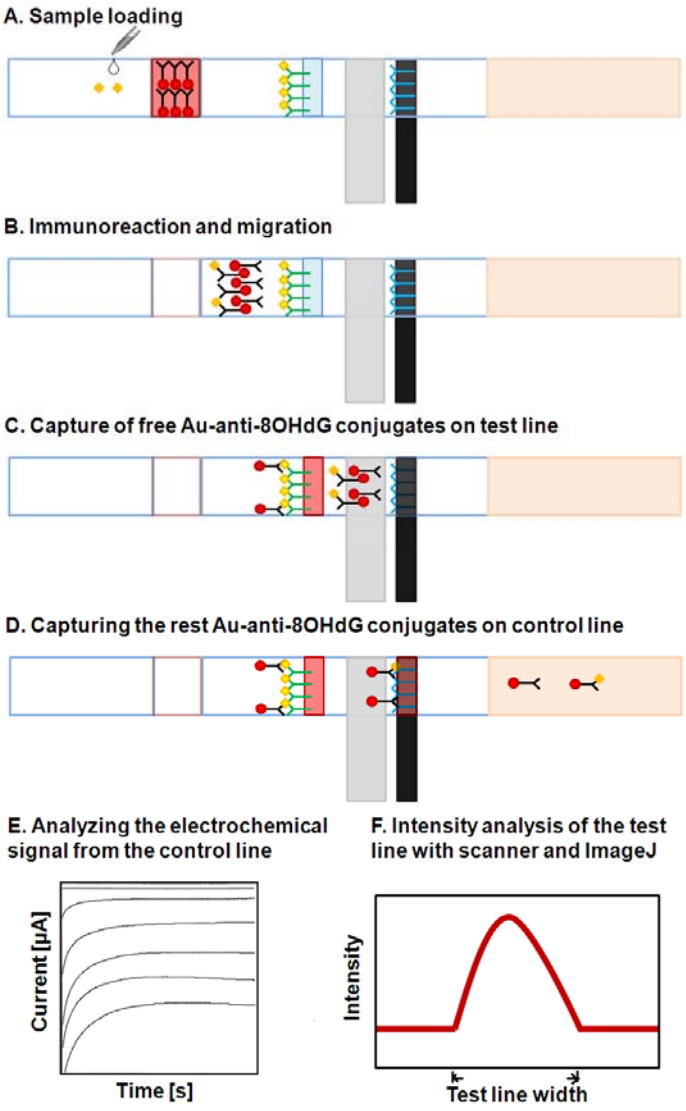

Figure 4.4 Principle of the ECIS for 8-OHdG quantitative detection.

4.3.3. Electrochemical characterization of CNT conductive paper-based electrodes

Before using ECIS devices for analytes measurement, the functionality of the electrodes was established. A potassium ferricyanide/ferrocyanide ($K_3Fe(CN)_6/K_4Fe(CN)_6$) mixture was used as a model redox-active compound to characterize electrochemical behavior of the CNTs conductive paper. 100 mM $K_3Fe(CN)_6/K_4Fe(CN)_6$ stock solution was prepared by dissolving these two chemicals in PBS (1X) buffer, corresponding working solutions can be obtained by altering the dilution. Figure 4.5 shows the cyclic voltammetric response for the compound in the two electrode system at various scan rates. The peak shape of CVs demonstrates a typical reversible electrochemical reaction, indicating that no side reactions take place and the kinetics of electron transfer is sufficiently rapid to maintain the surface concentrations of redox-active species at the values required by the Nernst equation. Next, the dependence of peak current on the square root of the scan rate was studied. The insert in Figure 4.5 shows that anodic and cathodic peak currents were directly proportional to the square root of the scan rate ($v^{1/2}$) between 10 and 200 mV s^{-1}. The linearity indicates that the mass transfer in this system is a diffusion controlled process similar to the behavior of traditional electrochemical cells.

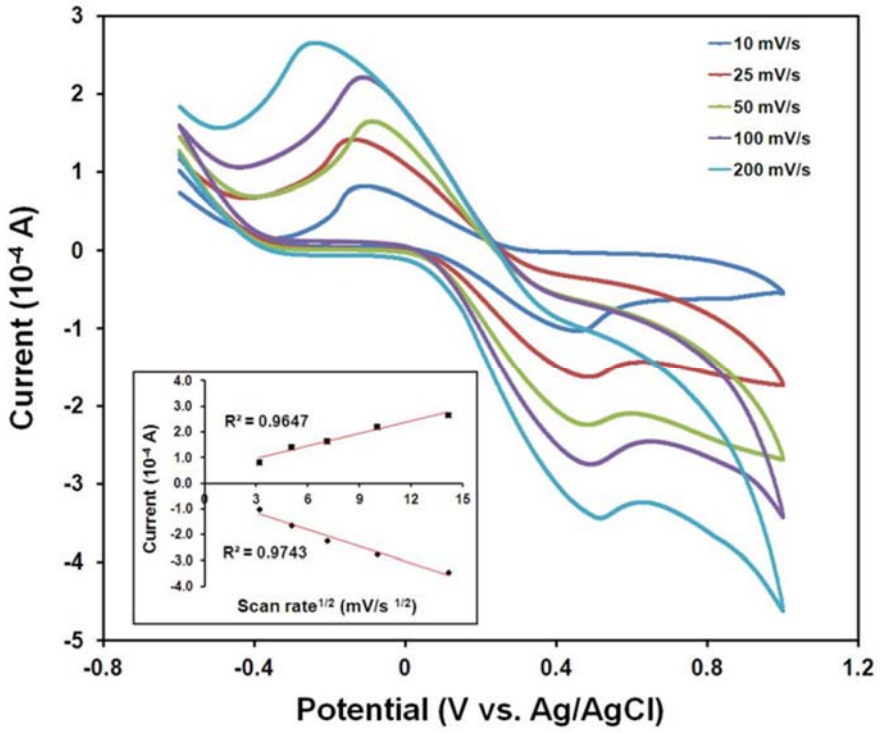

Figure 4.5 Representative cyclic voltammograms of 5.0 mM $K_3Fe(CN)_6/K_4Fe(CN)_6$ solution (pH=7.0) in two electrodes system at various scan rates: 10, 25, 50, 100, and 200 mV s^{-1}. We used a 2 mm by 6 mm CNT conductive paper electrode as the working electrode, and a printed Ag/AgCl electrode as the reference/counter electrode. The relationship between anodic and cathodic currents and the square root of the scan rate is shown in the insert. The red lines represent the linear regression line between $i_{p,ox}$ or $i_{p,re}$ and $(\nu)^{1/2}$, respectively.

4.3.4. Colorimetric measurement of analytes in buffer by ECIS

A series of 8-OHdG standard solutions with concentrations of 0, 1, 10, 20, 50, 80, 100, 150, 200, and 1000 ng mL^{-1} in 1X PBS buffer were prepared and applied to the sample pad. After 10 min, chronoamperometry at the electrodes and color intensity of the test lines were recorded according to the method in the methodology section 4.2.5. The color bar (Figure 4.6a) shows the typical responses on test lines of the strips to 8-OHdG with increasing concentrations from 0 to 1000 ng mL^{-1}. The color intensity deceased when the sample concentration increased which is consistent with the theory of competitive format detection.

The color bar can easily be used as a reference, each color representative of the results for equivalent concentration of the analyte.

Figure 4.6b demonstrates the calibration curve produced by introducing samples of varying concentrations of 8-OHdG into the strips, revealing a logarithmic relationship between the color intensity and the concentration. Normalized intensity defined by average sample density (ASD) / average blank density (ABD) of the test line is used as the y-axis. As these are intended to be single-use test strips, each data point represents the average response from three separate test strips. The error bars represent the standard deviation. Most commercialized ELISA kit can detect urinary 8-OHdG concentration in the range of 0.64 to 200 ng mL^{-1} (i.e. KOG-200SE, Genox). This range was used as a reference for linearity study. The insert for Figure 4.6b shows that a linear response is observed for the concentrations between 1 ng mL^{-1} and 200 ng mL^{-1} (logarithm scale) where the coefficient of determination (R^2) is greater than 0.99. The limit of detection (LOD), calculated based on three times the standard deviation of blank, was found to be 2.07 ng mL^{-1}. The result shows that this strip can potentially be used as a simple, rapid and low cost platform with acceptable detection limit and range for 8-OHdG measurement compared with other traditional methods.

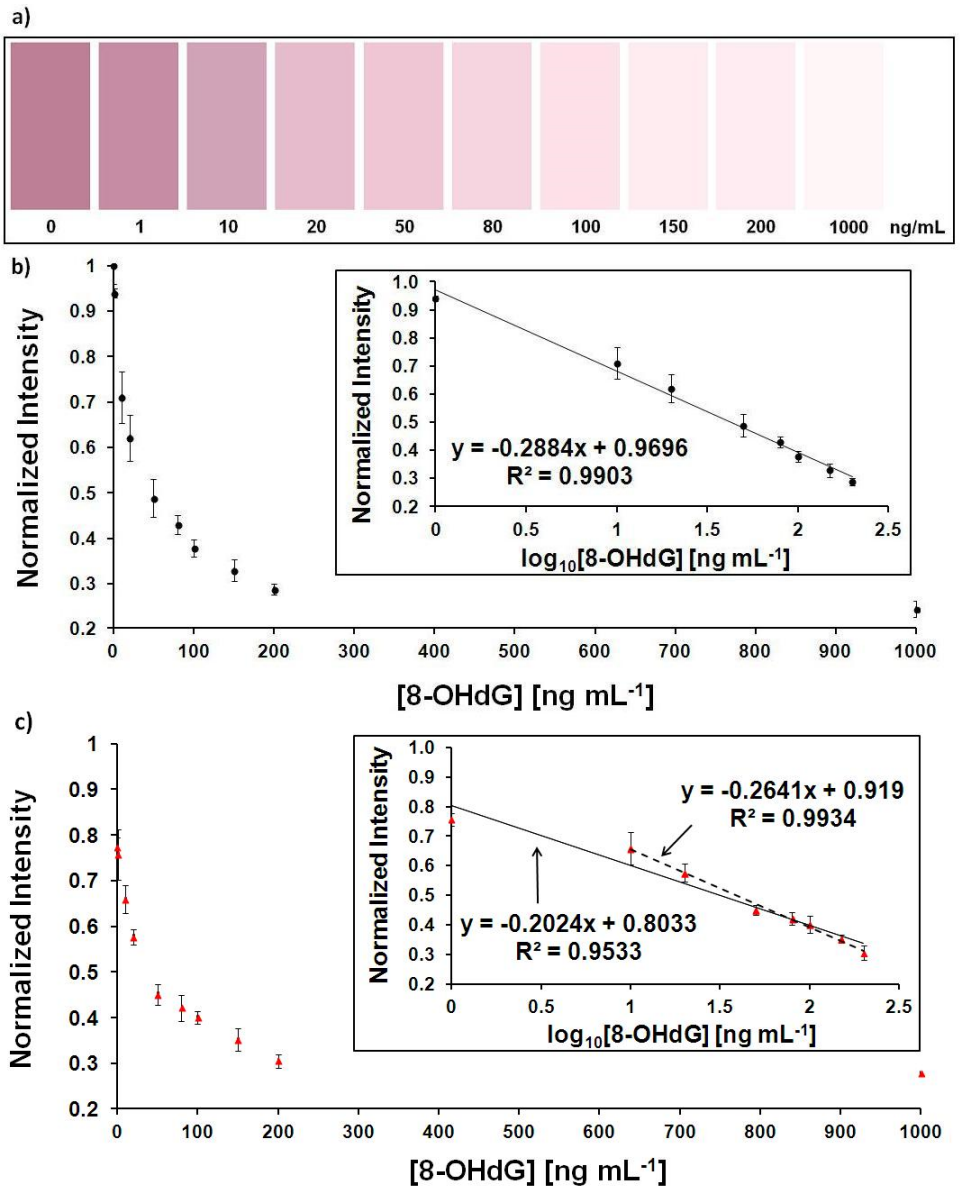

Figure 4.6 (a) Color bar represents 8-OHdG standard solutions with varying concentrations. (b) Dose-response curve for 8-OHdG based on optical density analysis using standard samples. Values are mean ± SD from three independent experiments. The normalized intensity of the test line is plotted against the concentration of 8-OHdG in the logarithm scale as shown in the insert. (c) Dose-response curve for 8-OHdG based on optical density analysis using urine samples. Values are mean ± SD from three independent experiments. The normalized intensity of the test line is plotted against the concentration of 8-OHdG in the logarithm scale as shown in the insert (solid line, 1-200 ng mL^{-1}; dash line, 10-200 ng mL^{-1}).

4.3.5. Colorimetric measurement of analytes in urine samples by ECIS

After confirming the feasibility of this device for standard 8-OHdG solutions measurement, it was evaluated as a tool for urine sample testing. A series of 8-OHdG spiked urine samples with the same concentrations of those in PBS buffer were prepared and applied to the strips.

Figure 4.6c shows the normalized intensity curve rendered from the urine samples spiked with varying 8-OHdG concentrations. As expected, the changing trend of the curve is similar to that of the standard solutions. We also drew two linear fitting curves for the urine samples over the whole and partial concentration range (solid line, 1-200 ng mL^{-1}; dash line, 10-200 ng mL^{-1}), shown in the insert. A linear response is also observed for concentrations between 1 ng mL^{-1} and 200 ng mL^{-1} (logarithm scale) where the coefficient of determination (R^2) is greater than 0.95. The LOD, calculated as previously, was found to be 5.76 ng mL^{-1}, which is still sensitive enough for 8-OHdG measurement in urine samples from both healthy and non-healthy patients (As mentioned previously, healthy human subjects have urinary 8-OHdG levels in the range of 10 to 60 ng mL^{-1}. While the levels go up 2~4 times higher for the non-healthy patients depend on different types of diseases).[146-148, 150, 153-155]

The slope obtained from the whole range fitting (solid line) is significantly bigger than that generated from spiked PBS samples, which maybe is the result of 8-OHdG originally present in the urine samples (2-8 ng mL^{-1} after 1/10 dilution), resulting in a considerable concentration shift for the left end data. For this reason the dash line produces a more accurate fitting with R^2 as high as 0.9934 and slope of -0.2641 which is much closer to that of spiked PBS sample.

Nevertheless, in reality there are various types of bio-molecules in urine which may affect the antigen-antibody interaction and stability of antibody-AuNP complex, leading to lower discrimination among different 8-OHdG concentrations. This presents one possible explanation for the bigger slope in spiked urine samples even after the deletion of first data point when compared to that of PBS. It is worth noting that, this is a universal problem for immunoassays, biological samples from different individuals may interfere with immuno-reactions differently. There are some easy methods that could be used, such as 1/10 dilution for personal testing and molecular size based filtration or centrifugation in laboratory, to minimize these difference in interference. A complete establishment of a marketed immunoassay for a particular molecule still requires the evaluation of different interference of samples from individuals across healthy individuals and patients, which is one of our follow-ups in future works.

4.3.6. Chronoamperometric analysis of 8-OHdG in the ECIS

At the start of our study, we employed numerous electrochemical techniques including cyclic voltammetry, square wave voltammetry, etc. for 8-OHdG measurement in the ECIS system. For most techniques, 8-OHdG can only be detected in high concentrations, making such techniques unsuitable for use in clinical research. Chronoamperometry, which offers a better signal-to-noise ratio than other electrochemical techniques, is able to detect 8-OHdG in lower concentrations. Thus, this method was used as the standard detection approach for the following study.

Prior to chronoamperometric measurement, cyclic voltammetry was used to determine the oxidation potential of 8-OHdG (0.42 V) in the ECIS system with high concentration.

Subsequently, chronoamperometric measurements were performed at a fixed step potential (0.42 V) after applying the 8-OHdG samples (standard or urine) to the strips for 10 min (prior to taking photographs for colorimetric tests). Figure 4.7a shows a representative chronoamperometric response to the measurements of 8-OHdG using ECIS. Over the range of concentrations of 8-OHdG examined (0–150 ng mL^{-1}), all the response curves reached a steady state 2 s after the step potential. Figure 4.7b shows the corresponding calibration curves for the detection of 8-OHdG in both standard and urine solutions (n = 6). When the concentration of 8-OHdG is in the range of 0-150 ng mL^{-1}, the current is linearly proportional to the 8-OHdG concentration with the correlation coefficient of R^2 = 0.99 in standard solutions and that of R^2 = 0.97 in urine samples. From the calibration plot, comparable detection limits (compared to the colorimetric method) of 3.11 ng mL^{-1} in standard solutions and 8.85 ng mL^{-1} in urine samples were calculated, which are still sensitive enough for 8-OHdG measurement in human urine samples.

Both the higher detection limitation and bigger slope in spiked urine samples indicate that background of urine lower the sensitivity of electrochemical detection of 8-OHdG. One reason for this is because the background urine has a completely different ionic environment compared with buffer where electrochemistry will occur quantitatively differently. Another is because 8-OHdG present in the urine samples resulting in a considerable concentration shift for the left end data. As discussed previously, there are some easy methods that could be used to minimize these difference in interference, such as 1/10 dilution of the background urine or using an artificial urine for calibration.

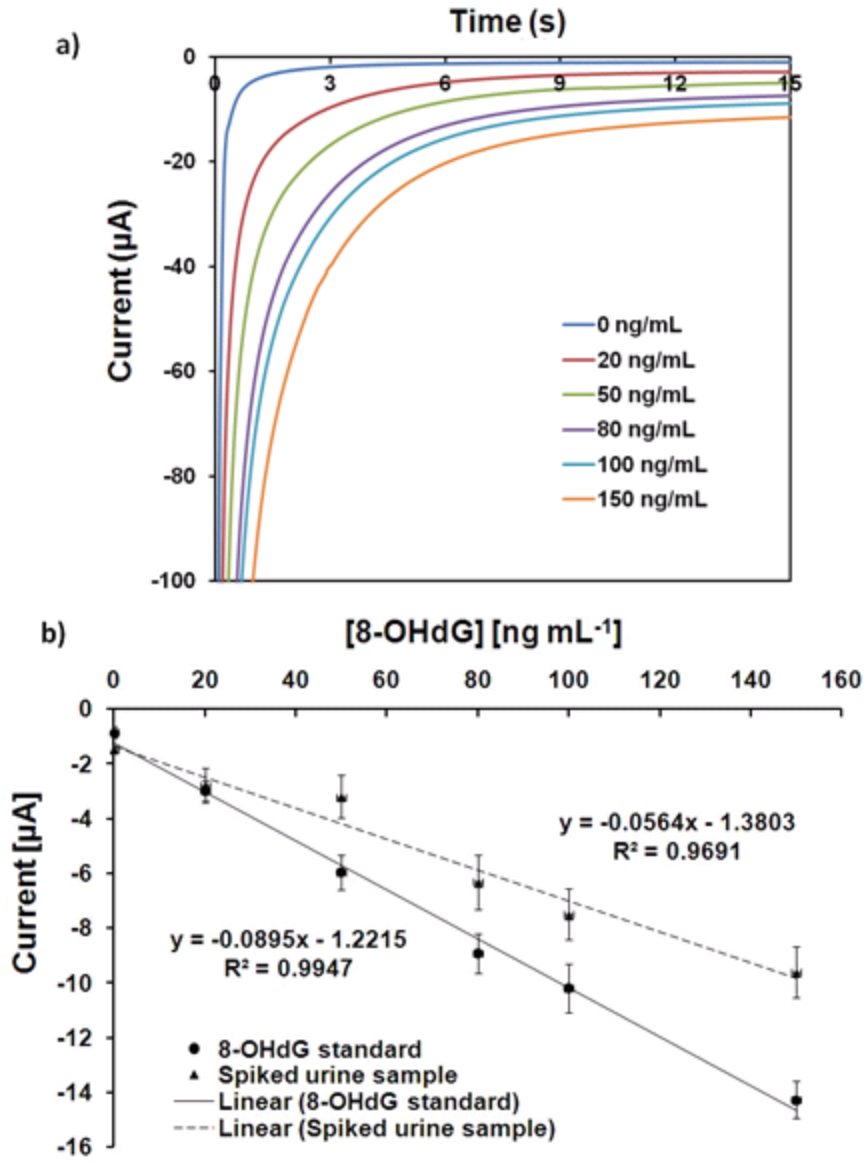

Figure 4.7 (a) Representative chronoamperometric curves for 8-OHdG concentrations (ng mL^{-1}): 0, 20, 50, 80, 100 and 150 in the ECIS; (b) Calibration plots of current as a function of the 8-OHdG concentration for its detection in standard solutions (black circle) and in urine samples (black triangle). We used CNTs conductive paper as the working electrode and silver/silver chloride as the counter/reference electrode, respectively. The working electrode had a surface area of 12 mm^2 in contact with the solution in both standard and urine. The distance between electrodes was 1.0 mm. A 420 mV step potential was used to generate the calibration curve. The solid lines represent a linear fit to standard with regression equation: y = -1.2215 – 0.0895x (R^2 = 0.9947, n=6). The dash line represents a linear fit to urine samples with the regression equation: y = -1.3803-0.0564x (R^2 = 0.9691, n=6).

In a strict sense, our device is not a complete POCT device at this research stage because of sample preparation (dilution) and electrochemical analyzer employment. However, these can be avoid by using artificial urine as the background urine for calibration and applying a portable analyzer which is compacted and can be connected to a wireless electronic device for reading in the near future. Therefore, we provide a protype here for concept demonstration, and optimizations are still needed for complete POCT and commercialization.

4.4. Conclusions

We demonstrate, for the first time, the coupling of CNTs conductive paper based electrochemical detection and traditional LFS based colorimetric detection to provide rapid (~10 min) quantitative measurement of DNA oxidative damage biomarkers (8-OHdG) in both PBS and spiked urine samples, exhibiting the feasibility of using this device in medical diagnosis. The two methods on one single strip are both able to quantitatively detect levels of 8-OHdG concentrations, with detection limitation of 2.07 ng mL^{-1} for colorimetric method and 3.11 ng mL^{-1} for electrochemical method that are low enough for patient testing in the field. Integration of these two detections provides a platform where cross check of 8-OHdG measurement could be achieved. Using this system, testers could get higher confidence on double positive or double negative results. In addition, this system minimizes the chance of false negative or false positive by compensation between these two methods differing in principle. Future efforts will be made to optimize our system to be suitable to be connected to a wireless-enabled electronic system for portable and quantitative assessment of oxidative stress induced DNA damage.

Chapter 5. Integrate a personal glucose meter with the traditional LFS for portable and quantitative detection of biomarkers

5.1. Introduction

We successfully coupled the electrochemical sensing platform to the LFS in the previous chapter. This sensing strategy, which is called ECIS, provides a simple and low cost platform for quantitative biomarker detection with high sensitive and accuracy. As mentioned previously, an important superiority for this platform is that it can be potentially connected to a portable electronic device for quantitative and instant measurements, which is a key perspective for the future POCT development. At the same time, electrochemical detection usually based on a fact that the analyte itself should be electrochemically detectable. Therefore, in this chapter, we tried to test an electrochemical integrated LFS platform by connecting to a portable device. This portable device can detect any analytes with or without electrochemical properties by electrochemical method. PGM is the most popular and accessible portable electronic device on the market and used here to demonstrate the concept of our design. A small molecule, 8-OHdG and a large protein molecule, prostate-specific antigen (PSA) are used as the representative non-glucose targets to test the feasibility of the device.

Prostate cancer (PCa) has become one of the most frequently diagnosed cancers and the third leading cause of cancer morbidity and mortality among males in the United States.[156] Therefore, early and sensitive diagnosis of PCa is needed to initiate therapy to avoid the progression of the disease. It has been shown that serum PSA is the most reliable tumor marker to detect PCa at the early stage and to monitor recurrence of the disease after treatment.[157-160] Currently, most PSA testings take place at dedicated centralized laboratories using large, automated analyzers, requiring sample transportation, increased waiting time and increased administration and medical costs.[161, 162] Near-patient or POCT is highly needed to

reduce the number of clinic visits, decrease costs to the patient and the healthcare system, increase patient satisfaction and improve clinical outcome. Recent advances in biosensor development based on nanomaterials and nanostructures as integral components have brought POCT for PSA closer to reality.

In recent years, much effort has been devoted toward developing POCT devices.[13, 24, 163-169] Among them, paper-based POCT devices is a special category due to the advantages of being simple, rapid, on-site, and cost-effective; they have been widely used in home healthcare and medical testing,[56, 61, 138] even environmental monitoring.[39, 40, 170] LFS is one of the simplest and most popular formats of paper-based POCT devices, and can be used to detect specific substances including small molecules,[40, 60, 171, 172] large proteins[15, 58, 173] and even whole pathogens,[138] in a sample by using an immunological reaction. However, most of these tests are based on qualitative colorimetry, which is not sufficient in many cases. To overcome this limitation, a number of devices capable of quantitative analysis have been developed.

As we know, medical devices for POCT are very costly to develop and manufacture, and are difficult to commercialize. As a result, few have been successfully commercialized. The PGM is one of the most successfully commercialized diagnostic devices on the market,[174, 175] and it has been widely used by millions of diabetes patients to monitor their blood glucose levels every day because of its low cost, compact size, simple operation and reliable quantitative results.[163] The recent successful launch of FDA-approved smartphone-enabled PGMs which enable the wireless transmission of reminders, test results, and data analysis through smartphone apps will attract even larger number of users.[176]

Most glucometers today use an electrochemical method (Figure 5.1). Test strips contain a capillary that sucks up a reproducible amount of blood. The glucose in the blood reacts with an enzyme electrode containing glucose oxidase (or dehydrogenase). The enzyme is reoxidized with an excess of a mediator reagent, such as a ferricyanide ion (a ferrocene derivative or osmium bipyridyl complex). The mediator in turn is deoxidized by reaction at the electrode, which generates an electrical current. The total charge passing through the electrode is proportional to the amount of glucose in the blood that has reacted with the enzyme. From this detection mechanism, we can conclude that the glucose meter is capable of detecting glucose as the unique target.

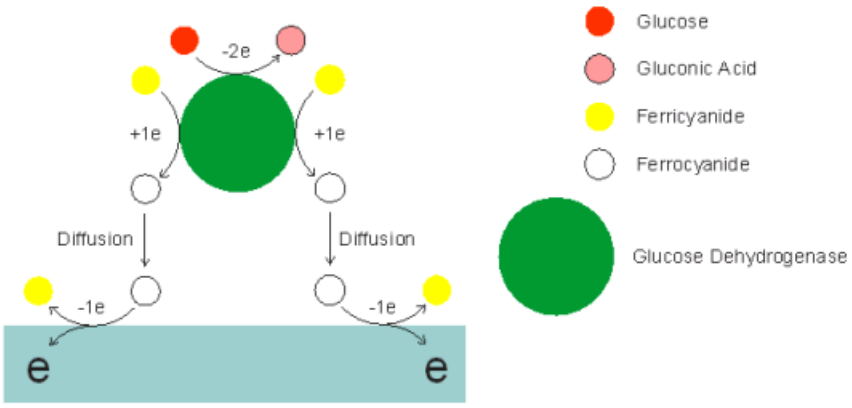

Figure 5.1 Detection mechanism of glucose meter. Image taken from Bioanalytical Systems Inc.

In order to realize non-glucose target detection by using a PGM, the relationship between target recognition and glucose generation must be established. Recently, many groups have reported methods establishing a direct relationship between the concentrations of the targets in the samples and the glucose detected by a PGM, enabling a number of non-glucose targets

to be detected quantitatively.[163, 177, 178] However, most of these methods included much liquid handling, such as adding and mixing solution, which should be avoided as much as possible to ensure ease of use. Conversely, a lateral flow device, as mentioned previously, is supposed to replace most of the manual solution addition and mixing involved in the above methods.

The basic design of the device is adapted from the previous colorimetric detection platform based on AuNPs based immunoreactions (in specific aim 1 and 2). However, visual detection can provide only qualitative and semi-quantitative results. Thus, to enable quantitative analysis, we establish a novel method that correlates the detection of non-glucose target to the detection of an enzyme-invertase by the target-induced immunoreactions. Subsequently, the enzyme converts sucrose into glucose for PGM readout.

5.2. Experimental

5.2.1. Materials

Bovine serum albumin, Invertase from baker's yeast, Sucrose, Gold chloride trihydrate, Sodium borohydride, Sodium periodate, Ethylene Glycol, Potassium carbonate, Boric acid, Sodium chloride and Prostate Specific Antigen from human semen (Sigma-Aldrich (St. Louis, MO)). NeutrAvidin Agarose, Streptavidin, EZ-Link Hydrazide-Biotin and Biotin Quantitation Kit (Pierce Biotechnology (Rockford, IL, USA)). Trehalose, PBS (1X, pH=7.4) and Tri-Sodium Citrate Dihydrate (VWR (West Chester, PA)). Tween 20 (Fisher Scientific (Fairlawn, NJ)). Plastic backing, Nitrocellulose membrane, Absorbing pad and cellulose paper (Millipore (Billerica, MA)). Streptavidin Conjugated Gold Nanoparticles (Nanocs Inc. (New York, NY)). 8-hydroxy-2-deoxy Guanosine and 8-hydroxy Guanosine (Cayman chemical (Ann Arbor, MI)). Mouse monoclonal antibodies to 8 hydroxyguanosine (biotin),

Mouse monoclonal [PS2] to prostate specific antigen (Biotin), Mouse monoclonal [PS6] to Prostate Specific Antigen and polyclonal Goat anti Mouse IgG (Abcam (Cambridge, MA)). PGM (TRUEtrack) and test strips (Walgreens (Springfield, IL)).

5.2.2. Preparation of streptavidin coated gold nanoparticles (STV-AuNPs)

The AuNPs were synthesized by the same protocol as described in section 2.2.1. For Streptavidin labeling, the AuNPs solutions was concentrated 5-fold (5X) in advance and the pH was adjusted to 6.8~7.2 with K_2CO_3 (0.1 M). Before conjugation, the optimal concentration of protein was determinated by the same protocol in section 2.2.2. Simply, streptavidin solutions (20 μL) with different concentrations (0, 0.1, 0.25, 0.5 and 1 mg mL^{-1}) were mixed with gold solution (5X, 100 μL, pH 6.8-~7.2) and incubated for 15 min at room temperature, and then 10% NaCl solution was added. The color of samples changes from brilliant red to blue as the concentration of Streptavidin decreases. The optimum concentration for labeling was the lowest concentration of mAb that did not change color, which is 0.25 mg mL^{-1}.

At the same time, we also measured the zeta potentials of the five mixtures (after 1 h incubation and two times purification). We found that the zeta potential (Table 5.1) became less negative when the concentration of streptavidin increased, but there was no obvious change when the concentration is larger than 0.5 mg mL^{-1}. Based on the previous two experiments, 0.5 mg mL^{-1} was chosen as the optimal concentration for labeling.

Table 5.1 Zeta potential of five mixtures

Sample (20 μL, mg mL^{-1})	Zeta potential (mV)	SD (n = 3)
0	-52.7	±2.21
0.1	-26.87	±0.29
0.25	-20	±0.82
0.5	-7.78	±0.43
1	-7.18	±0.44

5.2.3. Preparation of biotin-invertase

Biotin was conjugated to sialic acid residues of invertase by using a EZ-Link Hydrazide-Biotin kit. The efficiency of biotinylation was tested through NeutroAvidin Agarose. Briefly, an aliquot (30 μL) of agarose beads were separated and resuspended in 200 μL PBS buffer containing biotin-invertase (0.25 mg mL^{-1}), and the mixture was incubated for 1 h. Then the mixture was centrifuged for 2 min and the supernatant was collected. 10 μL of the supernatant and biotin-invertase solution (0.25 mg mL^{-1}) were mixed with 50 μL 0.5 M sucrose solution respectively. After 30 min, the readout of PGM (TRUEtrack Walgreen) was collected. From the result (Table 5.2), we can conclude that the efficiency of the biotinylation of the enzyme was greater than 70%.

Table 5.2 Efficiency of the biotinylation of the enzyme

PGM readout (mg dL^{-1})	Biotin-invertase (10 μL, 0.25 mg mL^{-1})	Supernatant (10 μL, 0.25 mg mL^{-1})
30 min	61 (n =3)	Low (<20) (n =3)

5.2.4. Preparation and characterization of invertase/Antibody-AuNPs

An aliquot (100 μL) of the streptavidin coated gold nanoparticles (STV-AuNPs) was centrifuged and resuspended with 100 μL PBS buffer containing biotin-invertase (2.5 mg mL^{-}

^{1}) and biotin-Ab (32.5 μg mL^{-1}) for 1 h. Then the invertase/Ab-AuNPs conjugates were separated, washed with 1 % BSA/PBS and finally resuspended in buffer (50 μL) for further use.

5.2.5. Preparation of BSA-8 Hydroxyguanosine conjugates

Details found in section 2.2.4.1

5.2.6. Assembly of the LFS

Details are simlar to the section 2.2.5 with slight modification: The sample pad was pretreated with buffer (50 mM borate buffer, 1% BSA and 0.2% Tween-20), and invertase/Ab-AuNPs conjugates (20 uL) was dispensed by pipette onto a conjugate pad.

5.3. Results and discussion

5.3.1. Design and detection mechanism of the strip for non-glucose target detection by a PGM

As shown in Figure 5.2, the test strip is composed of four components which were preloaded with different reagents and pasted onto a plastic backing plate. The sample pad pretreated with buffer (50 mM borate buffer, 1% BSA and 0.2% Tween-20) is where the strip contacts the liquid sample. Conjugation pad, which is composed of glass-fiber material, contains invertase/antibody (Ab)-conjugated AuNPs. Next to the conjugation pad is a flow membrane, which is made of nitrocellulose. There are two reaction zones on membrane, which are called test line and control line. BSA/8 hydroxyguanosine conjugates (1 mg mL^{-1}) or Mouse anti-PSA [PS6] antibody (1 mg mL^{-1}) was used as the test line capture reagent, while Goat anti-Mouse IgG Ab (1 mg mL^{-1}) was used as the control line capture reagent. These capture

reagents were dispensed by the Linomat 5 dispenser onto the nitrocellulose membrane. Sample moves along the strip due to capillary action and finally gets collected by the last part known as the absorption pad.

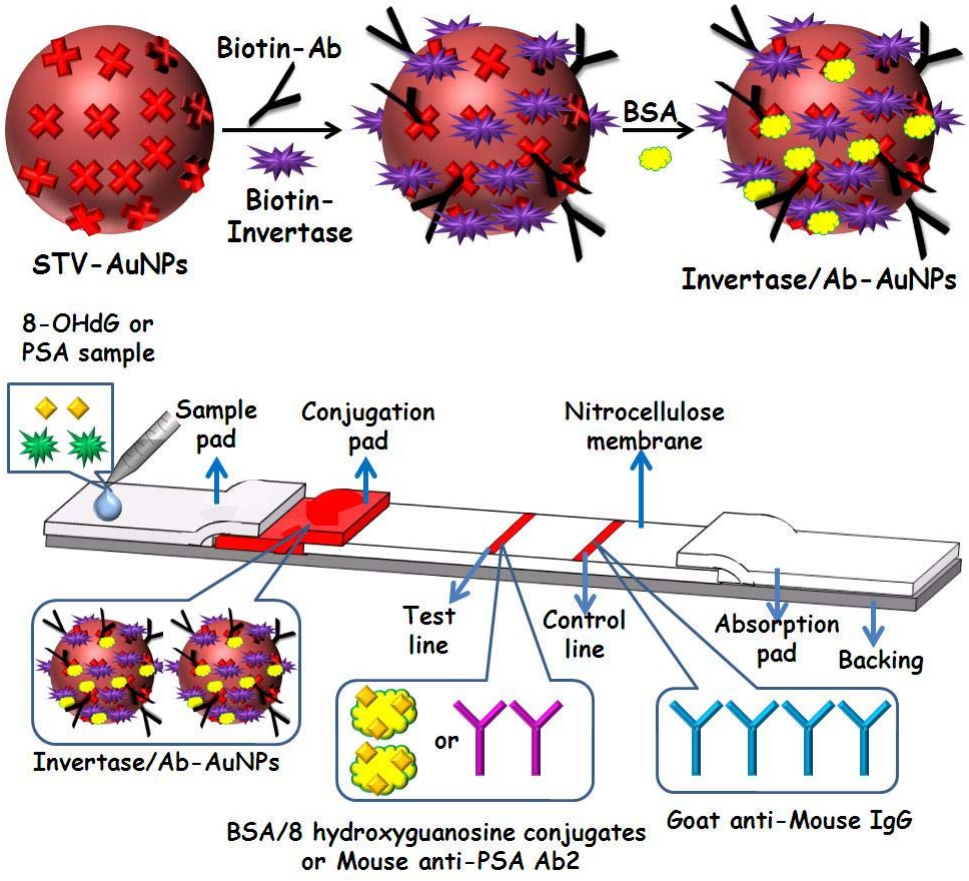

Figure 5.2 Design of test strip for quantitative detection of 8-OhdG or PSA

To realize non-glucose target detection using a PGM, the relationship between target recognition and glucose generation must be established. In our design, as illustrated in Figure 5.3 and Figure 5.4, the detection is based on two steps: the first step is that of competitive-type (for 8-OHdG, Figure 5.3 (A)(B)(C)(D)) or sandwich-type (for PSA, Figure 5.4 (A)(B)(C)(D)) immunoreactions in the LFS; the second step (Figure 5.3 (E)(F)(G) or Figure

5.4 (E)(F)(G)) contains an enzymatic reaction which converts sucrose into detectable glucose for measurement by a PGM.

Upon target introduction (Figure 5.3 (A) and 5.4 (A)), the target moves along the strip due to capillary force and rehydrate the conjugation pad, where the immunoreactions take place (Figure 5.3 (B) and 5.4 (B)). Subsequently, the invertase/Ab-AuNPs can be captured separately by the corresponding reaction zone based on the format of the Ab (Ab with free antigen-binding site will be captured by the BSA/8 hydroxyguanosine conjugates on the test line (Figure 5.3 (C); Ab saturated with 8-OHdG will be captured by the Goat anti-Mouse IgG on the control line (Figure 5.3 (D); Ab bounded with PSA will be captured by anti-PSA Ab2 on the test line (Figure 5.4 (C); the rest Ab will be fixed on the control line (Figure 5.4 (D)). Competitive-type immunoreactions make the target (sample) compete with the antigen (test line) for the antibody from conjugation pad. As a result, the color intensity of the test line as well as the amount of invertase captured on the test line are inversely proportional to the target concentration in the sample. Instead, the amount of invertase captured on the test line is proportional to concentration of PSA in the sandwich assay. Followed by the first step (<10 min), the test (2 mm) and control (2 mm) lines are cut by scissors and placed on a hydrophobic plate (Figure 5.3 (E) and 5.4 (E)). Then, 20 μL 0.5 M sucrose solutions are added on top of each zone (Figure 5.3 (F) and 5.4 (F)). After a specific period of time, the enzyme invertase fixed on each zone catalyzes the hydrolysis of sucrose to produce a specific amount of glucose for quantitative readout by the PGM (Figure 5.3 (G) and 5.4 (G)).

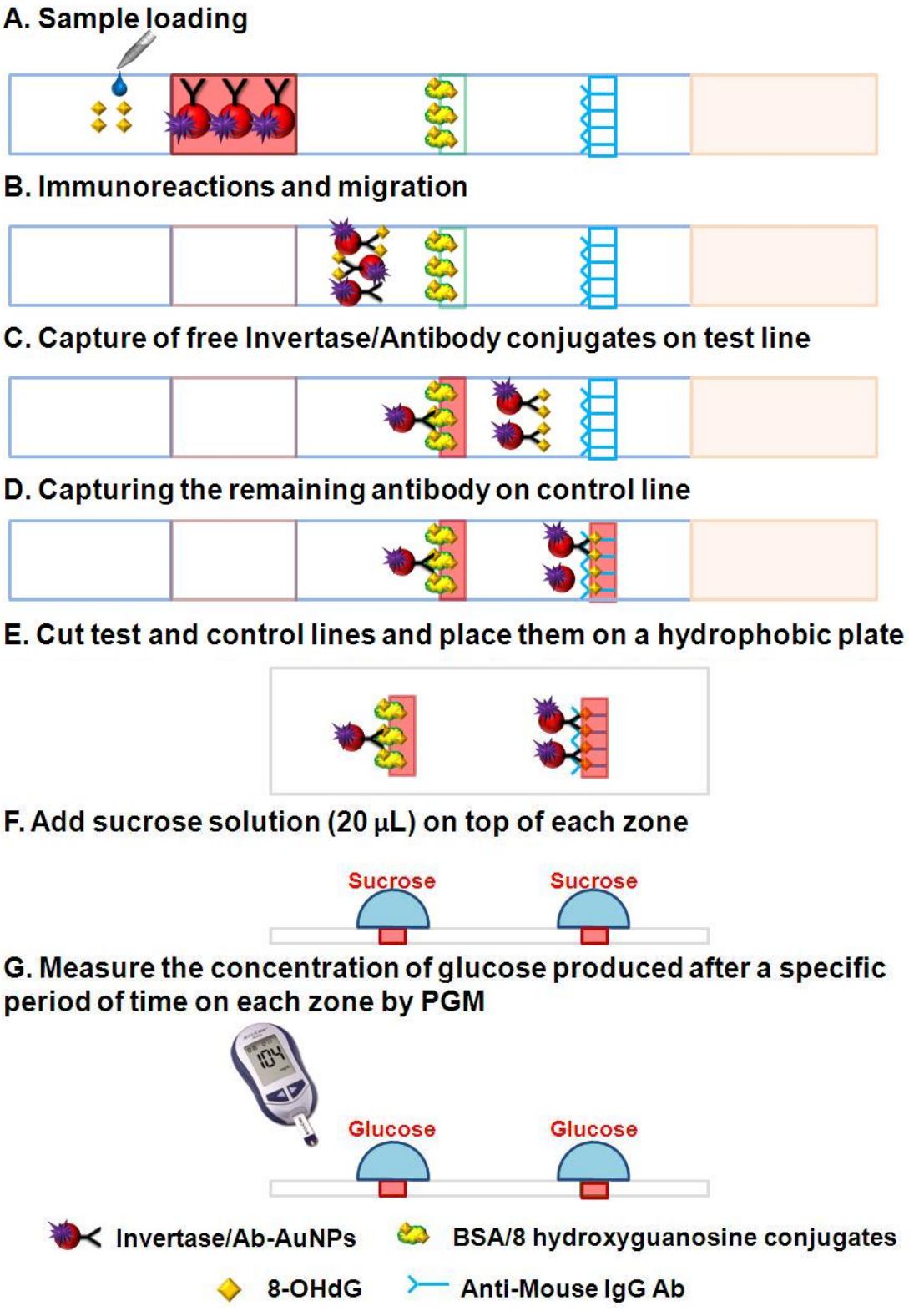

Figure 5.3 Mechanism for 8-OHdG detection by a PGM

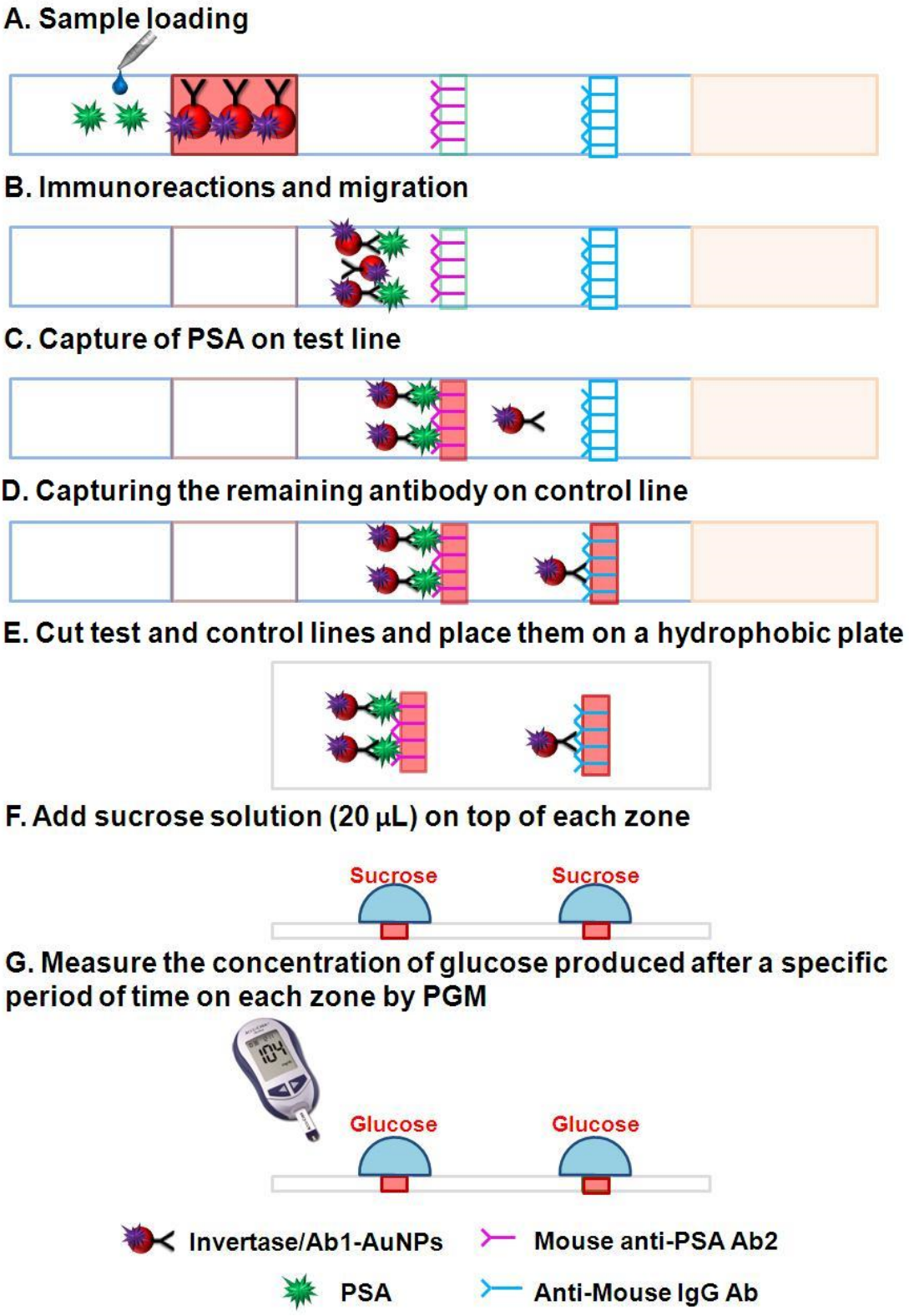

Figure 5.4 Mechanism for PSA detection by a PGM

5.3.2. Check the properties of Invertase/Antibody-AuNPs conjugates

The bifunctional AuNPs conjugated with invertase and antibody is one of the most important components in our design. The enzymatic product of invertase (glucose) can be monitored by a PGM. And the invertase/Ab-AuNPs are used as signal amplification labels, which can trigger each antibody-antigen recognition event into the capture of massive invertase. As a result, target-induced competitive or sandwich immunoreactions can lead to the capture of numerous invertases and generate a measurable amount of glucose that falls in the dynamic range of the PGM (0.6-33.3 mM or 10-600 mg dL^{-1}). Therefore, two aspects of the functions of the conjugates were examined before being used for the conjugation pad: enzymatic activity (invertase part) for glucose production and immunoreactivity (antibody part) for competitive or sandwich immunoreactions.

Firstly, the enzymatic activity of the conjugates was tested by mixing 10 μL conjugates solution with 50 μL 0.5 M sucrose solutions. The readout of PGM was 436 mg dL^{-1} (n = 3) after 10 min, indicating that conjugates possess a high enzymatic activity. Secondly, the immunoreactivity of the conjugates was tested through colorimetrical based antibody-antigen immunoreactions. Take 8-OHdG as an example, which is based on the theory of the competitive format of detection. 20 μL of the conjugates was applied onto the conjugation pad, which was subsequently assembled into a strip. 100 μL of samples with different concentrations were applied to the sample pad. After 10 min, photographs were taken by using digital camera. Figure 5.5 shows the typical responses of the strips to 8-OHdG with seven concentrations (0, 1, 2, 5, 10, 20, 100 ng mL^{-1}). The color intensity of the test line deceased when the sample concentration increased, which was consistent with the theory of

detection of competitive format and demonstrating the feasibility of the fuction of antibody in the conjugates for the following application.

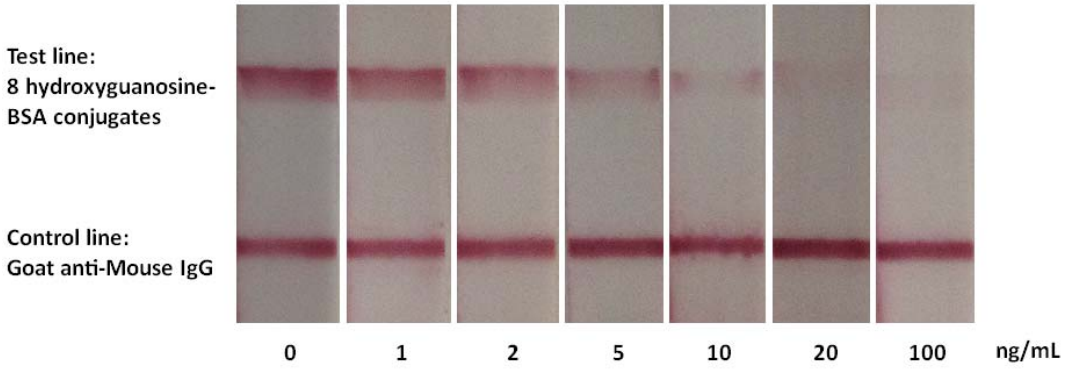

Figure 5.5 The photographs of test strips based on seven concentrations (0, 1, 2, 5, 10, 20, 100 ng mL^{-1}) of 8-OHdG. 8 hydroxyguanosine-BSA conjugates were used as the test line; Goat anti-Mouse IgG were used as the control line.

5.3.3. Quantitative analysis of 8-OHdG by integrating the PGM with the LFS

To demonstate the feasibility of our method for 8-OHdG detection, a series of 8-OHdG solutions with concentrations of 0, 0.1, 0.5, 1, 2, 5, 10, 20, 50, 100, 150 and 200 ng mL^{-1} in 1X PBS buffer were prepared and applied to the strips. After 10 min, the test (2 mm) and control (2 mm) lines were cut by scissors and placed on a hydrophobic plate. 20 μL of 0.5 M sucrose solution was put on top of each zone, and the PGM was used for readout after 45 min. As shown in Figure 5.6a, PGM readings (test line) decreased when the concentration increased, which is consist with the theory of the competitive format of detection. When the concentration is larger than 100 ng mL^{-1}, there was no obvious change in the PGM readings. However, elevated concentrations of 8-OHdG from 0.1 to 100 ng mL^{-1} lead to obviously decreased PGM readings. A dynamic range of 0 to 100 ng mL^{-1} can be obtained, and as low as 0.23 ng mL^{-1} of 8-OHdG can be detected.

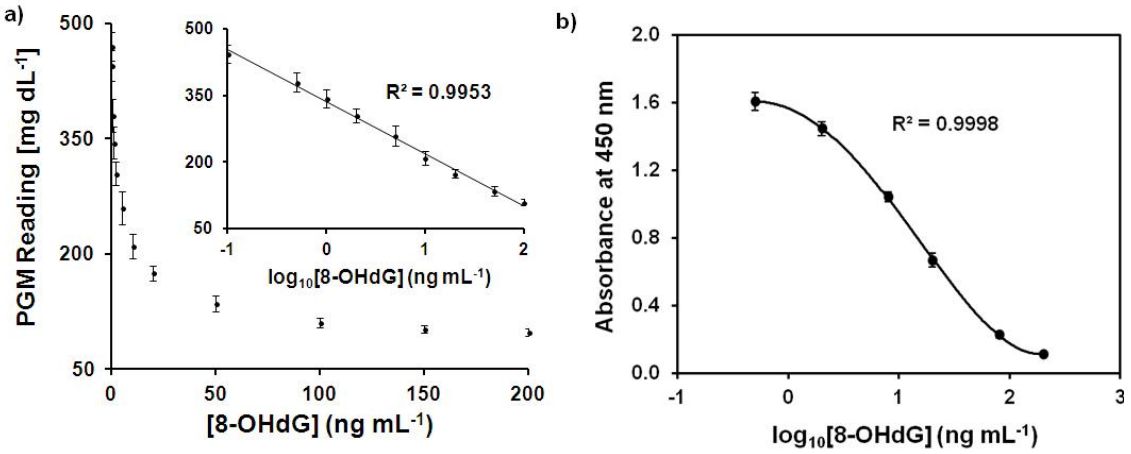

Figure 5.6 (a) Detection of 8-OHdG in buffer based on the PGM. The concentration of 8-OHdG was varied from 0 to 200 ng mL^{-1}. Error bars: SD, n = 6; (b) Conventional colorimetric ELISA for various concentrations of 8-OHdG. The absorbance spectra were recorded at 450 nm. Error bars: SD, n = 3.

In order to evaluate the analytical performance of the proposed method for 8-OHdG detection, a conventional ELISA approach was also performed for comparison. In the ELISA detection format, Horse Reddish Peroxidase (HRP) was used as a label to generate analytical signals. After the formation of the 8-OHdG-Ab1-Ab2/HRP in the ELISA plate wells, the 3,3',5,5'-tetramethylbenzidine (TMB) substrate for HRP was added and the UV-vis adsorption at 450 nm was recorded after acidification with sulfuric acid. As displayed in Figure 5.6b, the standard ELISA method for 8-OHdG indicates a detection range from 0.5 to 200 ng mL^{-1}, and the detection limit is about 0.64 ng mL^{-1}. We performed a comparison between our method and ELISA on the detection of 8-OHdG in buffer with known concentrations, which is shown in Table 5.3. From this table, we can see that the results obtained from our method are very close to those indicated in the first column. Table 5.4 illustrates that our PGM-based method can provide a simple, rapid, on-site and cost effective platform with acceptable detection limit and range in comparison with ELISA.

Table 5.3 Comparison between PGM-based method and ELISA on 8-OHdG detection in buffer samples (n = 6)

8-OHdG added in Buffer ($ng\ mL^{-1}$)	PGM-based method ($ng\ mL^{-1}$)	Commercial ELISA kit ($ng\ mL^{-1}$)
1	0.90±0.31	0.70±0.14
10	12.38±2.48	9.86±0.62
20	24.33±3.45	21.60±1.86
50	53.62±6.34	45.30±6.23

Table 5.4 PGM-based method vs. ELISA on 8-OHdG detection

	PGM-based method	Commercial ELISA kit
Detection limit ($ng\ mL^{-1}$)	0.23	0.64
Detection Range ($ng\ mL^{-1}$)	0.1-100	0.5-200
Time (h)	<1	3.5~4
Cost ($)	5/strip	700~800/test kit
Required Equipment	PGM ($20)	Microplate reader, computer, incubator, and many other lab supplies

5.3.4. Evaluate the PGM-based strip for 8-OHdG detection in human urine samples by comparing it with a conventional colorimetric ELISA

As mentioned previously, urinary 8-OHdG is considered to be an important biomarker of generalized and cellular oxidative stress. To evaluate the PGM-based strategy for the detection of 8-OHdG in real biomedical applications, urine samples from four individuals with varying 8-OHdG concentrations were tested. These samples were also assayed with a commercial 8-OHdG ELISA kit as reference. As shown in Table 5.5, the results obtained by the PGM-based method are in agreement with those obtained by the ELISA approach in the

investigated 8-OHdG concentration, which indicates the developed PGM-based method could be applied to clinical samples.

Table 5.5 Comparison between PGM-based method and ELISA on detection of 8-OHdG in human urine samples (n = 6)

Urine sample #	PGM-based method (ng mL^{-1})	Commercial ELISA kit (ng mL^{-1})
1	22.70 ± 1.25	17.72 ± 0.16
2	17.07 ± 0.97	13.70 ± 0.55
3	20.01 ± 1.83	15.24 ± 1.10
4	25.24 ± 2.12	18.81 ± 1.14

5.3.5. Quantitative analysis of PSA by integrating the PGM with the LFS

The platform was then used for PSA detection. A series of PSA solutions with concentrations of 1, 5, 10, 20, 50, 100 and 200 ng mL^{-1} in 1X PBS buffer were prepared and applied to the strips. After 10 min, the test lines (2 mm) were cut by scissors and placed on a hydrophobic plate. 20 μL of 0.5 M sucrose solution was put on top of each zone, and the PGM was used for readout after 30 min. As shown in Figure 5.7, PGM readings increased when the concentration increased, which is consist with the theory of the sandwich format of detection. A dynamic range of 0 to 100 ng mL^{-1} can be obtained, and as low as 1.26 ng mL^{-1} of PSA can be detected, by the definition of $3\sigma_b$/slope (σ_b, standard deviation of the blank samples). The detection limits achieved by the method indicate the promise for the detection of PSA in potential diagnosis applications of prostate cancer since the cutoff level of normal blood PSA concentration is 4 ng mL^{-1}.[179-183]

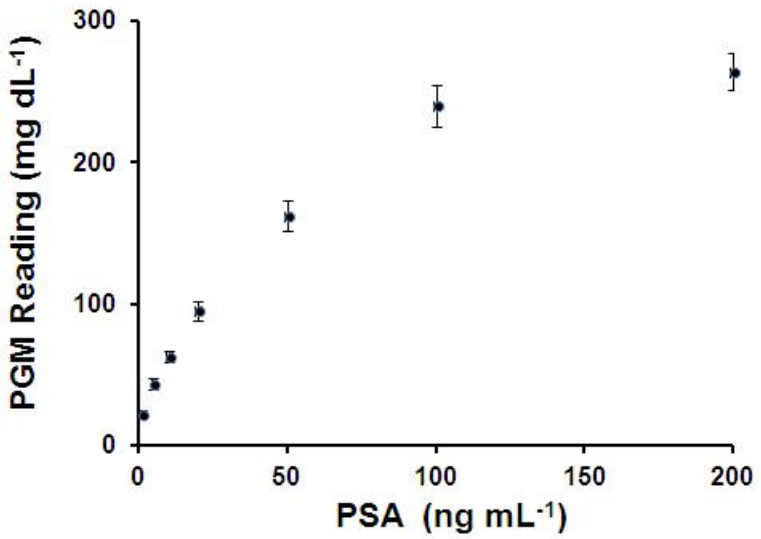

Figure 5.7. Detection of PSA in buffer based on the PGM. The concentration of PSA was varied from 0 to 200 ng mL^{-1}. Error bars: SD, n = 6.

We also compared our PGM-based method with a commercialized ELISA kit (Table 5.6) on the performance on PSA detection in aspect to the detection limit, detection range, assay time, assay cost as well as portability. It looks that our PGM-based method can provide a simple, rapid, low cost platform with acceptable detection limit and detection range for PSA detection.

Table 5.6 PGM-based method vs. ELISA on PSA detection

	PGM-based method	Commercial ELISA kit (R&D systems)
Detection limit (ng mL^{-1})	1.26	0.69
Detection Range (ng mL^{-1})	0.1-100	0.94-60
Time (h)	<1	4.5
Cost ($)	(5~10)/strip	500/test kit
Required Equipment	PGM ($20)	Microplate reader, computer, incubator, and many other lab supplies

The only disadvantage for this platform is that two steps are required to perform the measurements at this research stage which is not a proper POCT. However, this can be improved by future engineering design, which can separate the immunoreactions with enzymatic reaction automatically on strips. Therefore, the protype we designed here provides a potential novel concept for future POCT development and needs further optimizations for complete POCT and commercialization.

5.4. Conclusions

In conclusion, we have developed a simple approach for quantitative detection of 8-OHdG and PSA by using a low cost strip and an easily accessible PGM. The device was able to detect 8-OHdG concentrations in PBS as low as 0.23 ng mL^{-1} with a dynamic range of 0.1-100 ng mL^{-1} in less than 1 h. As low as 1.26 ng mL^{-1} PSA in buffer can also be detected through the same platform just replacing the antibodies. The strip was easy to fabricate and convenient to operate, and the assay did not require any specialized skills or sophisticated instrument. In addition, because of the advantages of the PGM, the demonstration of this approach will provide new opportunities for the detection of other targets.

Chapter 6. Conclusions and future work

6.1. Conclusions

This dissertation demonstrates noninvasive, rapid, visual, quantitative and convenient paper-based POCT biosensors for disease biomarker measurements. We have developed LFS sensing platforms with both sandwich and competitive formats for the detections of three BCa related biomarkers (Crestline, MMP-9 and VEGF) and a DNA oxidative damage biomarker (8-OHdG), respectively. The performance of the sensor was evaluated on the study of nanotoxicity of three metallic particles (CuO, TiO_2, CdO) on rat epithelial cells (CCL-149). We also successfully incorporated a paper electrode to the traditional LFS platform for quantitative analysis of 8-OHdG by both electrochemical and colorimetrical detection methods. Following this, a commercialized blood glucose meter was employed with an upgraded LFS platform for universal biomolecules detection, the feasibility of which was tested by a small molecule (8-OHdG) and a big protein molecule (PSA).

Chapter 1 introduces the objectives, the background and literature review on the dissertation topic. Three specific aims of this dissertation are also presented.

Chapter 2 summarizes the general experimental methods presented in the following chapters, which mainly including AuNPs based LFS fabrication, sample preparation and general detection mechanism.

Chapter 3 addresses specific aim 1. It deals with the development of simple and rapid AuNPs based LFS and its applications on three BCa related biomarkers detection and an oxidative DNA damage biomarker detection. LFS was the simplest and earliest design of paper-based POCT platform and has been widely used in many diagnostic areas. In this study, AuNPs

based LFS was developed for colorimetrical detection of biomarkers. The reliability of the strip was first evaluated by the detection of three BCa related biomarkers. The developed LFS was able to detect the biomarkers in both standard solutions and clinical urine samples with high sensitivity and specificity. This kind of comprehensive test for the levels of multiplex biomarkers could help us to better understand the underlying physiology of BCa and to monitor the BCa treatment progress in addition to BCa diagnosis. In the end, by comparing the results obtained from the strips to those of the commercial ELISA kits, we concluded that the strips can provide a useful tool for quick and non-invasive BCa diagnostic. Following this, we also upgraded the platform by incorporating an image processing program "ImageJ" for semi-quantitative analysis of a small DNA oxidative damage biomarker (8-oHdG). To the best of our knowledge, this is the first LFS-based sensing platform with the capability of 8-OHdG detection. The detection is quite quick (~10 minutes) and of high sensitivity (as low as 0.9 ng mL^{-1}). By using the same strip, we further assessed the nanotoxicity of three metal oxides (CuO, TiO2, CdO) NPs on rat epithelial cells (CCL-149) through measuring 8-OHdG concentrations produced in cells after NPs exposure. Feasibility of this method was validated by the comparison with two other established methods, Alamar Blue assay and Electrical impedance sensing (EIS) system on the level of cell proliferation/viability. This sensing platform could provide a useful tool for quantitative or qualitative 8-OHdG measurement and a high throughput analysis capable in mass screening in nanotoxicological investigations in future.

Chapter 4 addresses specific aim 2. It describes an upgraded sensing platform which combining electrochemical and colorimetric detection for the rapid measurement of 8-OHdG. The device takes advantage of the speed and low cost of the conventional strip test as well as

the high reliability and accuracy of the electrochemical assay. Competitive immunoreactions were performed on the LFS, and captured 8-OHdG on the control line was determined by chronoamperometric measurement with CNTs paper as the working electrode. At the same time, the color intensity of the test line was measured by a scanner and analyzed by ImageJ software. The device was able to detect 8-OHdG concentrations in PBS as low as 2.07 ng mL^{-1} by the colorimetric method and 3.11 ng mL^{-1} by the electrochemical method, both are comparable with the commercialized ELISA kit (detection limit is around 0.5 ng mL^{-1}). Since the normal range of urinary 8-OHdG is 10-60 ng mL^{-1}, either method is sensitive enough for 8-OHdG measurement in urine samples from both healthy and non-healthy patients (The levels of 8-OHdG go up 2~4 times higher for the non-healthy patients depend on different types of diseases). In conclusion, the integrated device with dual detection methods can provide a rapid, visual, quantitative and feasible detection method for 8-OHdG. The integration of these two methods holds two major advantages over tests based on a single method. Firstly, it can provide double confidence on the same assay. Secondly, by involving two methods that differ in principle, the integration could potentially avoid false results coming from one method. In addition, this method do not require expensive equipment or trained personnel, making it suitable for use as a simple, economical, portable field kit for on-site monitoring of 8-OHdG in a variety of clinical settings. Future efforts should be made to optimize the system for complete POCT development and commercialization. And the platform has a potential to be upgraded into a wireless-enabled biosensing system in future.

Chapter 5 addresses specific aim 3. It involves the integration of a personal glucose meters with the traditional LFS for portable and quantitative detection of biomarkers. The PGM is one of the most successfully commercialized diagnostic devices on the market and has been

widely used by millions of diabetes patients to monitor their blood glucose levels every day. Nevertheless, a glucose meter is capable of detecting glucose as the unique target. Herein, we established a novel method that transforms the detection of the target to the detection of an enzyme invertase. The enzyme converts sucrose into glucose for PGM readout. The concept was demonstrated by using a small molecule (8-OHdG) and a large protein molecule (PSA). The upgraded sensing platform was able to quantitatively detect 8-OHdG and PSA by using a low cost strip and an easily accessible wireless-enabled PGM with high sensitivity, specificity, speed of performance and simplicity. In addition, because of the advantages of the PGM, the demonstration of this approach will provide new opportunities for the detection of other targets. The only defect for this platform is that two steps are required to perform the measurements at this research stage which is not a proper POCT. Therefore, future efforts on the engineering design should be made to separate the immunoreactions with enzymatic reaction automatically on strips, which ensure the measurement can be done within single step. For future commercialization, more samples need to be tested and compared in the assay to ensure the reproducibility and accuracy.

6.2. Future work

The sensing platform developed in the chapter 5 for universal biomarker detection by using LFS and PGM could be further optimized and employed for the study of other disease biomarkers (both small and large molecules). The future areas of focus are: expanding the scope of the strip-PGM design to include other targets, further simplifying the design to eliminate the need for test line cutting, and optimizing the experimental conditions to acquire a more stable and accurate result.

Universality and wireless are two important factors for a sensing platform, as multiple detection and telemedicine are new perspectives for POCT sensor development. Therefore, a smartphone-enabled monitor system could be investigated and developed in future, which can be integrated with an upgraded LFS for instant biomarker detection, data collection and transmission.

REFERENCES

1. G. J. Kost, *Principles & Practice of Point-of-care Testing*, Lippincott Williams & Wilkins, Hagerstown, 2002.

2. C. P. Price and J. M. Hicks, *Point-of-care testing*, AACC Pres, Washington, 1999.

3. C. P. Chan, W. C. Mak, K. Y. Cheung, K. K. Sin, C. M. Yu, T. H. Rainer and R. Renneberg, *Annual review of analytical chemistry*, 2013, 6, 191-211.

4. S. Walter, *Chemie in unserer Zeit*, 2006, 40, 32-40.

5. M. Shibasaki, T. Ibuki and Y. Tanaka, *Journal of anesthesia*, 2010, 24, 643-645.

6. P. B. Luppa and H. Schlebusch, *POCT - Patientennahe Labordiagnostik*, Springer Medizin Verlag, Heidelberg, Germany, 2008.

7. A. M. Corstjens, J. J. Ligtenberg, I. C. van der Horst, R. Spanjersberg, J. S. Lind, J. E. Tulleken, J. H. Meertens and J. G. Zijlstra, *Critical care*, 2006, 10, R135.

8. J. L. Villalar, M. T. Arredondo, T. Meneu, V. Traver, M. F. Cabrera, S. Guillen and F. Del Pozo, *Journal of telemedicine and telecare*, 2002, 8 Suppl 2, 92-93.

9. P. Shah, X. Zhu and C. Z. Li, *Expert review of molecular diagnostics*, 2013, 13, 83-91.

10. W. Zhao and A. van der Berg, *Lab Chip*, 2008, 8, 1988-1991.

11. J. P. Comer, *Anal. Chem.,*, 1956, 28, 1748-1750.

12. P. von Lode, *Clin Biochem*, 2005, 38, 591-606.

13. A. W. Martinez, S. T. Phillips, G. M. Whitesides and E. Carrilho, *Anal Chem*, 2010, 82, 3-10.

14. A. W. Martinez, S. T. Phillips, M. J. Butte and G. M. Whitesides, *Angewandte Chemie*, 2007, 46, 1318-1320.

15. W. Wang, W. Y. Wu, W. Wang and J. J. Zhu, *Journal of chromatography. A*, 2010, 1217, 3896-3899.

16. E. M. Fenton, M. R. Mascarenas, G. P. Lopez and S. S. Sibbett, *ACS applied materials & interfaces*, 2009, 1, 124-129.

17. P. Kauffman, E. Fu, B. Lutz and P. Yager, *Lab Chip*, 2010, 10, 2614-2617.

18. E. Fu, B. Lutz, P. Kauffman and P. Yager, *Lab Chip*, 2010, 10, 918-920.

19. R. F. Carvalhal, M. S. Kfouri, M. H. Piazetta, A. L. Gobbi and L. T. Kubota, *Anal Chem*, 2010, 82, 1162-1165.

20. R. F. Carvalhal, E. Carrilho and L. T. Kubota, *Bioanalysis*, 2010, 2, 1663-1665.

21. L. Y. Shiroma, M. Santhiago, A. L. Gobbi and L. T. Kubota, *Anal Chim Acta*, 2012, 725, 44-50.

22. A. W. Martinez, S. T. Phillips and G. M. Whitesides, *Proc Natl Acad Sci U S A*, 2008, 105, 19606-19611.

23. S. A. Klasner, A. K. Price, K. W. Hoeman, R. S. Wilson, K. J. Bell and C. T. Culbertson, *Anal Bioanal Chem*, 2010, 397, 1821-1829.

24. A. W. Martinez, S. T. Phillips, E. Carrilho, S. W. Thomas, 3rd, H. Sindi and G. M. Whitesides, *Anal Chem*, 2008, 80, 3699-3707.

25. K. Abe, K. Suzuki and D. Citterio, *Anal Chem*, 2008, 80, 6928-6934.

26. W. Dungchai, O. Chailapakul and C. S. Henry, *Analytical Chemistry*, 2009, 81, 5821-5826.

27. Z. Nie, F. Deiss, X. Liu, O. Akbulut and G. M. Whitesides, *Lab Chip*, 2010, 10, 3163-3169.

28. Z. H. Nie, C. A. Nijhuis, J. L. Gong, X. Chen, A. Kumachev, A. W. Martinez, M. Narovlyansky and G. M. Whitesides, *Lab Chip*, 2010, 10, 477-483.

29. J. Yu, L. Ge, J. Huang, S. Wang and S. Ge, *Lab Chip*, 2011, 11, 1286-1291.

30. J. L. Delaney, C. F. Hogan, J. Tian and W. Shen, *Anal Chem*, 2011, 83, 1300-1306.

31. J. H. Leuvering, P. J. Thal, M. van der Waart and A. H. Schuurs, *Journal of immunoassay*, 1980, 1, 77-91.

32. C. D. Chin, V. Linder and S. K. Sia, *Lab Chip*, 2007, 7, 41-57.

33. S. Wang, L. Ge, X. Song, J. Yu, S. Ge, J. Huang and F. Zeng, *Biosens Bioelectron*, 2012, 31, 212-218.

34. G. Liu, Y. Y. Lin, J. Wang, H. Wu, C. M. Wai and Y. Lin, *Anal Chem*, 2007, 79, 7644-7653.

35. W. Dungchai, O. Chailapakul and C. S. Henry, *Anal Chim Acta*, 2010, 674, 227-233.

36. Y. He, S. Zhang, X. Zhang, M. Baloda, A. S. Gurung, H. Xu, X. Zhang and G. Liu, *Biosens Bioelectron*, 2011, 26, 2018-2024.

37. G. Liu, J. Wang, R. Barry, C. Petersen, C. Timchalk, P. L. Gassman and Y. Lin, *Chemistry*, 2008, 14, 9951-9959.

38. J. E. Adams, 3rd, D. R. Abendschein and A. S. Jaffe, *Circulation*, 1993, 88, 750-763.

39. A. Apilux, W. Dungchai, W. Siangproh, N. Praphairaksit, C. S. Henry and O. Chailapakul, *Anal Chem*, 2010, 82, 1727-1732.

40. L. Wang, W. Ma, W. Chen, L. Liu, W. Ma, Y. Zhu, L. Xu, H. Kuang and C. Xu, *Biosens Bioelectron*, 2011, 26, 3059-3062.

41. K. C. Grabar, R. G. Freeman, M. B. Hommer and M. J. Natan, *Analytical Chemistry*, 1995, 67, 735-743.

42. Q. Zeng, X. Mao, H. Xu, S. Wang and G. LIU, *Am. J. Biomed. Sci.*, 2009, 1, 70-79.

43. A. Kawde, X. Mao, H. Xu, Q. Zeng, Y. He and G. Liu, *Am. J. Biomed. Sci.*, 2010, 2, 23-32.

44. X. Mao, M. Baloda, A. S. Gurung, Y. H. Lin and G. D. Liu, *Electrochem Commun*, 2008, 10, 1636-1640.

45. J. J. Storhoff, A. A. Lazarides, R. C. Mucic, C. A. Mirkin, R. L. Letsinger and G. C. Schatz, *Journal of the American Chemical Society*, 2000, 122, 4640-4650.

46. H. X. Li and L. Rothberg, *P Natl Acad Sci USA*, 2004, 101, 14036-14039.

47. Y. Zhao, G. Zhang, Q. Liu, M. Teng, J. Yang and J. Wang, *J Agric Food Chem*, 2008, 56, 12138-12142.

48. S. H. Paek, S. H. Lee, J. H. Cho and Y. S. Kim, *Methods*, 2000, 22, 53-60.

49. F. Peng, Z. Wang, S. Zhang, R. Wu, S. Hu, Z. Li, X. Wang and D. Bi, *Clinical and vaccine immunology : CVI*, 2008, 15, 569-574.

50. S. Qian and H. H. Bau, *Analytical biochemistry*, 2004, 326, 211-224.

51. X. Wang, K. Li, D. Shi, N. Xiong, X. Jin, J. Yi and D. Bi, *J Agric Food Chem*, 2007, 55, 2072-2078.

52. C. Aprea, C. Colosio, T. Mammone, C. Minoia and M. Maroni, *J Chromatogr B Analyt Technol Biomed Life Sci*, 2002, 769, 191-219.

53. I. Y. Goryacheva, T. Y. Rusanova, N. A. Burmistrova and S. De Saeger, *Journal of Analytical Chemistry*, 2009, 64, 768-785.

54. C. M. Maragos, *Anal Bioanal Chem*, 2009, 395, 1205-1213.

55. M. G. Pikkemaat, *Anal Bioanal Chem*, 2009, 395, 893-905.

56. G. Liu, X. Mao, J. A. Phillips, H. Xu, W. Tan and L. Zeng, *Anal Chem*, 2009, 81, 10013-10018.

57. Q. H. Yang, X. Q. Gong, T. Song, J. M. Yang, S. J. Zhu, Y. H. Li, Y. Cui, Y. X. Li, B. B. Zhang and J. Chang, *Biosens Bioelectron*, 2011, 30, 145-150.

58. Y. Y. Lin, J. Wang, G. Liu, H. Wu, C. M. Wai and Y. Lin, *Biosens Bioelectron*, 2008, 23, 1659-1665.

59. S. W. Oh, Y. M. Kim, H. J. Kim, S. J. Kim, J. S. Cho and E. Y. Choi, *Clin Chim Acta*, 2009, 406, 18-22.

60. D. Tang, J. C. Sauceda, Z. Lin, S. Ott, E. Basova, I. Goryacheva, S. Biselli, J. Lin, R. Niessner and D. Knopp, *Biosens Bioelectron*, 2009, 25, 514-518.

61. M. Pattarawarapan, S. Nangola, T. R. Cressey and C. Tayapiwatana, *Talanta*, 2007, 71, 462-470.

62. F. Lu, K. H. Wang and Y. H. Lin, *Analyst*, 2005, 130, 1513-1517.

63. X. Mao, Y. Q. Ma, A. G. Zhang, L. R. Zhang, L. W. Zeng and G. D. Liu, *Analytical Chemistry*, 2009, 81, 1660-1668.

64. P. Pisani, D. M. Parkin, F. Bray and J. Ferlay, *International journal of cancer. Journal international du cancer*, 1999, 83, 18-29.

65. K. K. Aben and L. A. Kiemeney, *European urology*, 1999, 36, 660-672.

66. F. Millan-Rodriguez, G. Chechile-Toniolo, J. Salvador-Bayarri, J. Palou, F. Algaba and J. Vicente-Rodriguez, *The Journal of urology*, 2000, 164, 680-684.

67. N. Yang, S. Feng, K. Shedden, X. Xie, Y. Liu, C. J. Rosser, D. M. Lubman and S. Goodison, *Clinical cancer research : an official journal of the American Association for Cancer Research*, 2011, 17, 3349-3359.

68. A. Jemal, R. Siegel, J. Xu and E. Ward, *CA: a cancer journal for clinicians*, 2010, 60, 277-300.

69. C. J. Rosser, L. Liu, Y. Sun, P. Villicana, M. McCullers, S. Porvasnik, P. R. Young, A. S. Parker and S. Goodison, *Cancer Epidemiol Biomarkers Prev*, 2009, 18, 444-453.

70. R. O. Stuart, W. Wachsman, C. C. Berry, J. Wang-Rodriguez, L. Wasserman, I. Klacansky, D. Masys, K. Arden, S. Goodison, M. McClelland, Y. Wang, A. Sawyers, I. Kalcheva, D. Tarin and D. Mercola, *Proc Natl Acad Sci U S A*, 2004, 101, 615-620.

71. Y. Sun, S. Goodison, J. Li, L. Liu and W. Farmerie, *Bioinformatics*, 2007, 23, 30-37.

72. Y. Sun, V. Urquidi and S. Goodison, *Breast cancer research and treatment*, 2010, 119, 593-599.

73. N. Bandyopadhyay, T. Kahveci, S. Goodison, Y. Sun and S. Ranka, *Advances in bioinformatics*, 2009, 532989.

74. Y. Sun, S. Todorovic and S. Goodison, *IEEE transactions on pattern analysis and machine intelligence*, 2010, 32, 1610-1626.

75. M. Ruschhaupt, W. Huber, A. Poustka and U. Mansmann, *Statistical applications in genetics and molecular biology*, 2004, 3, Article37.

76. M. P. Washburn, D. Wolters and J. R. Yates, 3rd, *Nat Biotechnol*, 2001, 19, 242-247.

77. P. Kreunin, J. Zhao, C. Rosser, V. Urquidi, D. M. Lubman and S. Goodison, *Journal of proteome research*, 2007, 6, 2631-2639.

78. S. Goodison, C. J. Rosser and V. Urquidi, *Expert review of proteomics*, 2009, 6, 507-514.

79. K. R. Martin and J. C. Barrett, *Hum Exp Toxicol*, 2002, 21, 71-75.

80. B. Halliwell and J. M. C. Gutteridge, *Free Radicals in Biology and Medicine*, Oxford University Press, New York, 2007.

81. L. L. Wu, C. C. Chiou, P. Y. Chang and J. T. Wu, *Clin Chim Acta*, 2004, 339, 1-9.

82. R. A. Floyd, J. J. Watson, P. K. Wong, D. H. Altmiller and R. C. Rickard, *Free Radic Res Commun*, 1986, 1, 163-172.

83. M. Valko, H. Morris and M. T. Cronin, *Curr Med Chem*, 2005, 12, 1161-1208.

84. M. Valko, C. J. Rhodes, J. Moncol, M. Izakovic and M. Mazur, *Chem Biol Interact*, 2006, 160, 1-40.

85. L. Risom, P. Moller and S. Loft, *Mutat Res*, 2005, 592, 119-137.

86. M. D. Pulido and A. R. Parrish, *Mutat Res*, 2003, 533, 227-241.

87. J. E. Rundhaug and S. M. Fischer, *Cancers (Basel)*, 2010, 2, 436-482.

88. A. Valavanidis, T. Vlachogianni and C. Fiotakis, *J Environ Sci Health C Environ Carcinog Ecotoxicol Rev*, 2009, 27, 120-139.

89. H. Kasai, *Mutat Res-Rev Mutat*, 1997, 387, 147-163.

90. M. K. Shigenaga, C. J. Gimeno and B. N. Ames, *Proc Natl Acad Sci U S A*, 1989, 86, 9697-9701.

91. S. Koide, Y. Kinoshita, N. Ito, J. Kimura, K. Yokoyama and I. Karube, *J Chromatogr B Analyt Technol Biomed Life Sci*, 2010, 878, 2163-2167.

92. A. M. Domijan and M. Peraica, *Arh Hig Rada Toksikol*, 2008, 59, 277-282.

93. H. S. Lin, A. M. Jenner, C. N. Ong, S. H. Huang, M. Whiteman and B. Halliwell, *Biochem J*, 2004, 380, 541-548.

94. M. Harri, H. Kasai, T. Mori, J. Tornaeus, K. Savela and K. Peltonen, *J Chromatogr B Analyt Technol Biomed Life Sci*, 2007, 853, 242-246.

95. A. Weimann, D. Belling and H. E. Poulsen, *Free Radic Biol Med*, 2001, 30, 757-764.

96. M. S. Cooke, R. Singh, G. K. Hall, V. Mistry, T. L. Duarte, P. B. Farmer and M. D. Evans, *Free Radic Biol Med*, 2006, 41, 1829-1836.

97. E. Hondroulis, Z. Q. Zhang, C. Y. Chen and C. Z. Li, *Anal Lett*, 2012, 45, 272-282.

98. P. Shah, X. Zhu, C. Chen, Y. Hu and C. Z. Li, *Biomedical microdevices*, 2014, 16, 35-41.

99. J. C. Chow, J. G. Watson, N. Savage, C. J. Solomon, Y. S. Cheng, P. H. McMurry, L. M. Corey, G. M. Bruce, R. C. Pleus, P. Biswas and C. Y. Wu, *J Air Waste Manag Assoc*, 2005, 55, 1411-1417.

100. V. L. Colvin, *Nat Biotechnol*, 2003, 21, 1166-1170.

101. R. Owen and M. Depledge, *Mar Pollut Bull*, 2005, 50, 609-612.

102. C. F. Jones and D. W. Grainger, *Adv Drug Deliv Rev*, 2009, 61, 438-456.

103. R. Landsiedel, M. D. Kapp, M. Schulz, K. Wiench and F. Oesch, *Mutat Res*, 2009, 681, 241-258.

104. P. Moller, N. R. Jacobsen, J. K. Folkmann, P. H. Danielsen, L. Mikkelsen, J. G. Hemmingsen, L. K. Vesterdal, L. Forchhammer, H. Wallin and S. Loft, *Free Radic Res*, 2010, 44, 1-46.

105. G. Oberdörster, Stone Vicki, Donaldson Ken, *Nanotoxicology*, 2007, 1, 2-25.

106. N. Singh, B. Manshian, G. J. Jenkins, S. M. Griffiths, P. M. Williams, T. G. Maffeis, C. J. Wright and S. H. Doak, *Biomaterials*, 2009, 30, 3891-3914.

107. W. MacNee and K. Donaldson, *Eur Respir J Suppl*, 2003, 40, 47s-51s.

108. H. Y. Jia, Y. Liu, X. J. Zhang, L. Han, L. B. Du, Q. Tian and Y. C. Xu, *J Am Chem Soc*, 2009, 131, 40-41.

109. S. Durocher, A. Rezaee, C. Hamm, C. Rangan, S. Mittler and B. Mutus, *J Am Chem Soc*, 2009, 131, 2475-2477.

110. J. M. Hillegass, A. Shukla, S. A. Lathrop, M. B. MacPherson, N. K. Fukagawa and B. T. Mossman, *Wiley Interdiscip Rev Nanomed Nanobiotechnol*, 2010, 2, 219-231.

111. S. M. Poonam Takhar, *Archives of Applied Science Research*, 2011, 3, 389-403.

112. K. Bhattacharya, M. Davoren, J. Boertz, R. P. Schins, E. Hoffmann and E. Dopp, *Part Fibre Toxicol*, 2009, 6, 17.

113. H. L. Karlsson, P. Cronholm, J. Gustafsson and L. Moller, *Chem Res Toxicol*, 2008, 21, 1726-1732.

114. B. Fahmy and S. A. Cormier, *Toxicol In Vitro*, 2009, 23, 1365-1371.

115. I. Pujalte, I. Passagne, B. Brouillaud, M. Treguer, E. Durand, C. Ohayon-Courtes and B. L'Azou, *Part Fibre Toxicol*, 2011, 8, 10.

116. Q. Saquib, A. A. Al-Khedhairy, M. A. Siddiqui, F. M. Abou-Tarboush, A. Azam and J. Musarrat, *Toxicology in Vitro*, 2012, 26, 351-361.

117. D. Napierska, L. C. Thomassen, V. Rabolli, D. Lison, L. Gonzalez, M. Kirsch-Volders, J. A. Martens and P. H. Hoet, *Small*, 2009, 5, 846-853.

118. R. M. Mroz, R. P. Schins, H. Li, L. A. Jimenez, E. M. Drost, A. Holownia, W. MacNee and K. Donaldson, *Eur Respir J*, 2008, 31, 241-251.

119. M. J. Akhtar, M. Ahamed, M. Fareed, S. A. Alrokayan and S. Kumar, *J Toxicol Sci*, 2012, 37, 139-148.

120. J. C. Lai, M. B. Lai, S. Jandhyam, V. V. Dukhande, A. Bhushan, C. K. Daniels and S. W. Leung, *Int J Nanomedicine*, 2008, 3, 533-545.

121. S. Q. Li, R. R. Zhu, H. Zhu, M. Xue, X. Y. Sun, S. D. Yao and S. L. Wang, *Food Chem Toxicol*, 2008, 46, 3626-3631.

122. Y. Pan, A. Leifert, D. Ruau, S. Neuss, J. Bornemann, G. Schmid, W. Brandau, U. Simon and W. Jahnen-Dechent, *Small*, 2009, 5, 2067-2076.

123. N. Mei, Y. Zhang, Y. Chen, X. Guo, W. Ding, S. F. Ali, A. S. Biris, P. Rice, M. M. Moore and T. Chen, *Environ Mol Mutagen*, 2012, 53, 409-419.

124. M. F. Song, Y. S. Li, H. Kasai and K. Kawai, *J Clin Biochem Nutr*, 2012, 50, 211-216.

125. E. Hondroulis, C. Liu and C. Z. Li, *Nanotechnology*, 2010, 21, 315103.

126. R. Frick, B. Muller-Edenborn, A. Schlicker, B. Rothen-Rutishauser, D. O. Raemy, D. Gunther, B. Hattendorf, W. Stark and B. Beck-Schimmer, *Toxicology letters*, 2011, 205, 163-172.

127. M. Urner, A. Schlicker, R. Z'Graggen B, A. Stepuk, C. Booy, K. P. Buehler, L. Limbach, C. Chmiel, W. J. Stark and B. Beck-Schimmer, *Environmental science & technology*, 2014, 48, 13960-13968.

128. X. Han, N. Corson, P. Wade-Mercer, R. Gelein, J. Jiang, M. Sahu, P. Biswas, J. N. Finkelstein, A. Elder and G. Oberdorster, *Toxicology*, 2012, 297, 1-9.

129. S. M. Hussain, K. L. Hess, J. M. Gearhart, K. T. Geiss and J. J. Schlager, *Toxicology in vitro : an international journal published in association with BIBRA*, 2005, 19, 975-983.

130. C. Liu, Q. Jia, C. Yang, R. Qiao, L. Jing, L. Wang, C. Xu and M. Gao, *Anal Chem*, 2011, 83, 6778-6784.

131. V. Sharma, R. K. Shukla, N. Saxena, D. Parmar, M. Das and A. Dhawan, *Toxicol Lett*, 2009, 185, 211-218.

132. Z. Z. Wei Bai, Wenjing Tian, Xiao He, Yuhui Ma, Yuliang Zhao, Zhifang Chai, *Journal of Nanoparticle Research*, 2010, 12, 1645-1654.

133. E. Burello and A. P. Worth, *Nanotoxicology*, 2011, 5, 228-235.

134. C. S. J. H. Chang, C.H. Lo, T.T. Tsung, M.J. Kao, H.M. Lin, *REVIEWS ON ADVANCED MATERIALS SCIENCE*, 2005, 10, 128-132.

135. R. W. Kebin Zhou, Boqing Xu and Yadong Li, *Nanotechnology*, 2006, 17, 3939-3943.

136. S. Richard J. Lewis, 1997.

137. F. Tian, D. Cui, H. Schwarz, G. G. Estrada and H. Kobayashi, *Toxicol In Vitro*, 2006, 20, 1202-1212.

138. C. Z. Li, K. Vandenberg, S. Prabhulkar, X. Zhu, L. Schneper, K. Methee, C. J. Rosser and E. Almeide, *Biosens Bioelectron*, 2011, 26, 4342-4348.

139. M. Raoof, S. J. Corr, W. D. Kaluarachchi, K. L. Massey, K. Briggs, C. Zhu, M. A. Cheney, L. J. Wilson and S. A. Curley, *Nanomedicine : nanotechnology, biology, and medicine*, 2012, 8, 1096-1105.

140. Z. Yang, H. Suzuki, S. Sasaki and I. Karube, *Anal Lett*, 1997, 30, 1797-1807.

141. R. N. Goyal, N. Jain and D. K. Garg, *Bioelectroch Bioener*, 1997, 43, 105-114.

142. S. Prabhulkar and C. Z. Li, *Biosens Bioelectron*, 2010, 26, 1743-1749.

143. A. J. Bard and L. R. Faulkner, *Electrochemical Methods: Fundamentals and Applications*, Wiley, John & Sons, Incorporated, New York, 2000.

144. M. S. Cooke, J. Lunec and M. D. Evans, *Free Radic Biol Med*, 2002, 33, 1601-1614.

145. M. S. Cooke, M. D. Evans, K. E. Herbert and J. Lunec, *Free Radic Res*, 2000, 32, 381-397.

146. H. W. Kuo, S. F. Chang, K. Y. Wu and F. Y. Wu, *Occupational and environmental medicine*, 2003, 60, 590-594.

147. G. W. Xu, Q. H. Yao, Q. F. Weng, B. L. Su, X. Zhang and J. H. Xiong, *Journal of pharmaceutical and biomedical analysis*, 2004, 36, 101-104.

148. F. K. Chang, I. F. Mao, M. L. Chen and S. F. Cheng, *The Annals of occupational hygiene*, 2011, 55, 519-525.

149. D. J. Weiss and C. E. Lunte, *Electrophoresis*, 2000, 21, 2080-2085.

150. C. C. Chiou, P. Y. Chang, E. C. Chan, T. L. Wu, K. C. Tsao and J. T. Wu, *Clin Chim Acta*, 2003, 334, 87-94.

151. K. Kaneko, T. Kimata, S. Tsuji, A. Ohashi, Y. Imai, H. Sudo and N. Kitamura, *Clin Chim Acta*, 2012, 413, 1822-1826.

152. M. Erhola, S. Toyokuni, K. Okada, T. Tanaka, H. Hiai, H. Ochi, K. Uchida, T. Osawa, M. M. Nieminen, H. Alho and P. Kellokumpu-Lehtinen, *FEBS letters*, 1997, 409, 287-291.

153. L. C. Rall, R. Roubenoff, S. N. Meydani, S. N. Han and M. Meydani, *The Journal of nutritional biochemistry*, 2000, 11, 581-584.

154. T. S. Lin, C. C. Wu, J. D. Wu and C. H. Wei, *Toxicology and industrial health*, 2012, 28, 513-521.

155. S. Mei, Q. Yao, C. Wu and G. Xu, *J Chromatogr B Analyt Technol Biomed Life Sci*, 2005, 827, 83-87.

156. A. Jemal, R. Siegel, E. Ward, T. Murray, J. Xu, C. Smigal and M. J. Thun, *CA: a cancer journal for clinicians*, 2006, 56, 106-130.

157. M. C. Benson, I. S. Whang, C. A. Olsson, D. J. McMahon and W. H. Cooner, *The Journal of urology*, 1992, 147, 817-821.

158. T. J. Bradford, S. A. Tomlins, X. Wang and A. M. Chinnaiyan, *Urologic oncology*, 2006, 24, 538-551.

159. M. K. Brawer, *CA: a cancer journal for clinicians*, 1999, 49, 264-281.

160. C. Stephan, M. Klaas, C. Muller, D. Schnorr, S. A. Loening and K. Jung, *Clinical chemistry*, 2006, 52, 59-64.

161. B. Acevedo, Y. Perera, M. Ruiz, G. Rojas, J. Benitez, M. Ayala and J. Gavilondo, *Clin Chim Acta*, 2002, 317, 55-63.

162. D. A. Healy, C. J. Hayes, P. Leonard, L. McKenna and R. O'Kennedy, *Trends Biotechnol*, 2007, 25, 125-131.

163. Y. Xiang and Y. Lu, *Nature chemistry*, 2011, 3, 697-703.

164. S. Wang, X. Zhao, I. Khimji, R. Akbas, W. Qiu, D. Edwards, D. W. Cramer, B. Ye and U. Demirci, *Lab Chip*, 2011, 11, 3411-3418.

165. L. Shen, J. A. Hagen and I. Papautsky, *Lab Chip*, 2012, 12, 4240-4243.

166. S. Wang, F. Inci, T. L. Chaunzwa, A. Ramanujam, A. Vasudevan, S. Subramanian, A. Chi Fai Ip, B. Sridharan, U. A. Gurkan and U. Demirci, *Int J Nanomedicine*, 2012, 7, 2591-2600.

167. S. Wang, M. Esfahani, U. A. Gurkan, F. Inci, D. R. Kuritzkes and U. Demirci, *Lab Chip*, 2012, 12, 1508-1515.

168. Y. H. Tennico, D. Hutanu, M. T. Koesdjojo, C. M. Bartel and V. T. Remcho, *Anal Chem*, 2010, 82, 5591-5597.

169. A. M. Foudeh, T. Fatanat Didar, T. Veres and M. Tabrizian, *Lab Chip*, 2012, 12, 3249-3266.

170. Z. Nie, C. A. Nijhuis, J. Gong, X. Chen, A. Kumachev, A. W. Martinez, M. Narovlyansky and G. M. Whitesides, *Lab Chip*, 2010, 10, 477-483.

171. X. Zhu, E. Hondroulis, W. Liu and C. Z. Li, *Small*, 2013, 9, 1821-1830.

172. X. Zhu, P. Shah, S. Stoff, H. Liu and C. Z. Li, *Analyst*, 2014, 139, 2850-2857.

173. Q. Yang, X. Gong, T. Song, J. Yang, S. Zhu, Y. Li, Y. Cui, Y. Li, B. Zhang and J. Chang, *Biosensors & bioelectronics*, 2011, 30, 145-150.

174. A. Heller and B. Feldman, *Chemical reviews*, 2008, 108, 2482-2505.

175. M. Montagnana, M. Caputo, D. Giavarina and G. Lippi, *Clin Chim Acta*, 2009, 402, 7-13.

176. A. E. Carroll, D. G. Marrero and S. M. Downs, *Diabetes technology & therapeutics*, 2007, 9, 158-164.

177. Y. Xiang and Y. Lu, *Chem Commun (Camb)*, 2013, 49, 585-587.

178. J. Su, J. Xu, Y. Chen, Y. Xiang, R. Yuan and Y. Chai, *Chem Commun (Camb)*, 2012, 48, 6909-6911.

179. C. S. Thaxton, R. Elghanian, A. D. Thomas, S. I. Stoeva, J. S. Lee, N. D. Smith, A. J. Schaeffer, H. Klocker, W. Horninger, G. Bartsch and C. A. Mirkin, *Proc Natl Acad Sci U S A*, 2009, 106, 18437-18442.

180. X. Yu, B. Munge, V. Patel, G. Jensen, A. Bhirde, J. D. Gong, S. N. Kim, J. Gillespie, J. S. Gutkind, F. Papadimitrakopoulos and J. F. Rusling, *J Am Chem Soc*, 2006, 128, 11199-11205.

181. Y. P. Bao, T. F. Wei, P. A. Lefebvre, H. An, L. He, G. T. Kunkel and U. R. Muller, *Anal Chem*, 2006, 78, 2055-2059.

182. X. Liu, Q. Dai, L. Austin, J. Coutts, G. Knowles, J. Zou, H. Chen and Q. Huo, *J Am Chem Soc*, 2008, 130, 2780-2782.

183. H. Nie, S. Liu, R. Yu and J. Jiang, *Angewandte Chemie*, 2009, 48, 9862-9866.

VITA

XUENA ZHU

Born, Yuyao, Zhejiang, P.R.China

2005-2009	B.S., Biotechnology Zhejiang University of Technology Hangzhou, Zhejiang, P.R.China
2010-present	Ph.D. Candidate, Biomedical Engineering Expected Graduation: August, 2015 Florida International University Miami, Florida
2010-2013	FIU Presidential Fellowship
2012	FIU Graduate & Professional Student Committee conference travel award ($500)
2012	Best oral presentation award NanoFlorida 2012 Conference
2014	FIU Dissertation Year Fellowship

PUBLICATIONS AND PRESENTATIONS

C. Z. Li, K. Vandenberg, S. Prabhulkar, X. Zhu, L. Schneper, K. Methee, C.J. Rosser, E. Almeide, "Paper based point-of-care testing disc for multiplex whole cell bacteria analysis", *Biosens. Bioelectron*. 26(11):4342-4348, 2011.

X. Zhu, E. Hondroulis, W. Liu, and C. Z. Li, "Biosensing Approaches for Rapid Genotoxicity and Cytotoxicity Assays upon Nanomaterial Exposure", *Small*, 9(9-10), 1821-1830, 2013.

P. Shah, X. Zhu and C. Z. Li, "Development of paper-based analytical kit for point-of-care testing", *Expert Rev. Mol. Diagn.* 13(1), 83–91, 2013.

P. Shah, X. Zhu, C. Z. Li, " Development of a Cell-Chip Array for Single Cell Capturing Using Dielectrophoresis", *29th Southern Biomedical Engineering Conference (SBEC)*, 125-126, 2013.

X. Zhu, P. Shah, C. Z. Li, "Paper-based Immunosensor for Oxidative DNA Damage Biomarker Detection", *29th Southern Biomedical Engineering Conference (SBEC)*, 125-126, 2013.

X. Zhu, P. Shah, S. Stoff, H. Liu and C. Z. Li, "A paper electrode integrated lateral flow immunosensor for quantitative analysis of oxidative stress induced DNA damage", *Analyst*, 139 (11), 2850 – 2857, 2014.

X. Zhu, S. Ross, V. Urquidi, C. J. Rosser, C. Zhang, C. Z. Li, "Immuno strip based point-of-care testing for bladder cancer biomarkers detection", *Chemical Sensors*, 4 : 12, 2014.

P. Shah, X. Zhu, C. Chen, Y. Hu, C. Z. Li, "Lab-on-chip device for single cell trapping and analysis", *Biomedical Microdevices*, Volume 16, Issue 1, pp 35-41, 2014.

P. Shah, A. Kaushik, X. Zhu, C. Zhang and C. Z. Li, "Chip based single cell analysis for nanotoxicity assessment", *Analyst*, 139, 2088-2098, 2014.

E. Hondroulis, P. Shah, X. Zhu, C. Z. Li, "Chapter 5. Biosensing Devices for Toxicity Assessment of Nanomaterials", *Biointeractions of Nanomaterials*, CRC press 2014, Pages 117-130, 2014.

P. Zhang, Z. He, C. Wang, J. Chen, J. Zhao, X. Zhu, C. Z. Li, Q. Min, J. J. Zhu, "In situ Amplification of Intracellular MicroRNA with MNAzyme Nanodevices for Multiplexed Imaging, Logic Operation, and Controlled Drug Release", *ACS nano*, 9 (1), pp 789–798, 2015.

X. Zhu, P. Shah, C. Z. Li, “Paper Based Point of Care Biosensor for Toxic Exposure Assessment”, FIU BME Graduate Research Day, Miami, Florida, 2011.

X. Zhu, C. Z. Li, “Paper based Point of Care testing sensor for DNA oxidative damage biomarker detection”, Pittsburgh Conference, 2012, Orlando, Florida, 2012

X. Zhu, C. Z. Li, “Paper based sensor for DNA damage biomarker detection”, 5th Annual NanoScience Technology Symposium (NanoFlorida 2012), Tampa, Florida, 2012.
*Awarded best oral presentation

X. Zhu, P. Shah, C. Z. Li, “Paper-based Electrochemical Immunosensor for Oxidative DNA Damage Biomarker Detection”, 29th Southern Biomedical Engineering Conference, Miami, Florida, 2013.

X. Zhu, C. Z. Li, “Paper Based Point of Care Testing Sensor for DNA Oxidative Damage Biomarker Detection”, 2013 BIOELECTRONICS AND BIOSENSING SYMPOSIUM, Morgantown, West Virginia, 2013.

X. Zhu, C. Z. Li, “Lateral flow immunostrip with personal glucose meter for quantitative detection of non-glucose target”, 7th Annual NanoScience Technology Symposium (NanoFlorida 2014), Miami, Florida, 2014